



January 2019

## An Evaluation Of Remote Sensing Methods For Ecological Management In Theodore Roosevelt National Park

Jenna Folluo

Follow this and additional works at: <https://commons.und.edu/theses>

---

### Recommended Citation

Folluo, Jenna, "An Evaluation Of Remote Sensing Methods For Ecological Management In Theodore Roosevelt National Park" (2019). *Theses and Dissertations*. 2848.  
<https://commons.und.edu/theses/2848>

This Thesis is brought to you for free and open access by the Theses, Dissertations, and Senior Projects at UND Scholarly Commons. It has been accepted for inclusion in Theses and Dissertations by an authorized administrator of UND Scholarly Commons. For more information, please contact [zeineb.yousif@library.und.edu](mailto:zeineb.yousif@library.und.edu).

AN EVALUATION OF REMOTE SENSING METHODS FOR ECOLOGICAL  
MANAGEMENT IN THEODORE ROOSEVELT NATIONAL PARK

by


Jenna Nicole Folluo  
Bachelor of Science, University of Missouri, 2017

A Thesis  
Submitted to the Graduate Faculty  
of the  
University of North Dakota  
in partial fulfillment of the requirements  
for the degree of  
Master of Science

Grand Forks, North Dakota  
December  
2019

Copyright 2019 Jenna Folluo

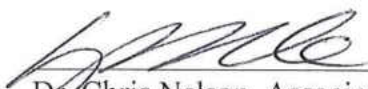
This thesis, submitted by Jenna Nicole Folluo in partial fulfillment of the requirements for the Degree of Master of Science from the University of North Dakota, has been read by the Faculty Advisory Committee under whom the work has been done and is hereby approved.

  
\_\_\_\_\_  
Dr. Robert A. Newman

  
\_\_\_\_\_  
Dr. Blake E. McCann

  
\_\_\_\_\_  
Dr. Bradley C. Rundquist

This thesis is being submitted by the appointed advisory committee as having met all of the requirements of the School of Graduate Studies at the University of North Dakota and is hereby approved.

  
\_\_\_\_\_  
Dr. Chris Nelson, Associate Dean  
School of Graduate Studies

12/10/19  
\_\_\_\_\_  
Date

## **PERMISSION**

Title            An Evaluation of Remote Sensing Methods for Ecological Management in Theodore Roosevelt National Park

Department    Biology

Degree         Master of Science

In presenting this thesis in partial fulfillment of the requirements for a graduate degree from the University of North Dakota, I agree that the library of this University shall make it freely available for inspection. I further agree that permission for extensive copying for scholarly purposes may be granted by the professor who supervised my thesis work or, in his absence, by the Chairperson of the department or the dean of the School of Graduate Studies. It is understood that any copying or publication or other use of this thesis or part thereof for financial gain shall not be allowed without my written permission. It is also understood that due recognition shall be given to me and to the University of North Dakota in any scholarly use which may be made of any material in my thesis.

Jenna Nicole Folluo

December 2019

## TABLE OF CONTENTS

LIST OF FIGURES .....	vii
LIST OF TABLES .....	xi
ACKNOWLEDGEMENTS .....	xii
ABSTRACT .....	xv
CHAPTERS .....	1
I. AN OVERVIEW OF ECOLOGICAL DYNAMICS IN THE GREAT PLAINS AND REMOTE SENSING TECHNOLOGY .....	1
INTRODUCTION .....	1
Prairie Grasslands and the Great Plains .....	1
Theodore Roosevelt National Park .....	4
The Rise of Remote Sensing .....	9
Objectives of Study .....	13
LITERATURE CITED .....	14
II. DETECTING AND MAPPING INVASIVE PLANTS IN THEODORE ROOSEVELT NATIONAL PARK .....	20
INTRODUCTION .....	20
METHODS .....	23
Study Area .....	23
Data Acquisition .....	24
Image Classification .....	26
Ground Truthing .....	31
Entire Unit Map .....	32
RESULTS .....	35
DISCUSSION .....	44
LITERATURE CITED .....	48
III. MAPPING VEGETATION COMMUNITIES IN THEODORE ROOSEVELT NATIONAL PARK .....	53
INTRODUCTION .....	53

METHODS .....	56
Study Area .....	56
Data Acquisition .....	56
Image Classification.....	59
RESULTS .....	61
DISCUSSION .....	69
LITERATURE CITED .....	72
IV. BLACK-TAILED PRAIRIE DOG COLONY MAPPING IN THEODORE ROOSEVELT NATIONAL PARK .....	75
INTRODUCTION .....	75
METHODS .....	78
Study Area .....	78
Data Acquisition .....	79
Image Classification.....	81
Perimeter Delineation .....	86
RESULTS .....	86
DISCUSSION.....	93
LITERATURE CITED .....	96
APPENDIX A:.....	100
CLASSIFICATION FIGURES .....	100
APPENDIX B: .....	129
CONFUSION MATRICES .....	129

## LIST OF FIGURES

- Figure 1: A map of the South Unit of Theodore Roosevelt National Park (TRNP) located in Billings County, North Dakota. The park boundary is depicted by the black outline, the local park road is shown in blue, and the United States Interstate 94 is shown in red. .... 6
- Figure 2: A map of the North Unit of Theodore Roosevelt National Park (TRNP) located in McKenzie County, North Dakota. The park boundary is depicted by the black outline, the local park road is shown in blue, and the North Dakota State Highway 85 is shown in red. .... 7
- Figure 3: Summary of image classification workflow: images are processed (top) and fed through the desired classifier (center branches), the researcher creates training samples and rulesets (rulesets in eCognition only) (center of diagram), error assessments and KHAT statistics are calculated for best classifications (bottom), and landscape metrics are performed to gain further understanding of the system (bottom center). .... 27
- Figure 4: Talkington mosaic image collected from low-altitude UAS. Each box represents a small subset that was used for classification via pixel-based and object-based methods. The box on the left corresponds to the Talkington75(1) classifications and the box on the right corresponds to the Talkington75(2) classifications. .... 28
- Figure 5: Object-based classification performed on an image taken via UAS (top) compared with a pixel-based (maximum likelihood) classification performed on



an image taken from NAIP (bottom). The UAS image was used as a near-ground-truth and the two images were compared to gain insight on errors. The red color in the NAIP classification corresponds to the vegetation of interest class and can be compared with the leafy spurge class (yellow) in the UAS classification..... 34

Figure 6: A) Talkington75(1) base image used for classification B) Classification produced using OBIA in eCognition C) Classification produced using maximum likelihood in ArcGIS D) Classification produced using SVM in ArcGIS. Classifications of leafy spurge are indicated by the color yellow. .... 36

Figure 7: Maximum likelihood classifications in ArcGIS of NAIP imagery; North Unit (left) and South Unit (right). Vegetation of interest indicated by the color orange. .... 39

Figure 8: Areas identified as “vegetation of interest” shown in the south unit of Theodore Roosevelt National Park. This classification identifies known areas of leafy spurge, but also areas of taller vegetation through error..... 40

Figure 9: Scatterplots showing correlations between classified imagery and ground truthed data with 95% confidence intervals displayed. .... 42

Figure 10: TRNP North Unit (left) and South Unit (right) classified via maximum likelihood in ArcGIS and corresponding producer's accuracies for each below the maps. The colors of the bars in the graphs correspond to the class color in the classification. Producer’s accuracy shows how often the classifier got it right; errors of omission are the inverse of producer’s accuracy. .... 63

Figure 11: Producer’s accuracy for individual classes produced using an equalized random accuracy assessment for object-based classification in eCognition (top), maximum likelihood pixel-based classification in ArcGIS (center), and SVM pixel-based classification in ArcGIS (bottom). The colors of the bars in the graphs correspond to the class color in the classification. Producer’s accuracy shows how often the classifier got it right; errors of omission are the inverse of producer’s accuracy. .... 66

Figure 12: Producer’s accuracy for individual classes produced using an equalized random accuracy assessment for object-based classification in eCognition (top) and for maximum likelihood pixel-based classification in ArcGIS (bottom). The colors of the bars in the graphs correspond to the class color in the classification. Producer’s accuracy shows how often the classifier got it right; errors of omission are the inverse of producer’s accuracy..... 67

Figure 13: Beef Corral prairie dog colony mosaic image collected from low-flying UAS. Each box represents a small subset that was used for classification via pixel-based and object-based methods. The box on top corresponds to the BeefCorral75(1) classifications and the box on the bottom corresponds to the BeefCorral75(2) classifications..... 82

Figure 14: Lindbo Flats prairie dog colony mosaic image collected via low-flying UAS. Each box represents a small subset that was used for classification via pixel-based and object-based methods. The box on top corresponds to the Lindbo75(1)

classifications and the box on the bottom corresponds to the Lindbo75(2) classifications.....	83
Figure 15: A) BeefCorral75(1) base image used for classification B) Classification produced using OBIA in eCognition C) Classification produced using maximum likelihood in ArcGIS D) Classification produced using SVM in ArcGIS. The brown color in the classification corresponds to prairie dog mounds, the off-white corresponds to bare ground, and the light green corresponds to short grasses. ....	88
Figure 16: Beef Corral colony perimeter (black line) as mapped by the <i>ConcaveHull</i> tool in ArcGIS. This perimeter accurately follows the edge of the image mosaic and correctly excludes small sections of trees where there were no prairie dog mounds. The perimeter was estimated from the classified map but displayed over the original mosaic to visualize the relationship.....	91
Figure 17: Colony perimeters for a central piece of the Beef Corral prairie dog colony. Ground data collected in 2016 is shown in blue, ground data collected in 2018 is shown in green, and the perimeter based on the image classification for 2018 is shown in red.....	92

## LIST OF TABLES

Table 1: Images used for classification and their temporal, spatial, and spectral characteristics. The full extent of UAS imagery was 0.43 – 0.59 km <sup>2</sup> . The images listed here are two different clips from the full mosaiced image.....	25
Table 2: Percent omission and commission error for classifications of Talkington taken via UAS.....	37
Table 3: Model of the percent classified spurge as a function of ground spurge coverage, area, density, and interaction terms for area * ground spurge coverage, and density * ground spurge coverage.....	43
Table 4: Images used for classification and their temporal, spatial, and spectral characteristics. I analyzed only portions of the full dataset from each site. ....	58
Table 5: Overall accuracy and Kappa statistics for all classification methods.....	68
Table 6: Images used for classification and their temporal, spatial, and spectral characteristics. Only portions of the full extent produced by each flight were classified. ....	80
Table 7: Percent omission and commission error for prairie dog mounds for each classification of Beef Corral and Lindbo Flats taken via UAS.....	89

## ACKNOWLEDGEMENTS

I would first like to thank my graduate advisor, Dr. Robert Newman, for your support and guidance throughout this project. Thank you for spending so much of your time and energy helping me to become a better scientist, and for teaching me to ask the hard and complicated questions. I cannot understate my appreciation for your contributions to my scientific growth throughout this process.

Thank you to my committee members, Dr. Blake McCann and Dr. Bradley Rundquist, for providing invaluable guidance, input, and feedback during this process. Thank you for providing me opportunities to grow and learn.

A huge thank you to Dr. Susan Felege for being my pilot and dedicating so much time into this project. Thank you for all your input, advice, and words of encouragement. You are a great example of what women in wildlife can accomplish and I am proud to have worked with you.

Thank you to the University of North Dakota Biology Department for providing me with funding and opportunities. Thank you to the National Park Service, particularly Theodore Roosevelt National Park, for offering me funding and work opportunities to get into the field and familiarize myself with the system.

I also want to thank my family of graduate students here in the Department of Biology. Thanks to my two main girls, Gaimi Davies and Taylor Holm, for always being there when I needed to vent, wanted to grab lunch, or forget about my project for a bit

and just laugh together. Thank you to Andrew Barnas for being the best human soundboard I've ever met. When I needed to talk through an idea or get your advice on something, you were always ready to help. I wouldn't have survived this project without amazing friends like you all.

A million thank-yous to my incredibly supportive boyfriend, Bradley Landis. You have been my rock throughout this entire process. Your unwavering support, constant encouragement, and undying love kept me going even on days when quitting seemed like the easiest option. Thank you for the nightly video-chats, for the many flights back and forth for visits, for ordering me pizza when I was craving, the 900 day snapstreak, and so much more. You're my guy. I love you forever.

Last but never least, thank you to my mom and dad, John and Deanna Folluo. Thank you for being willing to load all my belongings into a horse trailer and move me halfway across the country so I could chase after my goals and dreams. Thank you for supporting me throughout the process. I couldn't ask for better parents; I have been truly blessed.

For my Grandpa Leuthauser, who would have loved this.

## **ABSTRACT**

This thesis is comprised of four chapters that examine various aspects of remote sensing for ecological management in Theodore Roosevelt National Park. Chapter one reviews the use of remote sensing as a management tool and discusses its applications in TRNP. Chapter two describes the application of multiple remote sensing methods and how well they can detect and map invasive vegetation, particularly leafy spurge. Chapter three provides a study on defining and mapping vegetation communities in TRNP at varying spatial scales. Chapter four explores the use of remote sensing techniques to detect prairie dog mounds and map colonies.



## CHAPTER I

### AN OVERVIEW OF ECOLOGICAL DYNAMICS IN THE GREAT PLAINS AND REMOTE SENSING TECHNOLOGY

#### INTRODUCTION

##### *Prairie Grasslands and the Great Plains*

Covering an estimated 40% of the Earth's surface, grasslands have been intensely altered by anthropogenic activities (Anderson 2006); it is therefore crucial to understand their historical dynamics, recognize changes over time, and understand changes brought on to the system by humans. Remote sensing technologies look promising as a tool to monitor ecosystems because they can provide large amounts of high-quality data in short amounts of time and in places that were potentially inaccessible before (Toth and Jozkow 2016). High resolution imagery produced using unmanned aircraft systems (UAS) in combination with computational analysis techniques are hypothesized to produce high quality and accurate results (Watts et al. 2008). Managers and scientists hope to use these technologies to answer questions about the resources they manage. Theodore Roosevelt National Park (TRNP) has identified specific concerns and needs that include detection and mapping of invasive plants, mapping of vegetation communities, and detection and mapping of prairie dog colonies.

In North America, grasslands of the Great Plains make up much of the central portion of the continent. The Great Plains extend south into Texas and north into Canada, bounded by the Rocky Mountains to the west and mesic forests to the east. All grasslands

are dominated by graminoids but vary geographically in species composition and structure in relation to regional climate. North American prairie are categorized as short grass prairie, mixed grass prairie, and tall grass prairie (Li and Guo 2014). Graminoids are the most common species in these vast grasslands, with dominant genera being *Agropyron*, *Stipa*, and *Bouteloua* (Barker and Whitman 1988).

Periodic disturbances are characteristic of prairie grassland ecosystems and play an important role in maintaining species richness (Gibson 1989). Disturbances such as fire, soil alteration, and grazing increases grassland heterogeneity and productivity (Fuhlendorf and Engle 2001, McMillan 2017). Grasses in the Northern Great Plains (NGP) have evolved in tandem with grazing herbivores who used them for forage, which in turn led to evolution in grasses tolerant to grazing pressures (Milchunas et al. 1988). Prominent native grazers in North American prairies include the black-tailed prairie dog (*Cynomys ludovicianus*) and the American plains bison (*Bison bison*). Although at opposite ends of the body-size spectrum, both are considered iconic prairie herbivores and keystone species. However, these are not the only herbivores that graze in a prairie grassland system. Other important grazers include wildlife such as pronghorn, elk, and deer, as well as domestic cattle and horses. Prairie ecosystem structure and function is thus the result of interactions of climate, disturbance-adapted vegetation communities, and grazing herbivores.

Prairie dogs and bison evolved together with prairie grasslands, which created an ecosystem that was frequently disturbed. Prairie dogs are small, colonial members of the rodent family that historically lived throughout the NGP. Colonies are made up of multiple, closely related groups called “coteries” that inhabit separate burrow systems

(Crosby and Graham 1986). Through their burrowing activities, prairie dogs increase nutrient cycling (Coppock et al. 1983) and provide potential habitat for many other species (Hoogland 2013). Their alteration of the landscape leads to changes in vegetation community structure and ultimately increases biomass (Detling 1998). In addition, prairie dogs serve as prey for numerous predator species such as black-footed ferrets (*Mustela nigripes*), American badgers (*Taxidea taxus*), and coyotes (*Canis latrans*) (Hoogland 2013).

Bison are large-bodied ungulates that historically could be found throughout the NGP. Commonly referred to as “buffalo”, bison live in herd groups. Mature males spend most of the year living alone (Fischer 1967), and rejoin the large, mixed herds – containing mature cows and juveniles – during the breeding season (Hanson 1984). Bison change plant community structure through their indiscriminate grazing that promotes the growth of forbs, increases the amount of litter turned to soil, and increases the overall plant species richness. (Knapp et al. 1999).

Although indigenous humans have inhabited and been a part of the Great Plains ecosystem for millennia, human impacts increased dramatically in the last two centuries. Throughout the 19<sup>th</sup> century, Euro-American settlers expanded into the western U.S., building railroads and towns and plowing grassland to develop crop fields. Prairie dogs were quickly considered a nuisance species because they burrowed through potential farm- and ranchland and interfered with the placement of railroads (Wuerthner 1997, Miller et al. 2007). Bison, through hunting for their hides by Euro-American settlers, were reduced to near extinction. Bison populations experienced a massive bottleneck in

the late 19<sup>th</sup> century, with their numbers reduced from millions to only several hundred in a matter of decades (Halbert et al. 2006).

Loss or dramatic reduction in herbivore communities was only one of the fundamental changes that occurred with the arrival of Euro-American settlers. Fire, the other major, natural disturbance prevalent in grasslands was also suppressed. In addition, Europeans brought with them new plant species, many of which became established on the landscape (Dunn 1985). With seeds accidentally winding up in agricultural materials or products, humans aided in the spread of non-native plants across the U.S. (Guggisberg et al. 2012). These non-native species were able to thrive in their new environment, with many becoming established as exotic invasive species (Messersmith and Lym 1983). One exotic invasive species that is now prevalent in the NGP is leafy spurge (*Euphorbia esula*).

The NGP looks drastically different today than it did when settlers first moved here, with the majority of open space being converted to agricultural lands. Some portions of the landscape, however, remain less altered by human activities and give us a glimpse into the past. Theodore Roosevelt National Park (TRNP), although developed and ranched before its establishment as a National Park, is one such area that is working to restore natural ecology.

#### *Theodore Roosevelt National Park*

Located in southwestern North Dakota, TRNP provides a remnant of prairie grassland and badlands topography. TRNP (28,508.8 total hectares) was established in 1947 as Theodore Roosevelt Memorial Park and gained National Park status in 1978.

According to their purpose statement, Theodore Roosevelt National Park “...memorializes Theodore Roosevelt and pays tribute to his enduring contribution to the conservation of our nation’s resources by preserving and protecting the scenery, wildlife, and wilderness qualities of the North Dakota Badlands – the landscape that inspired Roosevelt and still inspires visitors today” (NPS 2014a). During its designation in 1978, 12,108.1 hectares of the park were established as Theodore Roosevelt Wilderness. The park comprises three, geographically separate units that all lie along the Little Missouri River corridor. The South Unit, off Interstate-94 in Billings County, is the largest of the units (Figure 1). Encompassing 18,756 hectares, the South Unit receives most visitors each year and contains resident bison, numerous prairie dog colonies, multiple species of wildlife, and a demonstration herd of feral horses. The North Unit, located off Highway-85 in McKenzie County (about 80 km north of the South Unit), is next in size (Figure 2). At around 9,741 hectares, the North Unit is a more rugged landscape that is also home to bison, a demonstration herd of longhorn cattle, prairie dogs, and other wildlife. Nearly the entirety of the North Unit is designated wilderness. The Elkhorn Ranch unit, also located in Billings County (about halfway between the north and south units) is the smallest unit at only 88.2 hectares and has no large resident wildlife; however, the Elkhorn Ranch is plagued with a large and difficult to control patch of leafy spurge.

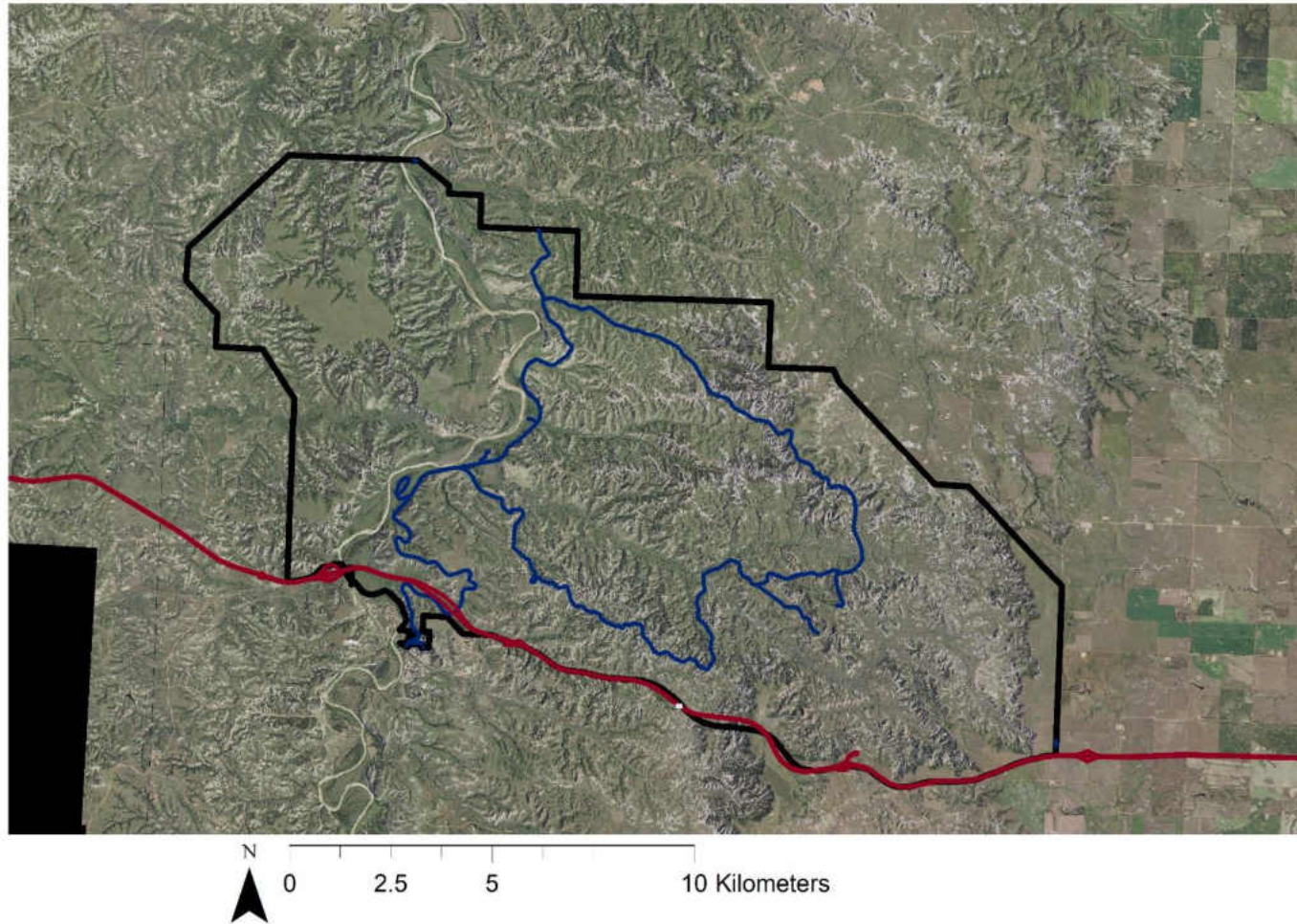


**Figure 1:** A map of the South Unit of Theodore Roosevelt National Park (TRNP) located in Billings County, North Dakota. The park boundary is depicted by the black outline, the local park road is shown in blue, and the United States Interstate 94 is shown in red.

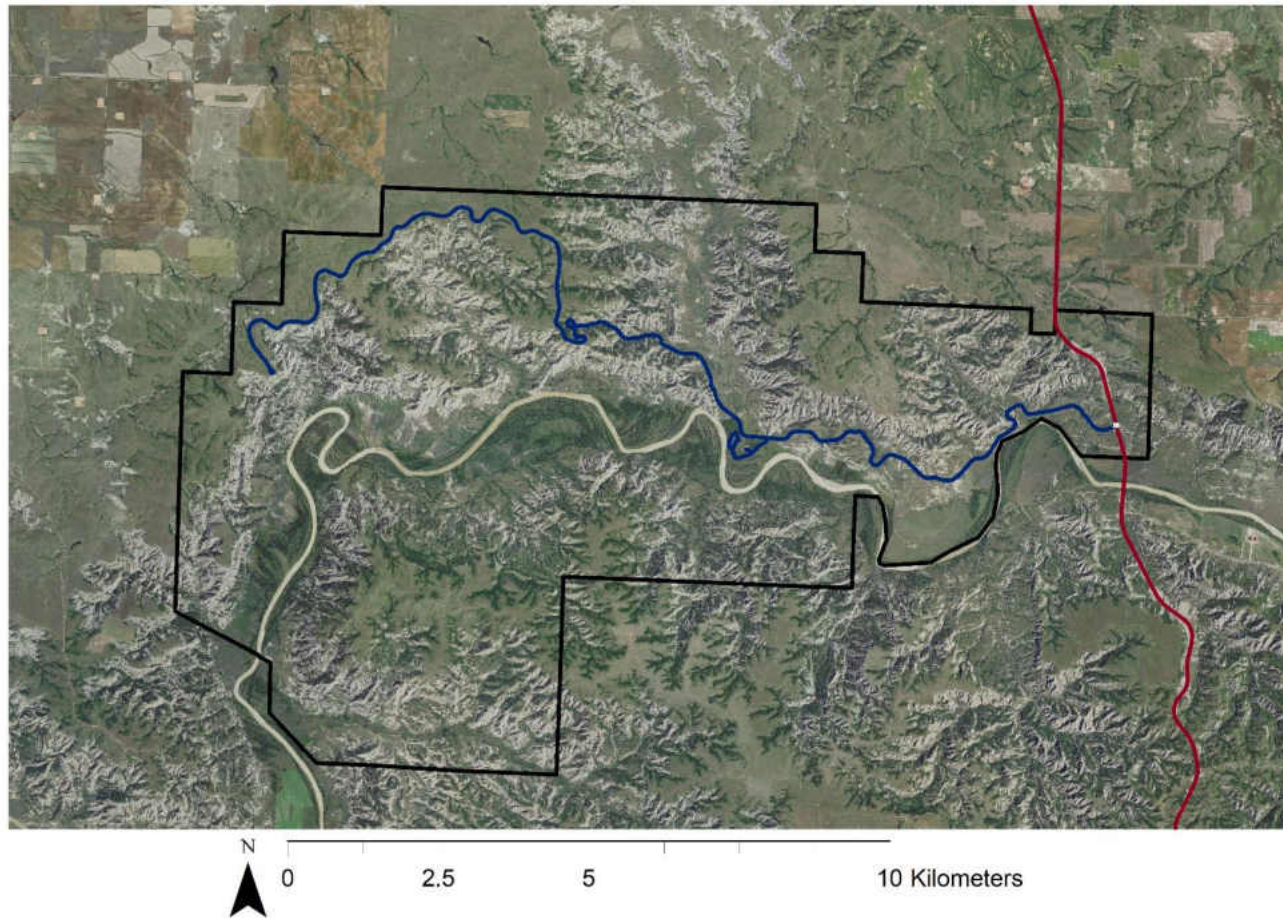


**Figure 2:** A map of the North Unit of Theodore Roosevelt National Park (TRNP) located in McKenzie County, North Dakota. The park boundary is depicted by the black outline, the local park road is shown in blue, and the North Dakota State Highway 85 is shown in red.

TRNP is located in the semi-arid region of North Dakota known for its topography and geologic features. Surrounded by the Little Missouri National Grasslands and privately-owned ranchland, TRNP managers strive to preserve the landscape in as similar of conditions to the 1800s as possible (NPS 1987). The restoration and preservation of natural areas such as TRNP is considered by some to be the single most important environmental effort scientists and managers can make for the future (Schramm 1990). The park maintains two conservation herds of bison, – numbering between 100 and 300 in the North Unit, and 300 and 500 in the South Unit – and is inhabited by a variety of other species, including around 18 prairie dog colonies of various sizes that cover approximately 485.6 hectares, elk, white-tail and mule deer, pronghorn antelope, a demonstration herd of around 150 feral horses, and many species of small mammals, birds, insects, plants, etc.

One of the factors preventing TRNP from occupying the natural state that Theodore Roosevelt himself enjoyed is the presence of exotic invasive plants. Leafy spurge grows throughout all three units of the park in all habitat types but can most commonly be found near stream beds and drainages (Anderson et al. 1996). Leafy spurge plagues the park and grows uncontrollably, choking out native vegetation and reducing forage for the herbivores that live there. Leafy spurge is not palatable to grazing wildlife because of the ingenol that is found in the latex of the plant, that acts as an irritant and can cause severe harm in the digestive system (Kronberg et al. 1993, Lym 1998). Established invasive plants have the potential to reduce forage by up to 75% in some instances (Lym and Messersmith 1985). This is not sustainable for wildlife such as bison,



and demonstration herds of feral horses and longhorn cattle that are confined to the park by the boundary fence.

Managers and scientists at TRNP have tried various control methods for eradicating invasive plants from natural areas. Mowing and manual removal have proven to be ineffective for leafy spurge. Currently, TRNP employs the use of various herbicides such as and Perspective® (Aminocyclopyrachlor) for leafy spurge as their primary control method. Additionally, flea beetles (*Aphthona* spp.) are used and have been successful as a biological control method. However, the success of control operations heavily relies on the ability to detect the plants in the first place.

### *The Rise of Remote Sensing*

Finding features of interest, such as invasive plants, in a national park with vast wilderness and roadless areas remains difficult, but remote sensing has the potential to help. Currently, employees travel by vehicle or by foot to locate features, but this leaves much undetected. With the increased availability of lower-cost high resolution imagery, remote sensing is being increasingly looked at as a viable method for surveillance (Lillesand et al. 2015). Remote sensing – which is any non-contact data collection method – allows researchers the possibility to detect and measure features over broader scales than they would be able to achieve from the ground (Whitehead and Hugenholtz 2014).

Remotely sensed data are characterized by their spatial, spectral, and temporal resolutions. Spatial resolution refers to the scale of the image and the size of the individual pixels in terms of their ground resolution, spectral resolution refers to the color

information contained within the imagery, and temporal resolution refers to the frequency of image acquisition (Liang et al. 2012). The “standard” spectral resolution includes the visible (to humans) red, green, and blue (RGB) wavelengths of light; this produces an image very similar to what humans can see. Multispectral resolution requires sensors (i.e. cameras) that can capture more than the standard 3-band RGB spectrum. Choosing the appropriate spatial resolution for remote sensing data requires an understanding of the size of the feature of interest and the amount of information needed (Atkinson and Curran 1997).

Remote sensing stepped into the global spotlight during the race to space in the mid-1900s and has evolved rapidly since then. Landsat-1 was launched in 1972 and became the first digital, civilian spaceborne remote sensor (Lulla et al. 2012). Landsat was groundbreaking, as it was equipped with a multispectral sensor (green, red, infrared 1, and infrared 2 bands) that took photos with 80-meter ground resolution (Williams et al. 2006). More than 40 years later, remote sensing via space technology has rapidly expanded; high resolution data can be acquired from satellites at more inexpensive prices than at the technology’s birth (Poli and Toutin 2012). Prior to the expansion of satellite imagery, manned aircraft surveys were considered the standard for remote sensing, however, now the gap in data quality is rapidly closing as many satellites have hyperspectral sensors that produce very high (sub-meter) resolution imagery (Toth and Jozkow 2016).

The development and subsequent rise of unmanned aircraft systems (UAS) offers another a potential method for obtaining even higher resolution imagery. UAS share some of the same benefits associated with satellite and manned aerial data collection but

have potentially greater flexibility and cost-savings (Koh and Wich 2012). UAS are now widely used in various applications including general mapping, detection of features, wildlife surveys and conservation, and overall landscape dynamics (Whitehead et al. 2014). For detection of invasive plants, UAS have shown promise for detection only under specific circumstances (Alvarez-Taboada et al. 2017). The potential for using UAS within the national park system, particularly TRNP, is appealing because they are thought to be low-impact systems that are unlikely to affect animal behavior or visitor experiences. UAS are currently banned for public use and may only be used under special circumstances such as search and rescue efforts or scientific research (NPS 2014b).

Image acquisition is just the first step in the application of remote sensing technology. Useful information must then be extracted from the imagery. Traditional computational analysis of remotely sensed imagery employs pixel-based classification, typically performed in a software such as ArcGIS (Environmental Systems Research Institute, Redlands, CA). Pixel-based classification relies on variations between pixels within the image and can use unsupervised or supervised methods. Unsupervised classification refers to a “hands-off” approach, where the only information the computer receives from the user is how many classes are desired. The program then works to cluster pixels into separate groupings using a statistical clustering algorithm based on the available spectral bands for the desired number of classes to produce a classified image. Supervised classification requires the user to specify the desired number of classes and creates specific representative samples for the program to match. The computer analyzes the spectral composition within the training set to estimate the probability distribution of values for each class, then matches similar pixels to the samples. Many different

supervised pixel-based classification algorithms have been developed: maximum likelihood, random forest, and support vector machines (SVM) (Khatami et al. 2016). However, any pixel-based approaches are insufficient when the most accurate classification relies on contextual information such as shape, texture, and spatial characteristics (Gupta and Bhadauria 2014).

Object-based image analysis (OBIA) was developed to overcome the limitations of pixel-based classifications. Rather than use only information contained in individual pixels, OBIA attempts to create and classify meaningful objects by grouping pixels together (Blaschke et al. 2014). Accuracy when using OBIA for vegetation classification is highly dependent on factors such as sample size, quality, and the distribution of vegetation on the ground (Yu et al. 2006). Classifications derived using OBIA in software such as eCognition Developer (Trimble, Inc., Sunnyvale, CA) tend to produce more accurate classifications than pixel-based methods (Blaschke 2010). This extra information comes at a price, however, since processing time and computational requirements are much greater; in addition, the price and complexity of the software involved in producing these types of classifications can deter potential users.

Although remote sensing has the potential to answer many questions that will inform ecological management, it is known to be highly context specific (Whitehead and Hugenholtz 2014). Detection of certain plants yields the best results only if the imagery were taken at the correct phenological stage (Müllerova et al. 2017). Using remote sensing to monitor biodiversity depends heavily on indirect approaches to identification (Turner et al. 2003). The use of remote sensing in combination with the above image classification methods has not been tested for fine-scale detection and mapping of

invasive plants, vegetation communities, and prairie dog colonies – all of which are important for managers at TRNP. Problem-specific data and experiments are needed to answer these ecological questions, which is what I aim to provide in this thesis.

### *Objectives of Study*

The purpose of this research is to provide insight on how remote sensing can best aid in meeting management objectives at Theodore Roosevelt National Park. Specifically, I hope to evaluate the use of unmanned aircraft systems (UAS) in combination with computational analyses such as pixel-based classification in ArcGIS and OBIA in eCognition. I will test the accuracy of these remote sensing techniques to detect, classify, and map invasive plants, vegetation communities, and prairie dog colonies. This will be addressed through the following objectives:

1. Detect, classify, and map leafy spurge using imagery obtained by UAS and analyzed computationally, compare results with established ground-truthed data, and create a unit-wide map of occurrence.
2. Define and map vegetation community structure using imagery obtained by UAS and analyzed computationally.
3. Detect, classify, and map prairie dog mounds and colonies using imagery obtained by UAS and analyzed computationally and compare results with established ground-truthed data by creating colony perimeters.

## LITERATURE CITED

- Alvarez-Taboada, F., C. Paredes, et al. (2017). "Mapping of the Invasive Species *Hakea sericea* Using Unmanned Aerial Vehicle (UAV) and WorldView-2 Imagery and an Object-Oriented Approach." *Remote Sensing* 9(9): 913.
- Anderson, G. L., J. Everitt, et al. (1996). "Mapping leafy spurge (*Euphorbia esula*) infestations using aerial photography and geographic information systems." *Geocarto International* 11(1): 81-89.
- Anderson, R. C. (2006). "Evolution and Origin of the Central Grassland of North America." *Journal of the Torrey Botanical Society* 133(4): 21.
- Atkinson, P. M. and P. J. Curran (1997). "Choosing an appropriate spatial resolution for remote sensing investigations." *Photogrammetric engineering and remote sensing* 63(12): 1345-1351.
- Barker, W. T. and W. C. Whitman (1988). "Vegetation of the Northern Great Plains." *Rangelands* 10(6).
- Blaschke, T. (2010). "Object based image analysis for remote sensing." *ISPRS Journal of Photogrammetry and Remote Sensing* 65(1): 2-16.
- Blaschke, T., G. J. Hay, et al. (2014). "Geographic Object-Based Image Analysis - Towards a new paradigm." *ISPRS J Photogramm Remote Sens* 87(100): 180-191.
- Coppock, D. L., J. Ellis, et al. (1983). "Plant-herbivore interactions in a North American mixed-grass prairie. II. Responses of bison to modification of vegetation by prairie dogs." *Oecologia*: 10-15.

- Crosby, L. A. and R. Graham (1986). Population Dynamics and Expansion Rates of Black-Tailed Prairie Dogs. Proceedings of the Twelfth Vertebrate Pest Conference.
- Detling, J. K. (1998). "Mammalian herbivores: ecosystem-level effects in two grassland national parks." *Wildlife Society Bulletin* 26(3).
- Dunn, P. H. (1985). "Origins of leafy spurge in North America." *Weed Science* 2(3).
- Fischer, W. A. (1967). Observations on Behavior of Lone Bull Bison. Proceedings of the Iowa Academy of Science.
- Fuhlendorf, S. D. and D. M. Engle (2001). "Restoring Heterogeneity on Rangelands: Ecosystem Management Based on Evolutionary Grazing Patterns." *BioScience* 51(8).
- Gibson, D. J. (1989). "Effects of Animal Disturbance on Tallgrass Prairie Vegetation." *The American Midland Naturalist* 121(1).
- Guggisberg, A., E. Welk, et al. (2012). "Invasion history of North American Canada thistle, *Cirsium arvense*." *Journal of Biogeography* 39(10): 1919-1931.
- Gupta, N. and H. S. Bhadauria (2014). "Object based Information Extraction from High Resolution Satellite Imagery using eCognition." *International Journal of Computer Science Issues* 11(3).
- Halbert, N. D., P. J. P. Gogan, et al. (2006). "Where the Buffalo Roam: the Role of History and Genetics in the Conservation of Bison on U.S. Federal Lands." *Park Science* 24(2).

- Hanson, J. R. (1984). "Bison Ecology in the Northern Plains and a Reconstruction of Bison Patterns for the North Dakota Region." *Plains Anthropologist* 29(104).
- Hoogland, J. (2013). *Conservation of the black-tailed prairie dog: saving North America's western grasslands*, Island Press.
- Khatami, R., G. Mountrakis, et al. (2016). "A meta-analysis of remote sensing research on supervised pixel-based land-cover image classification processes: General guidelines for practitioners and future research." *Remote Sensing of Environment* 177: 89-100.
- Knapp, A. K., J. M. Blair, et al. (1999). "The Keystone Role of Bison in North American Tallgrass Prairie." *BioScience* 49(1).
- Koh, L. P. and S. A. Wich (2012). "Dawn of drone ecology: low-cost autonomous aerial vehicles for conservation." *Tropical Conservation Science* 5(2).
- Kronberg, S. L., R. B. Muntifering, et al. (1993). "Cattle avoidance of leafy spurge: A case of conditioned aversion." *Journal of Range Management* 46.
- Li, M. and X. Guo (2014). "Long Term Effect of Major Disturbances on the Northern Mixed Grassland Ecosystem—A Review." *Open Journal of Ecology* 04(04): 214-233.
- Liang, S., X. Li, et al. (2012). *Advanced Remote Sensing: Terrestrial Information Extraction and Applications*, Elsevier Science.
- Lillesand, T., R. W. Kiefer, et al. (2015). *Remote sensing and image interpretation*, John Wiley & Sons.



- Lulla, K., M. D. Nellis, et al. (2012). Celebrating 40 years of Landsat program's Earth observation accomplishments, Taylor & Francis.
- Lym, R. G. (1998). "The Biology and Integrated Management of Leafy Spurge (*Euphorbia esula*) on North Dakota Rangeland." *Weed Technology* 12(2).
- Lym, R. G. and C. G. Messersmith (1985). "Leafy Spurge Control with Herbicides in North Dakota: 20-Year Summary." *Journal of Range Management* 38(2).
- McMillan, N. A. (2017). "Plant Community Responses to Bison Reintroduction within Montana's Northern Great Plains." *Wildlife and Fisheries Biology*, Clemson University. Master of Science.
- Messersmith, C. G. and R. G. Lym (1983). "Distribution and Economic Impacts of Leafy Spurge in North Dakota." *North Dakota Farm Research* 40.
- Milchunas, D. G., O. E. Sala, et al. (1988). "A Generalized Model of the Effects of Grazing by Large Herbivores on Grassland Community Structure."
- Miller, B. J., R. P. Reading, et al. (2007). "Prairie Dogs: An Ecological Review and Current Biopolitics." *Journal of Wildlife Management* 71(8): 2801-2810.
- Müllerová, J., J. Brůna, et al. (2017). "Timing Is Important: Unmanned Aircraft vs. Satellite Imagery in Plant Invasion Monitoring." *Frontiers in Plant Science* 8(887).
- National Park Service. (1987). "General Management Plan: Theodore Roosevelt National Park."

- National Park Service. (2014a). "Foundation Document: Theodore Roosevelt National Park."
- National Park Service. (2014b). "Director's Order: Policy Memorandum 14-05. N. P. Service. 36 CFR."
- Poli, D. and T. Toutin (2012). "Review of developments in geometric modelling for high resolution satellite pushbroom sensors." *The Photogrammetric Record* 27(137): 58-73.
- Schramm, P. (1990). "Prairie restoration: a twenty-five year perspective on establishment and management." *Proceedings of the Twelfth North American Prairie Conference, University of Northern Iowa Cedar Fall, Iowa.*
- Theodore Roosevelt National Park. (1987). "General management plan, development concept plans, land protection plan, environmental assessment: Theodore Roosevelt National Park, North Dakota." [Washington, D.C.?], U.S. Dept. of the Interior, National Park Service.
- Toth, C. and G. Józków (2016). "Remote sensing platforms and sensors: A survey." *ISPRS Journal of Photogrammetry and Remote Sensing* 115: 22-36.
- Watts, A. C., W. S. Bowman, et al. (2008). "Unmanned Aircraft Systems (UASs) for Ecological Research and Natural-Resource Monitoring (Florida)." *Ecological Restoration* 26(1).

Whitehead, K. and C. H. Hugenholtz (2014). "Remote sensing of the environment with small unmanned aircraft systems (UASs), part 1: a review of progress and challenges." *Journal of Unmanned Vehicle Systems* 2.

Whitehead, K., C. H. Hugenholtz, et al. (2014). "Remote sensing of the environment with small unmanned aircraft systems (UASs), part 2: scientific and commercial applications." *Journal of Unmanned Vehicle Systems* 2.

Williams, D. L., S. Goward, et al. (2006). "Landsat." *Photogrammetric Engineering & Remote Sensing* 72(10): 1171-1178.

Wuerthner, G. (1997). "Viewpoint: The black-tailed prairie dog - headed for extinction?" *Journal of Range Management* 50.

Yu, Q., P. Gong, et al. (2006). "Object-based Detailed Vegetation Classification with Airborne High Spatial Resolution Remote Sensing Imagery " *Photogrammetric Engineering & Remote Sensing* 72(7).

## CHAPTER II

### DETECTING AND MAPPING INVASIVE PLANTS IN THEODORE ROOSEVELT NATIONAL PARK

#### INTRODUCTION

Invasive plants remain one of the largest ecological problems across the globe because of the negative impacts they impose on functioning ecosystems (Vila et al. 2011). Invasive plants outcompete native species that provide vital food and nutrients for herbivores and pollinators, and they reduce overall plant species richness and biodiversity (Butler and Cogan 2004). In addition, exotic plant invasions have devastating global economic impacts (Pimentel et al. 2000). Once established, invasive exotics become difficult to control, allowing them to turn large areas of land into homogenous communities. These invasions become especially damaging when they occur in natural systems such as Theodore Roosevelt National Park (TRNP), where native species may still be well-represented, and ecological interactions intact. Invasives have the greatest potential for disruption in places that retain their original structure.

Leafy spurge (*Euphorbia esula*) has been identified as a serious concern not only in TRNP and other national parks (D'Antonio et al. 2004), but also in the entire Northern Great Plains (NGP) region (Lym and Messersmith 1985). In the early 1900s, homesteaders expanding westward brought a plethora of non-native vegetation with them, including leafy spurge (Stitt 2006). These introductions were often unintentional, with plants being brought over inadvertently in agricultural products such as hay or ship

ballasts (Messersmith and Lym 1983, Dunn 1985). Once in the new environment, these plants spread rapidly through seed contamination of agricultural equipment (Best et al. 1979), as well as via seed dispersal that was propagated by wild and domesticated animals, insects, waterways, and areas of development such as roads (Messersmith and Lym 1985).

Leafy spurge, a deep-rooted perennial weed, is one of the most abundant invasive plants in the NGP and infests roughly two million hectares of public and private land (Quimby and Wendel 1997), incurring a cost of \$34.5 billion to the U.S. economy (Pimentel et al. 2005). As of the year 2000, leafy spurge was estimated to cover between 5 – 10% of the south unit of TRNP and is extremely visible to park visitors (O’Neill et al. 2000).

Because of its overall hardiness, abundance in disturbed areas, and ability to rapidly infiltrate patches of native plants, leafy spurge has historically been difficult to control (Dunn 1979). Management success depends heavily on the stage of invasion, so managers and scientists must be able to detect and map these species before they become established. In addition, managers are looking for safe, cost-effective, and accurate tools for detection and mapping.

With advances in technology and increasing availability of high-resolution imagery, remote sensing has the potential to be a valuable management tool (Turner et al. 2003). Remotely sensed data are often limited by image quality, spectral composition, spatial resolution, sampling frequency in relation to flowering phenology – which has a large impact on detectability – and cost. I will test the utility of two data sources for detecting and mapping leafy spurge, including imagery from manned flights for the

National Agriculture Imagery Program (NAIP) and imagery from a fixed-wing unmanned aircraft system (UAS). Current NAIP products achieve 60 cm resolution and statewide coverage, whereas low altitude UAS imagery has a much higher spatial resolution of 2 to 3 cm but limited spatial extent (i.e. 0.5 – 3 km<sup>2</sup> per flight, depending on altitude and flight duration). Both of these data sources provide similar spectral composition using common sensors, such as affordable consumer-grade digital cameras (typically three spectral bands including red-green-blue, or RGB). Both may also contain a near infrared band that is commonly used for crop assessment.

Previous attempts to map leafy spurge in TRNP using aerial photography and light reflectance had limited success (Everitt and Anderson 1995); detections were only possible if patches of leafy spurge were large and already covered areas of at least 2.8 meters. Hyperspectral satellite imagery has also been tested for its utility in the detection of leafy spurge, often at lower resolutions than aerial imagery, and exhibited mixed results (Lawrence et al. 2006, Mairota et al. 2015). The limitations of these projects were similar, with small patches of leafy spurge remaining undetected. High resolution imagery that can be obtained through unmanned aircraft systems (UAS) promises a practical solution at detecting small patches of leafy spurge that offers cost-effective and flexibly timed data collection (Alvarez-Taboada et al. 2017).

Large volumes of data produced by remote sensors require efficient and accurate analytical methods to be useful for detecting features of interest, such as invasive plants. In addition to comparing UAS imagery to NAIP imagery, I will also compare two different computational approaches that have been used for image classification. Anderson et al. (1996) used a suitability analysis to create maps of leafy spurge in TRNP

based on aerial photography. Traditional approaches to classification have employed pixel-based classifiers, such as maximum likelihood and support vector machines (SVM) in ArcGIS (Khatami et al. 2016). The latter methods are both examples of supervised classification, for which an investigator provides examples of the features of interest within an image (the training set) on which to base computer classification of the entire image. Pixel-based methods attempt to match the spectral composition of individual pixels to properties of individual pixels in the training set. Alternatively, object-based image analysis (OBIA) attempts to account for additional information contained within the images that is not available in pixel-based classification techniques (Blaschke et al. 2014) such as size, shape, and texture of real-world objects, all of which are seen at a higher level than individual pixels. I used the software eCognition (version 9.1.2, Trimble 2015) for OBIA.

In this chapter, I will evaluate the use of remote sensing for invasive plant classification. Specifically, I will classify and map leafy spurge within TRNP based on NAIP imagery and UAS imagery and identify whether pixel-based classifications in GIS or OBIA in eCognition are more accurate at detection, and therefore which method produces the least error.

## METHODS

### *Study Area*

We obtained UAS imagery during the summer of 2018 in TRNP, located in the semi-arid region of southwestern North Dakota. TRNP is comprised of three geographically separate units. The largest unit, the South Unit, is located in Billings County and is approximately 18,756 hectares in size. One site of interest, the Talkington

trailhead, has a long-standing leafy spurge infestation and we selected that site for testing the utility of UAS imagery for mapping leafy spurge.

### *Data Acquisition*

In 2018, a University of North Dakota (UND) research crew from the Department of Biology flew a fixed-wing Trimble UX5 UAS at selected sites in TRNP, including Talkington. Flights occurred in late June to obtain imagery at a time when leafy spurge was flowering and most visible. Flights followed preprogrammed parallel line transects that permitted adequate overlapping photography of ground survey areas. Image overlap was 80%. We conducted flights at 75m and 90m. To facilitate analysis, I analyzed two portions clipped from the full extent photographed. Unmanned aircraft systems flight operations for this research were approved by the National Park Service (Study #THRO-00099, Permit #THRO-2018-SCI-0010). Aerial imagery was obtained from NAIP for 2016 and covers the entirety of both park units; NAIP imagery from 2018 was not included as it was not published at the time of data analysis. All remotely sensed data used in this research are listed in Table 1.



**Table 1: Images used for classification and their temporal, spatial, and spectral characteristics. The full extent of UAS imagery was 0.43 – 0.59 km<sup>2</sup>. The images listed here are two different clips from the full mosaiced image.**

<b>Image</b>	<b>Temporal Resolution</b>	<b>Spatial Resolution</b>	<b>Spatial Extent</b>	<b>Spectral Bands</b>
<b>NAIP</b>				
NUMosaic	June – August 2016	60 cm	97.40 km <sup>2</sup>	R-G-B-NIR
SUMosaic	June – August 2016	60 cm	186.79 km <sup>2</sup>	R-G-B-NIR
<b>UAS imagery</b>				
Talkington75(1)	June 2018	2.21 cm	124 m <sup>2</sup>	R-G-B
Talkington75(2)	June 2018	2.21 cm	898 m <sup>2</sup>	R-G-B
Talkington75NIR(1)	June 2018	2.35 cm	124 m <sup>2</sup>	R-G-NIR
Talkington75NIR(2)	June 2018	2.35 cm	124 m <sup>2</sup>	R-G-NIR
Talkington90(1)	June 2018	2.71 cm	124 m <sup>2</sup>	R-G-B

### *Image Classification*

The overall image classification workflow was structured in three main parts: data pre-processing, classification, and validation (Figure 3). All of the above steps were used for classifications performed in ArcGIS as well as eCognition. I created subsets of the Talkington image into two smaller portions to reduce processing time as seen in Figure 4.

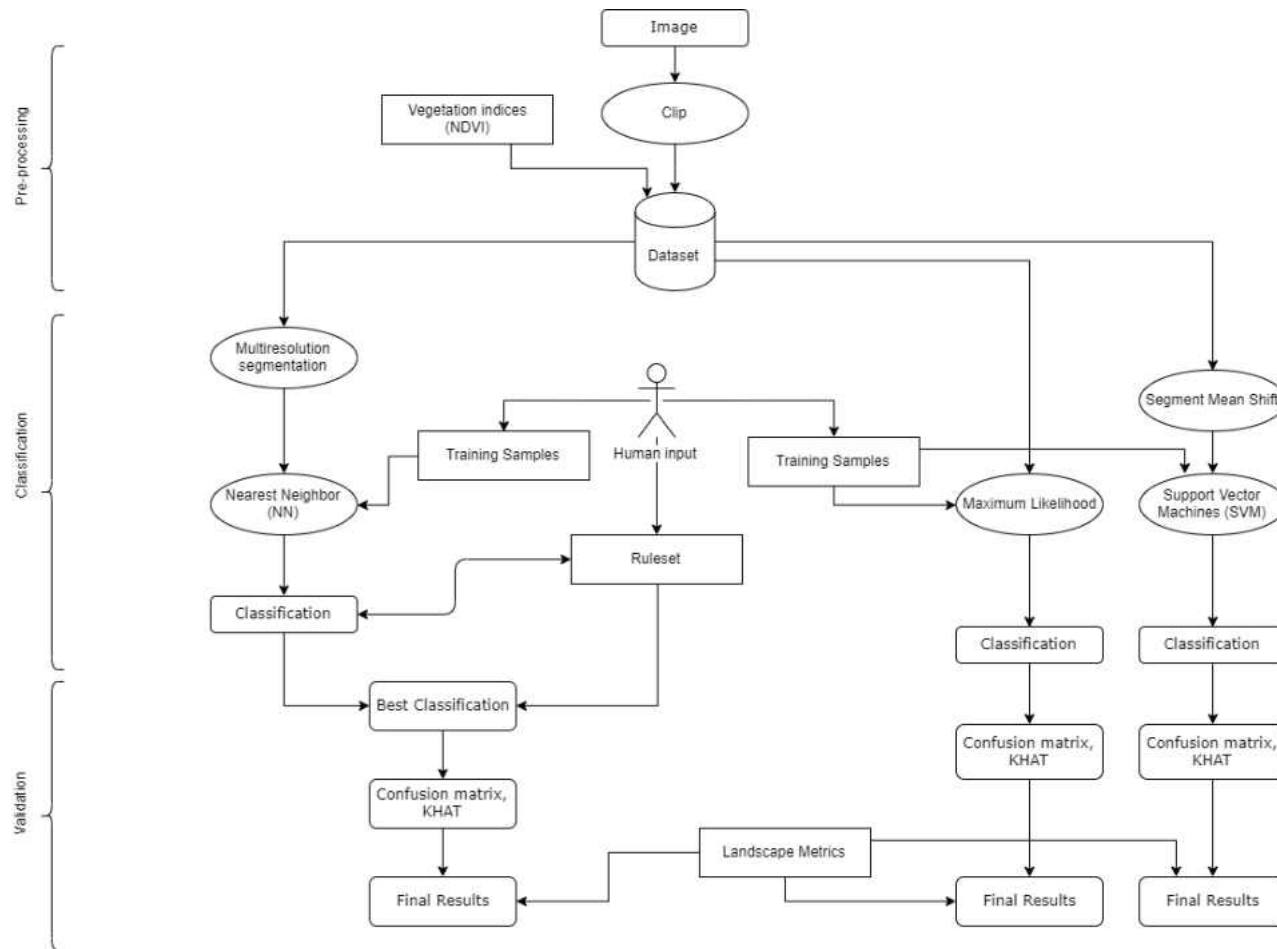


**Figure 3:** Summary of image classification workflow: images are processed (top) and fed through the desired classifier (center branches), the researcher creates training samples and rulesets (rulesets in eCognition only) (center of diagram), error assessments and KHAT statistics are calculated for best classifications (bottom), and landscape metrics are performed to gain further understanding of the system (bottom center).

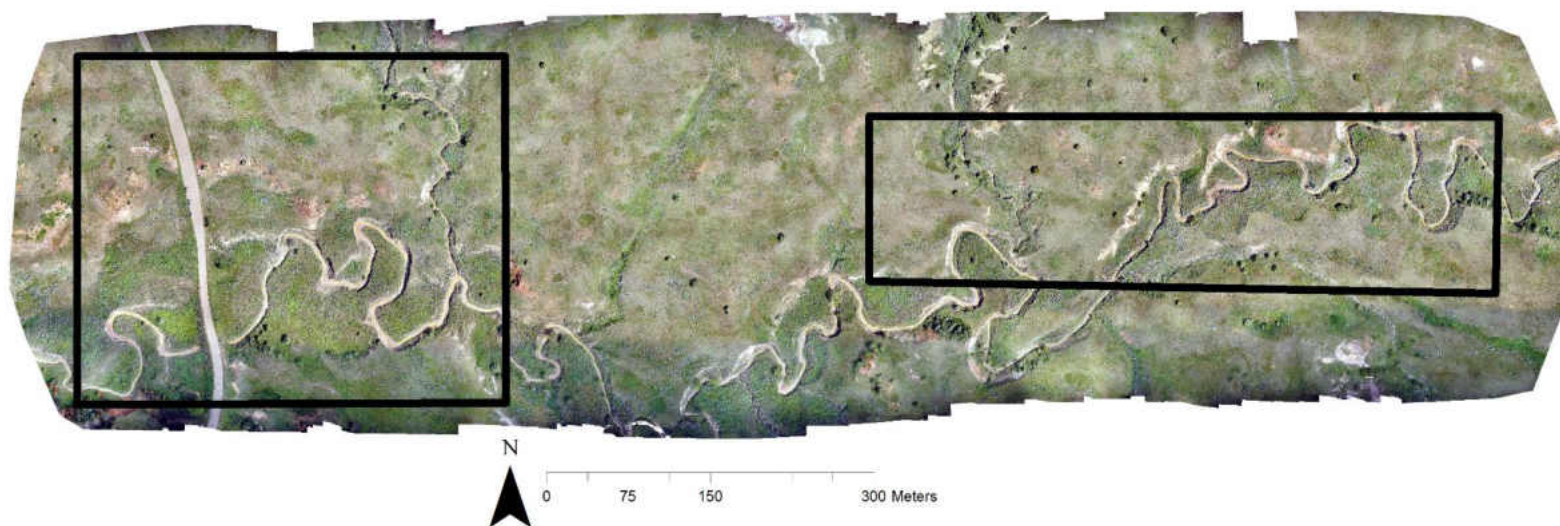


**Figure 4:** Talkington mosaic image collected from low-altitude UAS. Each box represents a small subset that was used for classification via pixel-based and object-based methods. The box on the left corresponds to the Talkington75(1) classifications and the box on the right corresponds to the Talkington75(2) classifications.

I used the image classification tools available in ArcGIS (version 10.6, ESRI) to perform pixel-based classifications of the imagery using supervised methods. I chose maximum likelihood and support vector machine (SVM) classifiers for this purpose. The maximum likelihood classifier is one of the best-known algorithms for supervised image classification and is commonly used for pixel-based classifications (Erdas Inc. 1999). The SVM classifier groups similar pixels based on spectral values and creates pseudo-objects in n-dimensional space (segmentation), which are then used to create training samples (Cortes and Vapnik 1995). A series of segmentations were tested by adjusting the parameters of spectral detail and spatial detail. The final image segmentations were achieved using a spectral detail of 15, spatial detail of 15, minimum segment size of 20, and band indexes of 1, 2, and 3. Multiple training samples were created for each class then merged to form a reliable sample for the whole image. These training samples were then used by the classifier to identify classes that I delineated and assign pixels to the appropriate classes.

I used eCognition Developer (version 9.1.2, Trimble 2015) to perform object-based image analysis (OBIA). A series of segmentations was tested by adjusting the parameters of scale, shape, compactness, and image weighting. Scale adjusts how large or small the desired image objects will be, shape adjusts the relationship between color and shape criteria for the resulting segments, compactness adjusts the overall area of the resulting segments, and image weighting refers to the importance given to each spectral band (El-naggar 2018). I tested the default scale parameter of 10 but this produced segments that were too small and cut features into multiple tiny parts. Additionally, I tested scale parameters of 50 and 100 but these produced segments that were undesirably

large and in that they incorporated multiple features into single segments that were not meaningful. The final image segmentations were achieved using parameters that appeared visually to represent a good compromise between these concerns (scale = 40, image layers (spectral bands) weighted equally, shape = 0.2, and compactness = 0.6). The Nearest Neighbor (NN) classifier was then used to classify objects based on training samples I created. I tested texture as a classification parameter, but the computer was still processing the image after two weeks so this attribute was eliminated from further consideration. Final classification parameters included mean color, brightness, standard deviation, maximum difference, area, shape, and mathematical band indices (Normalized difference vegetation index (NDVI) for images with an NIR spectral band). After initial classification, I examined the output and wrote rules to refine the classification based on misclassified regions. Each new rule had to be tested in an iterative fashion; when I wrote a new rule and it visibly did not resolve a misclassification, I removed that rule and wrote a new one. Commonly attempted rules included relative border, area, image object distance to vector layers, image object distance to other objects, and texture (GLCM quick 8/11). I repeated this process until further changes in the ruleset no longer corrected misclassifications and no additional options remained as indicated by program documentation, my own experience, and computational feasibility.

I ran error and accuracy assessments in the ArcGIS environment for both pixel based and OBIA classification techniques. I created confusion matrices where I examined omission (false negatives) and commission (false positives) errors. ArcGIS calculated a  $K_{HAT}$  (Kappa) statistic for each matrix, which gives an estimate for the measure of actual agreement within a confusion matrix (Congalton and Mead 1983). The Kappa statistic

can be used to show how your classification performs against a completely random classification (Kappa = 0) (Congalton and Green 1999). Since I was attempting to determine the accuracy of a feature of interest with low spatial coverage (leafy spurge), I used equalized accuracy assessments with a minimum of 100 sample points per class. I used this approach because rare-class sample sizes are often so small when using proportional stratified random sampling (Stehman and Foody 2009) and that too few pixels of leafy spurge were included. For equalized accuracy assessments, overall accuracy for the entire classification and Kappa are less informative. Instead, producer's accuracy (measure of omission error) and user's accuracy (measure of commission error) for leafy spurge specifically are better at showing how the classifier performed in the task of identifying leafy spurge.

### *Ground Truthing*

Ground-truthing data were collected in the summer of 2016 at Talkington. National Park Service (NPS) staff using a handheld GPS mapper walked around patches of leafy spurge to create polygons mapping the patch perimeters. The staff classified percent cover of spurge in each patch into broad cover classes as well as a description of the coverage type, i.e. dense, sparse, etc. I compared the classified images obtained using eCognition to the polygons created in the field to see if there was a correlation between on-the-ground and remotely sensed data. I used the *Tabulate Area* tool in ArcGIS to find the percent coverage of leafy spurge on the classified image, within the boundaries of each patch that had been delineated in the field. Then, I used the *Field Calculator* to determine the sum of the area and the percent cover of leafy spurge based on the

classified images, within the field-delimited polygons. I exported percent coverage into R (version 3.5.1, R Core Team 2018) and plotted against the ground-sampled patches.

As a second verification method, I modeled percent cover of spurge from the classified images as a function of the ground truthing coverage, the area of the polygons (hectares), vegetation density characteristics (categorical with four levels: patchy, scattered, uniform, and dense), and interaction terms for area by ground truthing coverage, and vegetation density by ground truthing coverage. I log-transformed percent cover to meet the assumption of normally distributed errors and conducted the analysis in R (version 3.5.1, R Core Team 2018).

### *Entire Unit Map*

The benefit of wider-area coverage available with NAIP imagery is only attainable if the wider area can be efficiently classified. OBIA is much more time-consuming, so for the purposes of my thesis I only classified NAIP imagery using maximum likelihood pixel-based classification. Classes included bare ground, grasses, vegetation of interest, sagebrush, trees, and water. Since the yellow color of leafy spurge cannot be seen in the NAIP images, training samples for leafy spurge were created from knowledge of where it existed on the ground. In the final classification, I called the class that contained leafy spurge “vegetation of interest”, rather than simply “leafy spurge”; because the classifier commonly grouped other vegetation types in as well. This analysis yielded a map of the entire south unit.

I compared a small subset of the NAIP classification with the object-based classification derived from UAS imagery. I used UAS imagery to test the accuracy of the



NAIP classification. Because of its very high resolution, UAS imagery served as a near-ground truth for both image sources. The vegetation of interest class (shown in red) was compared with the leafy spurge class in the UAS classification using 700 validation points (Figure 5).

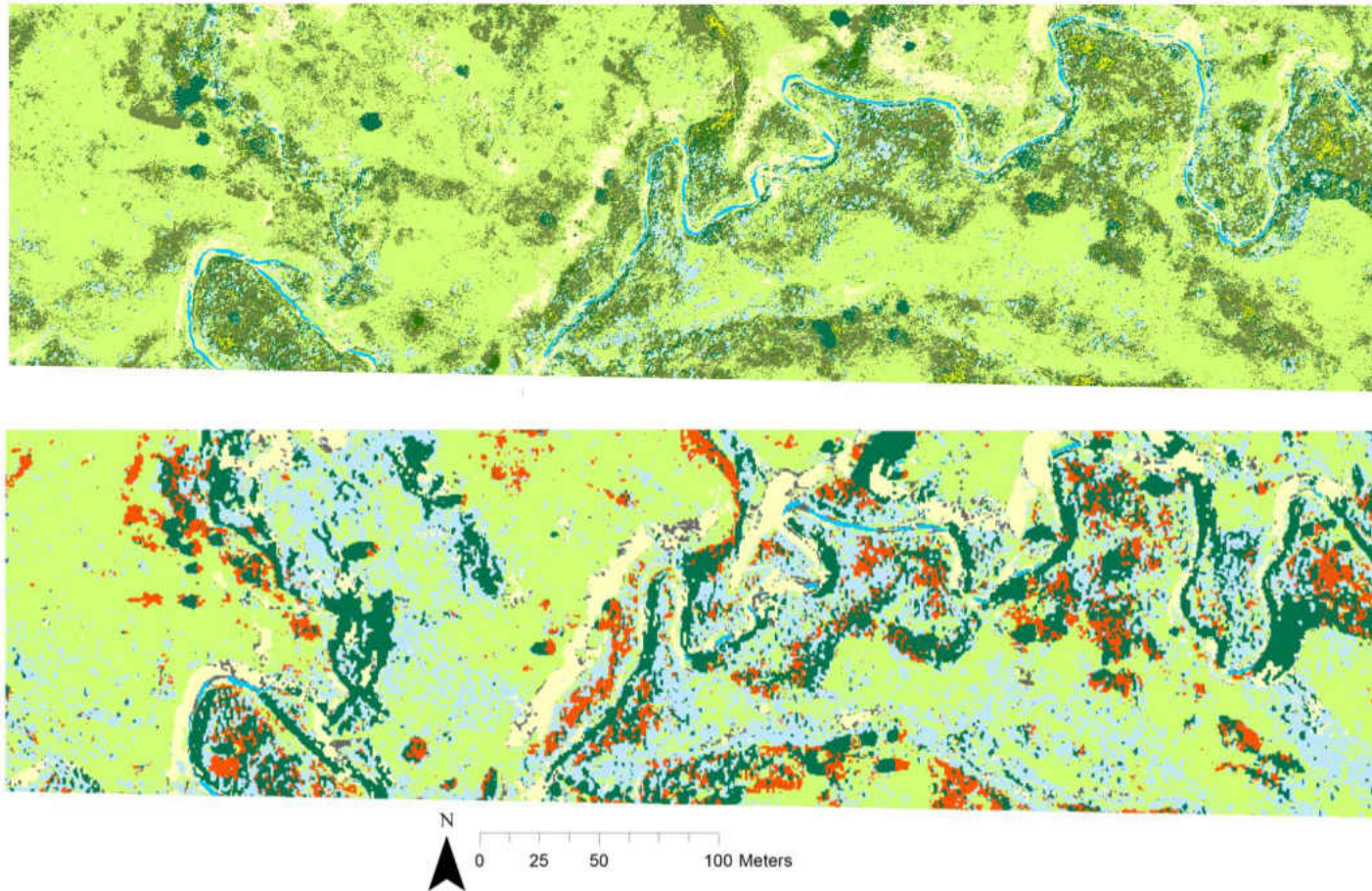


**Figure 5:** Object-based classification performed on an image taken via UAS (top) compared with a pixel-based (maximum likelihood) classification performed on an image taken from NAIP (bottom). The UAS image was used as a near-ground-truth and the two images were compared to gain insight on errors. The red color in the NAIP classification corresponds to the vegetation of interest class and can be compared with the leafy spurge class (yellow) in the UAS classification.

## RESULTS

SVM and maximum likelihood classifications of UAS imagery (Figure 6A) in ArcGIS both yielded limited accuracy for leafy spurge. Errors of omission ranged from 41% to 61%, and errors of commission ranged from 21% to 82%. Light conditions were variable when flights were occurring (i.e. clouds were moving across the sky throughout the day, creating shadows) and the effects of this can be seen in the imagery. SVM is not well-suited to handle variations in light when segmenting the images and created large segments that were not meaningful; grasses, bare ground, water, and leafy spurge were often lumped together into large continuous objects in shadowed areas (Figure 6D). This caused accuracy to decrease. The maximum likelihood classifier seemed to handle variations in light slightly better than SVM, but that was not reflected in accuracy for leafy spurge (Figure 6C).

OBIA classifications of UAS imagery using eCognition produced the classifications with the highest accuracy for detecting leafy spurge (Figure 6B). Errors of omission ranged from 15% to 49%, and errors of commission ranged from 39% to 85%. By all classification modes, UAS images that contained R-G-B bands performed better than images with R-G-NIR. All measures of omission and commission error for leafy spurge for all classification modes can be found in Table 2.

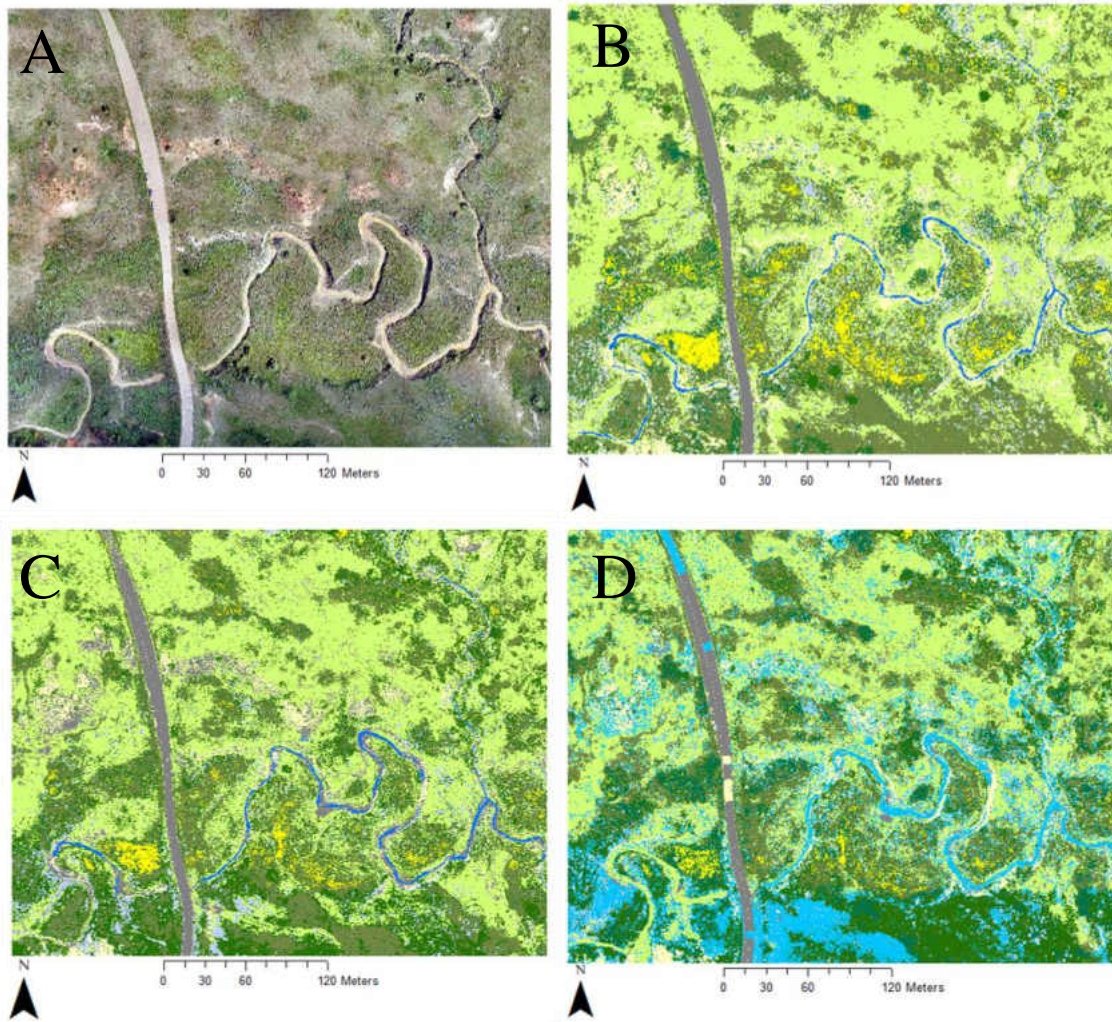


**Figure 6:** A) Talkington75(1) base image used for classification B) Classification produced using OBIA in eCognition C) Classification produced using maximum likelihood in ArcGIS D) Classification produced using SVM in ArcGIS. Classifications of leafy spurge are indicated by the color yellow.

**Table 2: Percent omission and commission error for classifications of Talkington taken via UAS**

<b>Classification Method</b>	<b>No. Accuracy Points</b>	<b>Percent Omission Error</b>	<b>Percent Commission Error</b>
<b>SVM</b>			
Talkington75(1)	111	41%	21%
Talkington75(2)	111	54%	80%
<b>MAXL</b>			
Talkington75(1)	111	44%	26%
Talkington75(2)	111	46%	80%
Talkington75NIR(1)	111	60%	69%
Talkington75NIR(2)	111	61%	82%
Talkington90(1)	111	43%	49%
<b>ECOG</b>			
Talkington75(1)	111	17%	46%
Talkington75(2)	125	15%	54%
Talkington75NIR(1)	111	42%	71%
Talkington75NIR(2)	111	49%	85%
Talkington90(1)	111	24%	39%

Notes: All UAS images are R-G-B unless otherwise stated in the image name. The higher the percentage, the more errors the classifier made.

NAIP images that were classified using maximum likelihood in ArcGIS were not successful at detecting leafy spurge (Figure 7). For the south unit map, errors of omission were only 12%, whereas errors of commission were 92%. This means that leafy spurge was correctly found within the “vegetation of interest” class 88% of the time. However, many other groups – particularly taller vegetation – were also grouped into the “vegetation of interest” classification. This is what produced the 92% commission error. Approximately 10.18% (or 1,877 hectares) of the south unit is covered by this vegetation of interest (Figure 8), which may be an overestimate.

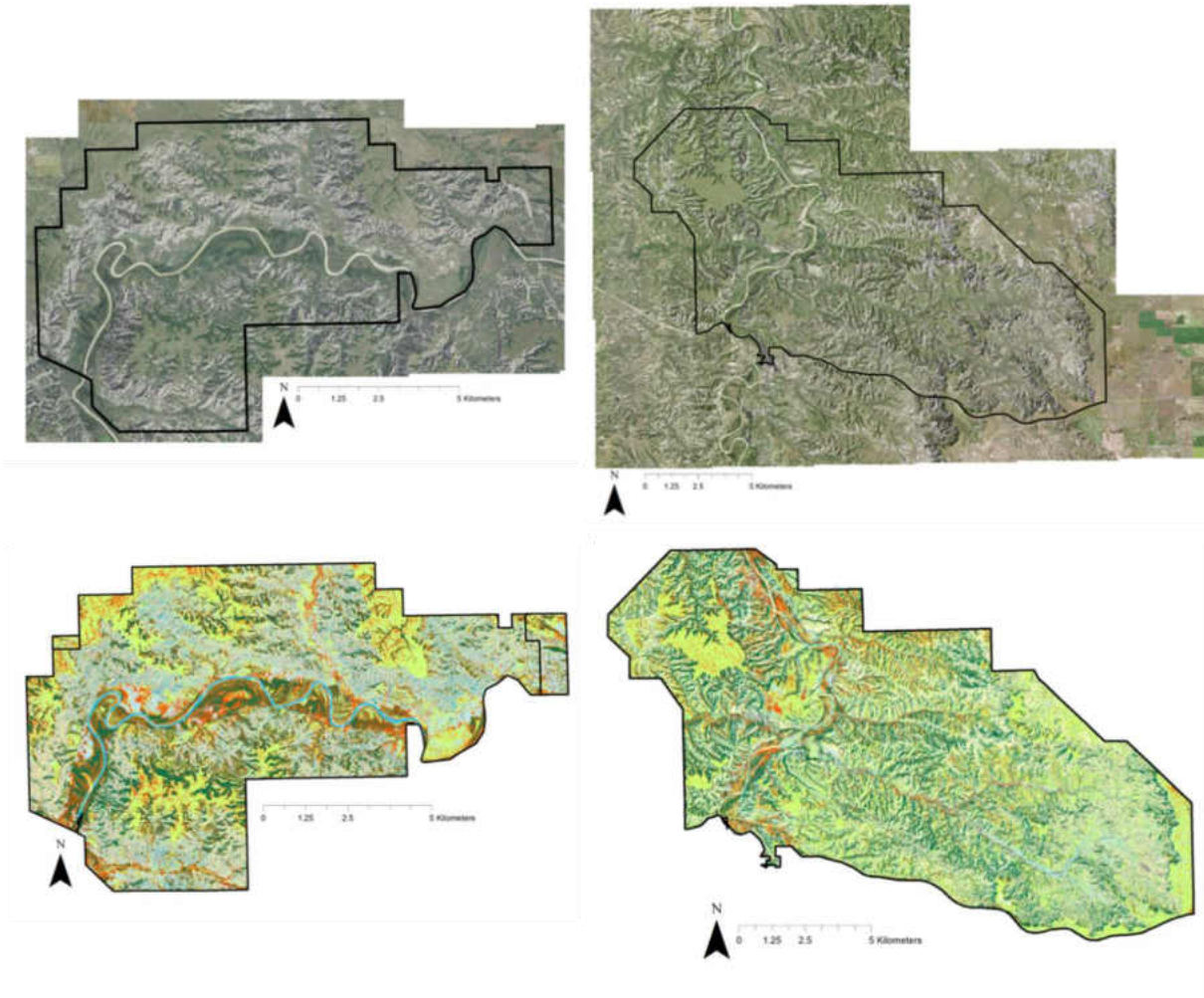


**Figure 7:** Maximum likelihood classifications in ArcGIS of NAIP imagery; North Unit (left) and South Unit (right). Vegetation of interest indicated by the color orange.

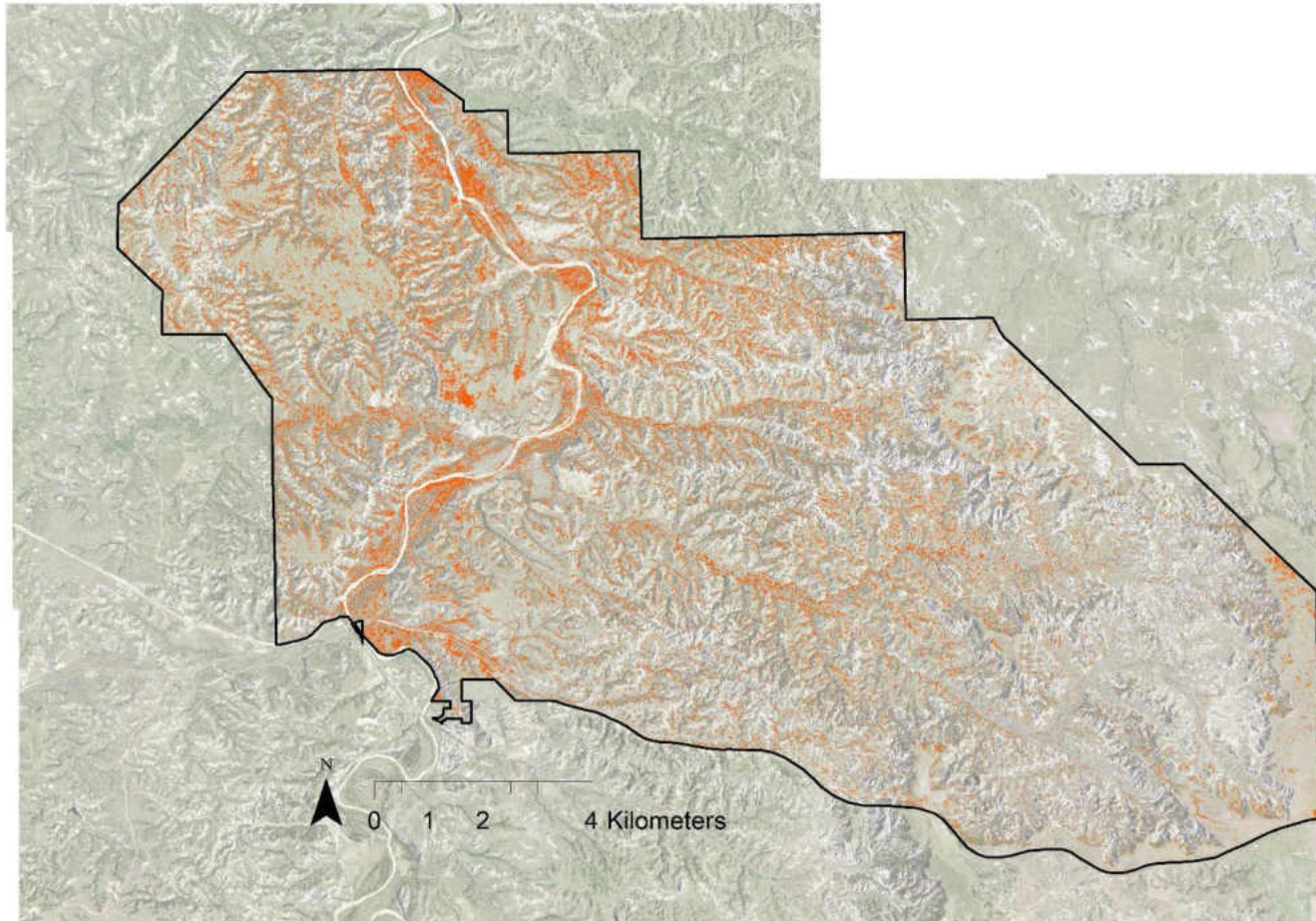


**Figure 8:** Areas identified as “vegetation of interest” shown in the south unit of Theodore Roosevelt National Park. This classification identifies known areas of leafy spurge, but also areas of taller vegetation through error.



Leafy spurge percent cover in UAS images classified in eCognition was moderately correlated with ground truthed data, with the largest correlation coefficient being 0.64 ( $p = 0.00002$ ) for the Talkington90(1) image and the smallest being 0.067 ( $p = 0.68$ ) for the Talkington75(2) image. The NIR images produced lower correlations with ground data, whereas RGB images – aside from Talkington75(2) – produced higher correlations, which can be seen in the scatterplots in Figure 9. In the linear regression model, I was unable to estimate parameters for Dense area classifications since there was only a single observation in the dataset. Area ( $p = 0.0052$ ), and the interaction term for area by ground truthed coverage ( $p = 0.0115$ ) were the only significant terms in the model (Table 3), with Patch Area having a positive effect on classification.

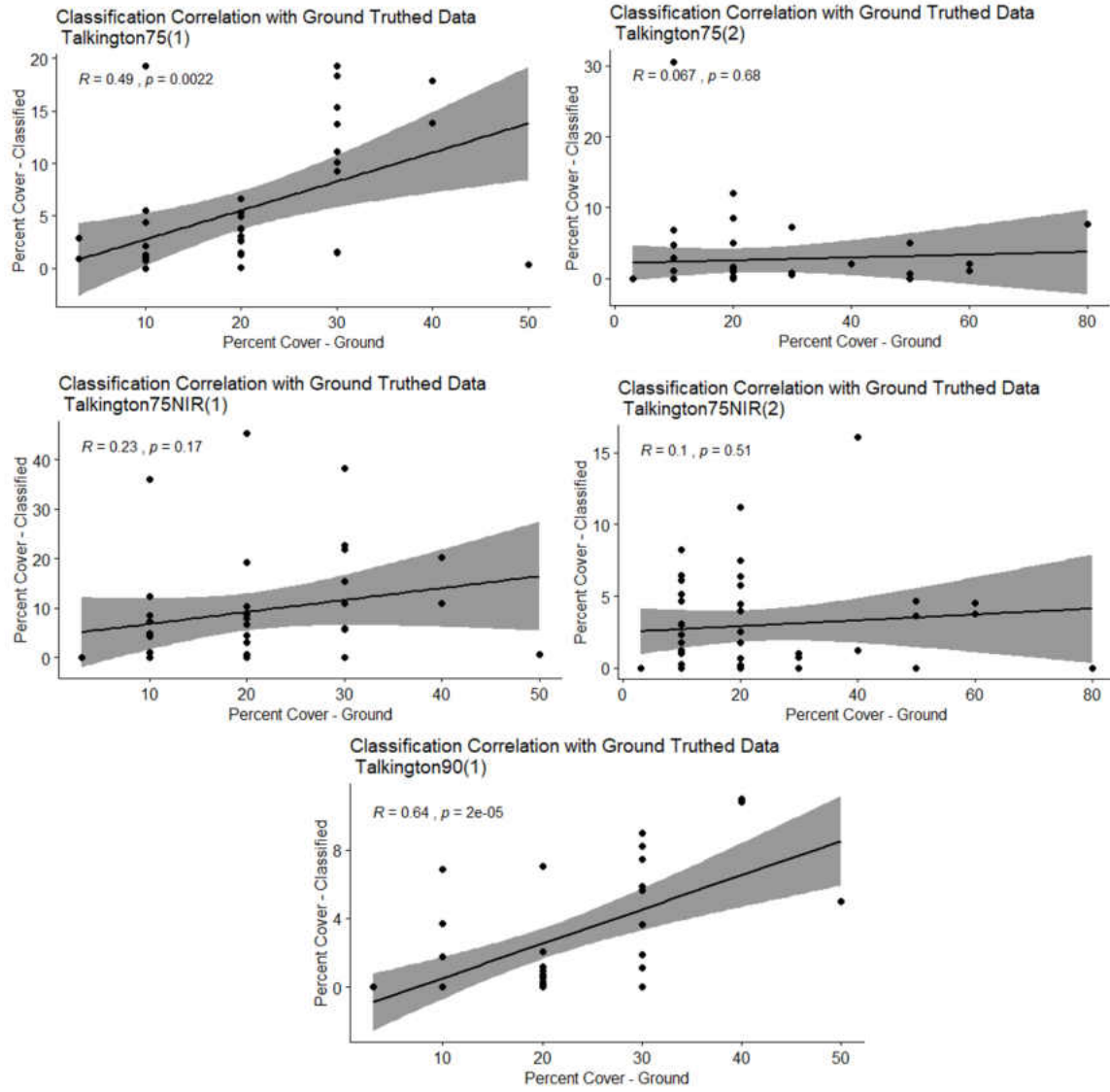


**Figure 9:** Scatterplots showing correlations between classified imagery and ground truthed data with 95% confidence intervals displayed.

**Table 3: Model of the percent classified spurge as a function of ground spurge coverage, area, density, and interaction terms for area \* ground spurge coverage, and density \* ground spurge coverage**

<b>Parameter</b>	<b>Estimate</b>	<b>Std. Error</b>	<b>P-value</b>
Ground Spurge Coverage	0.36	0.19	0.0677
Area	159.6	55.30	0.0052
Density Patchy	9.24	12.80	0.4730
Density Scattered	11.76	10.52	0.2675
Density Uniform	-7.78	5.77	0.1815
Ground Spurge * Area	-4.94	1.90	0.0115
Ground Spurge * Patchy Density	0.02	0.32	0.9556
Ground Spurge * Scattered Density	-0.14	0.20	0.4848
Ground Spurge * Uniform Density	NA	NA	NA

Notes: Residual standard error was 4.075 on 69 degrees of freedom. Multiple R-squared = 0.3642, adjusted R-squared = 0.2905, F-statistic = 4.941 on 8 and 69 DF, p-value = 7.452e-05.

## DISCUSSION

Overall, RGB images obtained via a low-flying UAS and processed using object-based image analysis in eCognition showed the best results and accuracies for detecting leafy spurge in TRNP. Both pixel-based classifiers performed similarly and only displayed limited success in detecting leafy spurge. In most classifications of all modes, errors of commission were more prevalent than errors of omission. Errors of commission mean the classification returned a false positive and errors of omission mean the classification returned a false negative. This means the maps produced may be accurate in some respects (i.e. for estimating potential area of invasion), there may be some slight overestimation due to errors of commission.

NAIP images that were classified using maximum likelihood in ArcGIS were not informative for detecting invasive plants. The images were taken on June 26, 2016 which corresponds to the peak phenology of spurge, but no visible spurge can be seen in the imagery. It has been previously established that the yellow-green color of leafy spurge bracts is necessary for detection (Everitt et al. 1995, Müllerova et al. 2017). A broad class that I named vegetation of interest was used to estimate the existence of leafy spurge in the NAIP imagery. Vegetation in this class was picked up by the computer as being a different shade of green than the background vegetation, since no yellow can be seen. The amount of vegetation of interest was overestimated due to the incorporation of taller vegetation into the class. Because of the lack of visible leafy spurge and the computer processing requirements for multiple high-resolution NAIP images, NAIP classifications were not pursued in eCognition. Future work may wish to incorporate eCognition classifications to see if that reduces error. In addition, training data for NAIP

classifications should be derived from higher resolution UAS imagery when spurge is clearly visible, or from larger, high percent cover patches mapped on the ground.

For UAS imagery, images with R-G-NIR showed lower accuracy than those with RGB images. The dip in accuracy for this image may come from the missing information the B band may have provided, and also implies that the NIR band is not as informative for this purpose. Future work will include using a Micasense camera which is capable of 5-band imagery (R-G-B-RE-NIR) and this hypothesis can then be tested.

The classifications achieved using eCognition in this research were performed using the same ruleset for every image. This shows the transferability of rulesets from one image to another. Individual image accuracy could be increased by creating a new ruleset specific to each image, but that is inefficient. This work demonstrates that rulesets can be transferred between images, especially between images of the same spectral resolution (i.e. R-G-B to R-G-B).

For extremely high-resolution imagery, such as that derived from low altitude UAS flights, computational limitations of object-based classifications on single workstations remain a concern. Classifications run on a computer with dual processors and 128 GB of RAM took anywhere from between 14 hours at the fast end to 158 hours. When attempting to include texture (GLCM – quick 8/11) as a parameter, the classification was still running after 160 hours and the decision was made that this was not feasible to do on the computer we had available. Cloud or cluster computing is a potential option for this work in the future as it will drastically speed up processing times; however that increases the cost since additional software licenses will have to be purchased.

Previous studies have determined that a data fusion approach is sometimes useful for producing accurate studies of natural systems (Marvin et al. 2016), and the same can be applied for increasing accuracy in detecting leafy spurge via the methods described in this paper. Future work could look at including LiDAR (light detection and ranging) to aid in detecting leafy spurge as it has been used successfully in aiding image classifications (Li et al. 2006). If objects of interest stand taller than the grasses that surround them, vegetation height could be an important parameter to include. However, vertical scale needs to be considered. LiDAR collected from an aerial image flight may not be available at a fine enough resolution for UAS imagery. In addition, suitability analyses in ArcGIS (Anderson et al. 1996) and soil monitoring from the ground (Jordan et al. 2008) have shown to be useful for identifying invasive plants and have the potential for data fusion with classifications.

Additionally, ground truthed data can be used as a verification method. The ground truthed data used in this study was collected two years prior to when the UAS was flown, so this could account in part for the low correlations. Future flight plans should include some incorporation of same-year ground testing so these data sources can be adequately compared. Although area of the ground truthing polygons – or, the size of the patch of leafy spurge on the ground – was significant in the linear model I performed, this should be revisited before a minimum threshold patch size can be determined for detection via remote sensing. Patch sizes that were very small in 2016 may have grown larger in the two years before the area was flown in 2018. This would skew results since the patch size being classified from the UAS imagery is larger than stated in the ground truthed data.

This research has demonstrated that classification of UAS imagery via eCognition is a viable strategy for detecting and mapping leafy spurge. Additionally, the combination of classified and ground-truthed data can provide an overall estimate of leafy spurge coverage for the entire park. Although I was unable to identify a threshold patch size of leafy spurge for detection, I was able to confirm that area is a significant component. Future work should use ground data and classifications from UAS imagery from the same year to determine this threshold patch size. The knowledge gained from these types of analyses can be used to make management decisions for targeting eradication efforts in high-priority areas.

## LITERATURE CITED

- Alboukadel Kassambara (2019). ggpubr: 'ggplot2' Based Publication Ready Plots. R package version 0.2.3.
- Alvarez-Taboada, F., C. Paredes, et al. (2017). "Mapping of the Invasive Species *Hakea sericea* Using Unmanned Aerial Vehicle (UAV) and WorldView-2 Imagery and an Object-Oriented Approach." *Remote Sensing* 9(9): 913.
- Anderson, G. L., J. Everitt, et al. (1996). "Mapping leafy spurge (*Euphorbia esula*) infestations using aerial photography and geographic information systems." *Geocarto International* 11(1): 81-89.
- Best, K. F., G. G. Bowes, et al. (1979). "The Biology of Canadian Weeds .39 - *Euphorbia esula* L." *Canadian Journal of Plant Science*.
- Blaschke, T., G. J. Hay, et al. (2014). "Geographic Object-Based Image Analysis - Towards a new paradigm." *ISPRS J Photogramm Remote Sens* 87(100): 180-191.
- Butler, J. L. and D. R. Cogan (2004). "Leafy spurge effects on patterns of plant species richness." *Rangeland Ecology and Management* 57(3): 305-312.
- Congalton, R. G. and R. A. Mead (1983). "A quantitative method to test for consistency and correctness in photointerpretation." *Photogrammetric engineering and remote sensing* 49(1): 69-74.
- Congalton, R. G. and K. Green (1999). *Assessing the Accuracy of Remotely Sensed Data: Principles and Practices*. Boca Raton, FL, Lewis Publishers.



- Cortes, C. and V. Vapnik (1995). "Support-vector networks." *Machine learning* 20(3): 273-297.
- D'Antonio, C. M., N. E. Jackson, et al. (2004). "Invasive plants in wildland ecosystems: merging the study of invasion processes with management needs." *Frontiers in Ecology and the Environment* 2(10): 513-521.
- Dunn, P. H. (1979). "The Distribution of Leafy Spurge (*Euphorbia esula*) and Other Weedy *Euphorbia* spp. in the United States." *Weed Science* 27(5).
- Dunn, P. H. (1985). "Origins of leafy spurge in North America." *Weed Science* 2(3).
- El-naggar, A. M. (2018). "Determination of optimum segmentation parameter values for extracting building from remote sensing images." *Alexandria engineering journal*.
- Erdas Inc. (1999). "ERDAS Field Guide." Atlanta, Georgia 672: 94.
- ESRI. ArcGIS Desktop: Release 10. Redlands, CA: Environmental Systems Research Institute.
- Everitt, J. H. and G. L. Anderson (1995). "Use of Remote Sensing for Detecting and Mapping Leafy Spurge (*Euphorbia esula*)." *Weed Technology* 9(3).
- Jordan, N. R., D. L. Larson, et al. (2008). "Soil modification by invasive plants: effects on native and invasive species of mixed-grass prairies." *Biological Invasions* 10(2): 177-190.
- Khatami, R., G. Mountrakis, et al. (2016). "A meta-analysis of remote sensing research on supervised pixel-based land-cover image classification processes: General

- guidelines for practitioners and future research." *Remote Sensing of Environment* 177: 89-100.
- Lawrence, R. L., S. D. Wood, et al. (2006). "Mapping invasive plants using hyperspectral imagery and Breiman Cutler classifications (randomForest)." *Remote Sensing of Environment* 100(3): 356-362.
- Li, H., H. Gu, et al. (2006). Fusion of High-Resolution Aerial Imagery and Lidar Data for Object-Oriented Urban Land-Cover Classification Based on SVM. ISPRS Workshop on Updating Geo-spatial Databases with Imagery & The 5th ISPRS Workshop on DMGISs.
- Lym, R. G. and C. G. Messersmith (1985). "Leafy Spurge Control with Herbicides in North Dakota: 20-Year Summary." *Journal of Range Management* 38(2).
- Mairota, P., B. Cafarelli, et al. (2015). "Challenges and opportunities in harnessing satellite remote-sensing for biodiversity monitoring." *Ecological Informatics* 30: 207-214.
- Marvin, D. C., L. P. Koh, et al. (2016). "Integrating technologies for scalable ecology and conservation." *Global Ecology and Conservation* 7: 262-275.
- Messersmith, C. G. and R. G. Lym (1983). "Distribution and Economic Impacts of Leafy Spurge in North Dakota." *North Dakota Farm Research* 40.
- Messersmith, C. G., R. G. Lym, et al. (1985). "Biology of leafy spurge." *Weed Science* 5(3).

- Müllerová, J., J. Brůna, et al. (2017). "Timing Is Important: Unmanned Aircraft vs. Satellite Imagery in Plant Invasion Monitoring." *Frontiers in Plant Science* 8(887).
- O'Neill, M., S. L. Ustin, et al. (2000). Mapping the distribution of leafy spurge at Theodore Roosevelt National Park using AVIRIS. Proceedings of the Ninth JPL Airborne Earth Science Workshop, Pasadena, California, NASA Jet Propulsion Laboratory.
- Pimentel, D., L. Lach, et al. (2000). "Environmental and Economic Costs of Nonindigenous Species in the United States." *BioScience* 50(1): 53.
- Pimentel, D., R. Zuniga, et al. (2005). "Update on the environmental and economic costs associated with alien-invasive species in the United States." *Ecological economics* 52(3): 273-288.
- Quimby Jr, P. and L. Wendel (1997). "The ecological areawide management of leafy spurge: a demonstration of biologically based IPM strategies." Sidney, MT, USA: US Department of Agriculture–Agricultural Research Service.
- R Core Team (2013). *R: A language and environment for statistical computing*. R Foundation for Statistical Computing, Vienna, Austria.
- URL <http://www.R-project.org/>
- Stehman, S. V. and G. M. Foody (2009). "Accuracy assessment." *The SAGE handbook of remote sensing*: 297-309.

Stitt, S., R. Root, et al. (2006). "Classification of Leafy Spurge With Earth Observing-1 Advanced Land Imager." *Rangeland Ecology & Management* 59(5): 507-511.

Trimble. (2015). *eCognition Developer: Release 9*. Sunnyville, CA: Trimble.

Turner, W., S. Spector, et al. (2003). "Remote sensing for biodiversity science and conservation." *Trends Ecol Evol* 18(6): 306-314.

Vila, M., J. L. Espinar, et al. (2011). "Ecological impacts of invasive alien plants: a meta-analysis of their effects on species, communities and ecosystems." *Ecol Lett* 14(7): 702-708.

**CHAPTER III**  
**MAPPING VEGETATION COMMUNITIES IN THEODORE ROOSEVELT**  
**NATIONAL PARK**  
**INTRODUCTION**

Effective wildlife management requires an understanding and consideration of the vegetation communities that animals use to survive and reproduce. Vegetation influences habitat selection, so animals may be more likely to stay in certain areas if the vegetation can be used to meet their needs for food and shelter (Howe and Westley 1988). Because of the important link between wildlife and plants, it is important to understand and monitor vegetation communities. This is especially true for natural systems such as Theodore Roosevelt National Park (TRNP) that use forage allocation models to manage animal numbers (Irby et al. 2002) because of the park's boundary fence that constrains their movement. Because animals such as bison, feral horses, prairie dogs, pronghorn, elk, and deer among many others all depend directly on vegetation composition and quality, mapping and monitoring the vegetation communities that support them is critically important.

Past research has identified and defined the vegetation communities in TRNP. Hansen et al. (1984) delineated habitat types within the park using techniques and ideas proposed by Daubenmire and Daubenmire (1968). They identified 11 vegetation associations defined by different combinations of numerically dominant species. That

same year, Norland (1984) created 14 physiographic and vegetational classes; seven classes were unique to one unit or the other, while the rest were found in both units.

These classes were breaks, cottonwood forests, wooded draws, upland grasslands, old river terraces, grassland flats, bottom grasslands, toe slopes, rolling grasslands, Achenbach hills, ridge and ravine, scoria hills, sagebrush bottoms, and prairie dog towns. Irby et al. (2002) created vegetation community categories specifically for a forage allocation model for ungulates. The Upland Grasslands category contained subcategories of graminoids, forbs, litter, climax grass species, and western wheatgrass, while the Hardwood Draws category contained green ash stems, chokecherry, serviceberry stems, snowberry stems, all species, bare ground, climax graminoids, exotic graminoids, invasive forbs, and palatable forbs.

Traditional methods of vegetation sampling and monitoring, such as walking on foot to designated plots as presented by Daubenmire 1959, are impractical in areas as large as TRNP. Using remote sensing as a monitoring tool for vegetation can help identify important or critical areas where employees could then be sent to sample on foot, as well as cover large areas that would not be entirely sampled on foot. Remote sensing has been used extensively to estimate to map and monitor vegetation (Kastens and Legates 2002, Luscier et al. 2006, Walton et al. 2013, Dandois and Ellis 2013).

Advances in technology have resulted in a variety of platforms from which to collect imagery, ranging from satellite to high altitude aircraft, to very low altitude unmanned aircraft systems (UAS). Different platforms with different sensors have different capabilities in relation to temporal frequency of sampling, spatial coverage, image resolution, and spectral resolution and breadth. The choice of platform and sensors

will depend on the specific problem and data needs, with spatial scale being an important factor to consider. Mapping vegetation communities for bison, for example, who move at a relatively large scale, might require the use of a different platform and sensor than when mapping for prairie dogs, who are more limited in their spatial extent. Different sources of imagery, therefore, may be most useful for each application. I had two sources of imagery available to me, each potentially most useful at different scales. Specifically, I used imagery obtained from manned flights as part of the National Agriculture Imagery Program (NAIP) to estimate vegetation classification at broader scales, and much higher resolution but more spatially limited imagery obtained using a UAS. The former produces 60 cm resolution (in recent years) and covers very large areas (e.g. statewide), whereas the latter has a much higher resolution of 2 to 3 cm but covers only small sections of the park per flight.

In addition to testing the performance of imagery collected at different spatial scales for classifying vegetation communities in the park, I will also compare image classification methods for their performance for vegetation classification. Two methods for computational analysis that have been used for this purpose in the past are pixel-based and object-based classifications. Pixel-based methods often implemented in geographic information systems (GIS) have been used for vegetation monitoring to estimate forest types in India (Reddy et al. 2015) among many other examples. More advanced methods such as object-based image analysis (OBIA) implemented in eCognition software have been used for estimating percent ground cover of various species (Luscier et al. 2006). GIS is readily available at many higher education institutions, state and federal agencies, and in open source formats for anyone, whereas eCognition is less commonly used and

available only as a commercial product. A comparative study by Yu et al. (2006) found that the object-based classification from eCognition yielded higher overall accuracy, but the maximum likelihood classification from GIS performed better for vegetation classes of small sample sizes. In addition, Hussain et al. (2013) found that object-based image analysis has a higher potential of accurately detecting changes in very-high resolution imagery.

In this chapter I will evaluate the use of remote sensing for vegetation community classification. I will classify the vegetation communities at multiple sites in TRNP based on NAIP imagery and UAS imagery and identify whether pixel-based or object-based methods yield better accuracy for each spatial scale.

## METHODS

### *Study Area*

This research was conducted in TRNP, located in southwestern North Dakota. This semi-arid region exhibits a prairie grassland ecosystem and badlands topography. TRNP is comprised of three geographically separate units, two of which are included in this study: the South Unit (18,756 hectares) is the largest and is located in Billings County, whereas the North Unit (9,741 hectares) is noticeably smaller and located about 80 km to the north in McKenzie County. I used UAS imagery collected at sites in the South Unit and NAIP imagery for both units for this thesis.

### *Data Acquisition*

In the summer of 2018, a University of North Dakota (UND) research crew from the Department of Biology flew a fixed-wing Trimble UX5 at three sites at two altitudes. These sites were selected because of them containing either invasive vegetation or prairie



dog colonies. Flights followed preprogrammed line transects that permitted 80% overlapping photography of ground survey areas. Flights were conducted at 75m and then 90m for each site. Unmanned aircraft systems flight operations for this research were approved by the National Park Service (Study #THRO-00099, Permit #THRO-2018-SCI-0010). Aerial imagery that covers the entirety of both park units was obtained from the National Agriculture Imagery Program (NAIP) for 2016; NAIP imagery from 2018 was not included as it was not published at the time of data analysis. All remotely sensed data used in this research are listed in Table 4.

**Table 4: Images used for classification and their temporal, spatial, and spectral characteristics. I analyzed only portions of the full dataset from each site.**

<b>Image</b>	<b>Temporal Resolution</b>	<b>Spatial Resolution</b>	<b>Spatial Extent</b>	<b>Spectral Bands</b>
<b>NAIP imagery</b>				
NAIPNUMosaic	June – August 2016	60 cm	97.40 km <sup>2</sup>	R-G-B-NIR
NAIPSUMosaic	June – August 2016	60 cm	186.79 km <sup>2</sup>	R-G-B-NIR
<b>UAS imagery</b>				
Talkington75(1)	June 2018	2.21 cm	124 m <sup>2</sup>	R-G-B
Talkington75(2)	June 2018	2.21 cm	898 m <sup>2</sup>	R-G-B
Talkington75NIR(1)	June 2018	2.35 cm	124 m <sup>2</sup>	R-G-NIR
Talkington75NIR(2)	June 2018	2.35 cm	124 m <sup>2</sup>	R-G-NIR
Talkington90(1)	June 2018	2.71 cm	124 m <sup>2</sup>	R-G-B
Lindbo75(1)	June 2018	2.24 cm	134 m <sup>2</sup>	R-G-B
Lindbo75(2)	June 2018	2.24 cm	105 m <sup>2</sup>	R-G-B
Lindbo75NIR(1)	June 2018	2.18 cm	134 m <sup>2</sup>	R-G-NIR
Lindbo90(1)	June 2018	2.7 cm	134 m <sup>2</sup>	R-G-B
BeefCorral75(1)	June 2018	2.26 cm	612 m <sup>2</sup>	R-G-B
BeefCorral75(2)	June 2018	2.26 cm	662 m <sup>2</sup>	R-G-B

## *Image Classification*

The overall image classification workflow was structured in three main parts: data pre-processing, classification, and validation (Chapter 2, Figure 3). This is true for classifications performed in ArcGIS as well as eCognition. The workflow is described in more detail in Chapter 2. All classified images can be found in Appendix A.

I used the image classification tools available in ArcGIS (version 10.6, ESRI) to perform pixel-based classifications of the imagery using supervised methods. I chose maximum likelihood and support vector machine (SVM) classifiers for this purpose. The maximum likelihood classifier is the best-known algorithm for supervised image classification (Erdas Inc. 1999) and is commonly used for pixel-based classifications. The SVM classifier groups similar pixels based on spectral values and creates pseudo-objects in n-dimensional space (segmentation), which are then used to create training samples (Cortes and Vapnik 1995). A series of segmentations were tested by adjusting the parameters of spectral detail (level of importance given to spectral features) and spatial detail (level of importance given to the proximity between features). The final image segmentations were achieved using a spectral detail of 15, spatial detail of 15, minimum segment size of 20, and band indexes of 1, 2, and 3. Multiple training samples were created for each class then merged to form a reliable sample for the whole image. These training samples were then used by the classifier to identify classes that I delineated and assign pixels to the appropriate classes.

I performed object-based image analysis (OBIA) using eCognition Developer (version 9.1.2, Trimble 2015). I then tested a series of segmentations by adjusting the parameters of scale, shape, compactness, and image weighting. Scale adjusts how large or

small the desired image objects will be, shape adjusts the relationship between color and shape criteria for the resulting segments, compactness adjusts the overall area of the resulting segments, and image weighting refers to the importance given to each spectral band (El-naggar 2018). The final image segmentations were achieved using a scale of 40, image layer weights of 1, 1, and 1, shape of 0.2, and compactness of 0.6. Then, I used the Nearest Neighbor (NN) classifier to classify objects based on training samples I created. Classification parameters included mean color, brightness, standard deviation, maximum difference, area, shape, and mathematical band indices. After initial classification, I examined the output and wrote additional rules to refine the classifier.

For all classifiers, I defined classes as bare ground, grasses, leafy spurge (in images that included the invasive plant), prairie dog mounds (in images that included a prairie dog colony), the paved park road, sagebrush, taller and shrubby vegetation, trees, water, and areas of no data. In the NAIP imagery, I defined a “vegetation of interest” class that included leafy spurge as well as other taller vegetation. This is because the yellow color of leafy spurge could not be distinguished in the NAIP imagery. Areas of no data were present on the outer edges of the image mosaic and were not included in accuracy assessments.

I ran error and accuracy assessments in the ArcGIS environment for both pixel based and OBIA classification techniques. To evaluate the accuracy of the overall landscape classification, I performed an accuracy assessment with stratified random points. Stratified random accuracies assign points proportional to the percent cover. A multinomial equation from Congalton & Green (1999) was used to calculate the appropriate number of points based on a 95% confidence interval. Confusion matrices

were created where omission (false negatives) and commission (false positives) errors were quantified and examined. ArcGIS calculated a  $K_{HAT}$  (Kappa) statistic for each matrix, which gives an estimate for the measure of actual agreement between true and estimated classification within a confusion matrix (Congalton and Mead 1983). The Kappa statistic can be used to show how your classification performs against a completely random classification ( $Kappa = 0$ ) (Congalton and Green 1999).

For these assessments, overall accuracy – which is calculated by dividing the total correct by the overall total (Jensen 1996) – for the entire classification and the Kappa statistic are informative for classifier performance. Because of this, I performed proportional stratified random accuracy assessments. However, to gain insight on performance for individual classes, I performed equalized random accuracy assessments with each class getting a minimum of 100 accuracy points. I used this approach because rare-class sample sizes are often small when using stratified random sampling (Stehman and Foody 2009) and therefore introduces a sampling deficiency for looking at accuracy of individual classes. I examined the producer's accuracy (measure of omission error) and the user's accuracy (measure of commission error) for the equalized confusion matrices. All confusion matrices for all classifications can be found in Appendix B.

## RESULTS

NAIP imagery classified in ArcGIS using the maximum likelihood classifier produced low accuracies (Figure 10). The North Unit classification had an overall accuracy of 59% (overall error of 41%) and a Kappa of 0.49, while the South Unit classification had an overall accuracy of 61% (overall error of 39%) and a Kappa of 0.50. Water was considerably more accurate in the South Unit classification. Both units

showed higher errors of commission for water at 61% and 74%, respectively. Trees were identified at similar accuracy levels in both units. Sagebrush was more accurately identified in the North Unit than in the South Unit, whereas “vegetation of interest” was more accurately identified in the South than in the North Unit. Individual class accuracies for both units using an equalized random accuracy assessment can be found in Figure 10.

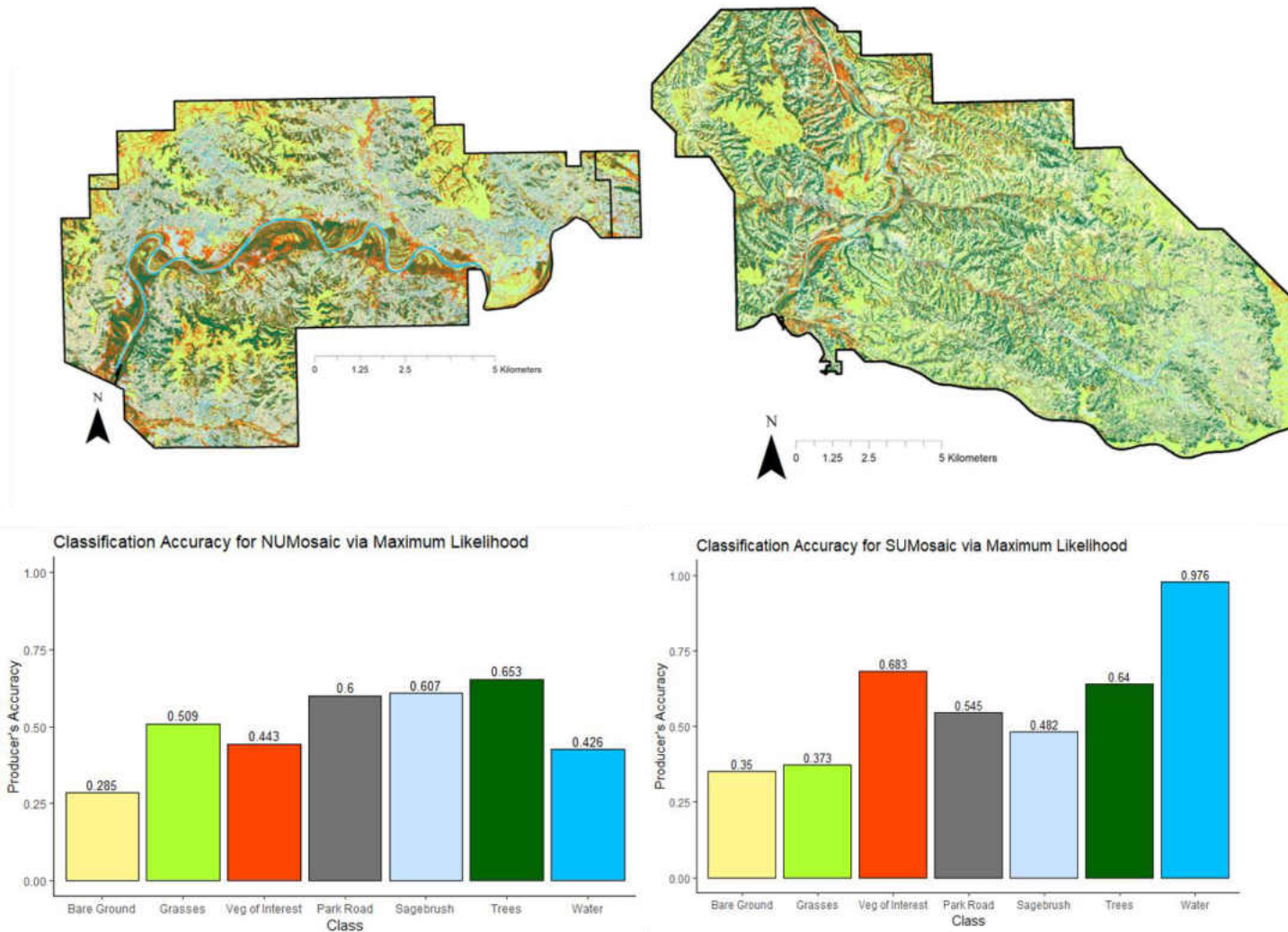


**Figure 10:** TRNP North Unit (left) and South Unit (right) classified via maximum likelihood in ArcGIS and corresponding producer's accuracies for each below the maps. The colors of the bars in the graphs correspond to the class color in the classification. Producer's accuracy shows how often the classifier got it right; errors of omission are the inverse of producer's accuracy.

UAS images classified by the SVM classifier in ArcGIS had relatively low accuracy (Figure 11). Images with prairie dog colonies (BeefCorral and Lindbo) had higher overall accuracies (65% and 72%), but low Kappa values (0.43 and 0.40). Maximum likelihood classifications of UAS imagery yielded higher accuracies than SVM. Overall accuracy ranged from 41% (Kappa = 0.27) to 76% (Kappa = 0.44). Images with prairie dog colonies produced the highest accuracies, whereas images that showed mostly vegetation produced slightly less accurate classifications. Light conditions were variable when UAS flights were occurring (i.e. clouds were moving across the sky throughout the day) and the effects of this can be seen in the form of shadows in the imagery. SVM is not well-suited to handle variations in light when segmenting the images and created large segments that were not meaningful. This caused accuracy to drastically decrease. The maximum likelihood classifier seemed to handle variations in light slightly better than SVM, but that was only slightly reflected in the accuracy assessments.

OBIA classifications of UAS imagery produced the classifications with the highest accuracies. Accuracies ranged from 50% (Kappa = 0.35) to 85% (Kappa = 0.74) for the overall image accuracy, and images displaying R-G-B bands performed best. These classifications also produced higher overall accuracy for images that contained prairie dog colonies. OBIA was able to handle variations in light and therefore the changing light conditions did not cause any noticeable decreases in accuracy.

Producer's accuracies for individual classes in a vegetation dominated image (Talkington75(1)) are shown in Figure 11. Producer's accuracy shows how often the classifier got it right; errors of omission are the inverse of producer's accuracy. The



paved park road and water classes had high accuracy in all three classification modes. Producer's accuracies for individual classes in a prairie dog colony dominated image (Lindbo75(1)) are shown in Figure 12. Individual classes performed differently in each classification mode, which is likely because of how similar classes such as bare ground, grasses, and prairie dog mounds are – the more similar the classes, the more likely the classification is to confuse them. Overall accuracy and Kappa statistics produced via stratified random accuracy assessments for all classification methods can be found in Table 5.

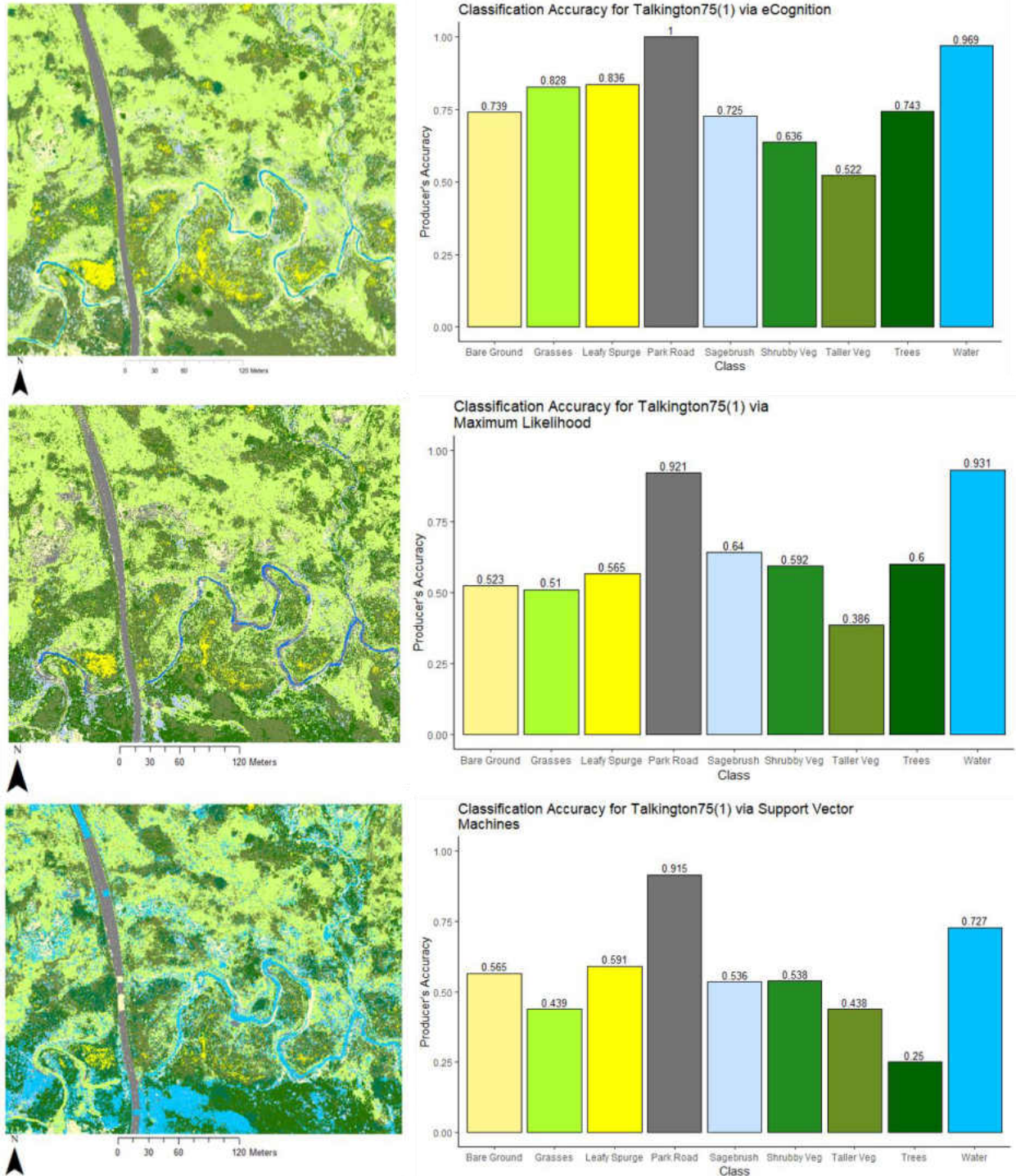


**Figure 11:** Producer’s accuracy for individual classes produced using an equalized random accuracy assessment for object-based classification in eCognition (top), maximum likelihood pixel-based classification in ArcGIS (center), and SVM pixel-based classification in ArcGIS (bottom). The colors of the bars in the graphs correspond to the class color in the classification. Producer’s accuracy shows how often the classifier got it right; errors of omission are the inverse of producer’s accuracy.

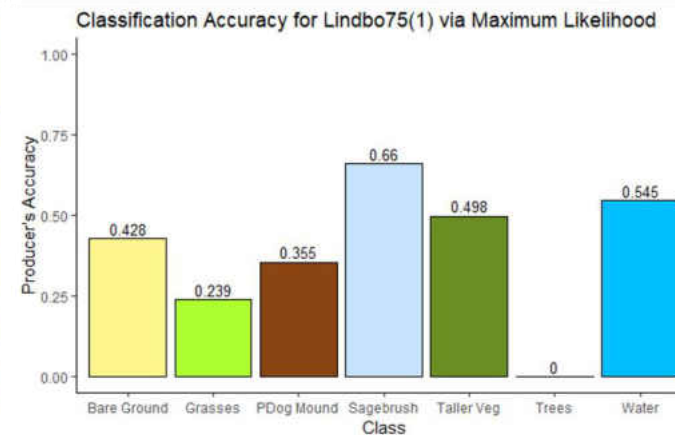
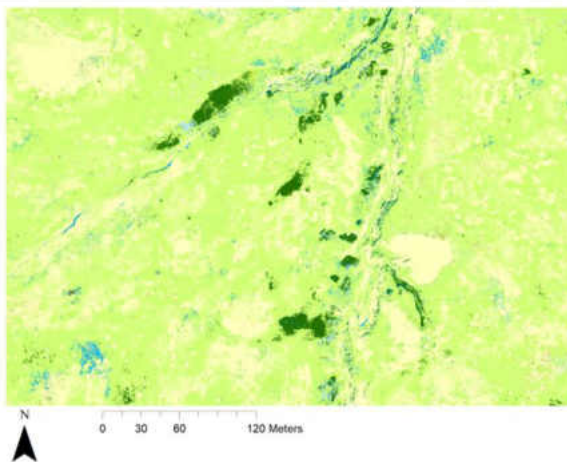
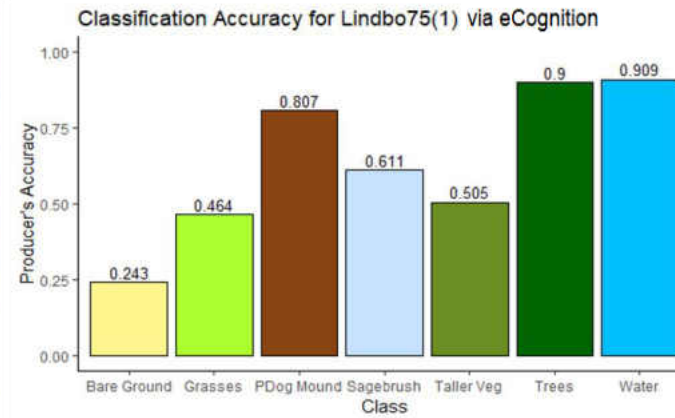
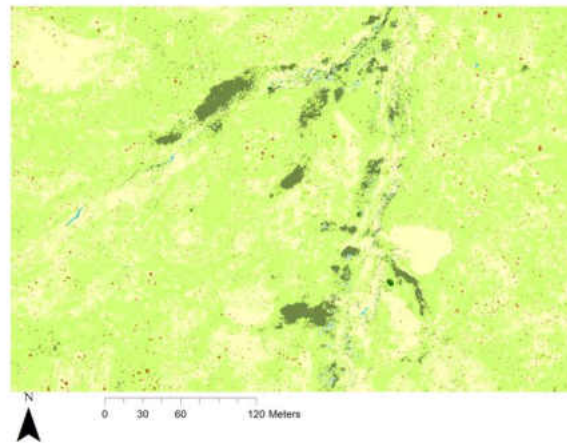


**Figure 12:** Producer's accuracy for individual classes produced using an equalized random accuracy assessment for object-based classification in eCognition (top) and for maximum likelihood pixel-based classification in ArcGIS (bottom). The colors of the bars in the graphs correspond to the class color in the classification. Producer's accuracy shows how often the classifier got it right; errors of omission are the inverse of producer's accuracy.

**Table 5: Overall accuracy and Kappa statistics for all classification methods**

<b>Classification Method</b>	<b>Main Feature in Imagery</b>	<b>Overall Accuracy</b>	<b>Kappa</b>
<b>SVM</b>			
Talkington75(1)	Vegetation	0.47	0.34
Talkington75(2)	Vegetation	0.60	0.44
BeefCorral75(1)	Prairie Dogs	0.65	0.43
BeefCorral75(2)	Prairie Dogs	0.72	0.40
<b>MAXL</b>			
NUMosaic	NAIP	0.59	0.49
SUMosaic	NAIP	0.61	0.50
Talkington75(1)	Vegetation	0.58	0.45
Talkington75(2)	Vegetation	0.63	0.44
Talkington75NIR(1)	Vegetation	0.46	0.27
Talkington75NIR(2)	Vegetation	0.54	0.32
Talkington90(1)	Vegetation	0.41	0.24
Lindbo75(1)	Prairie Dogs	0.70	0.43
Lindbo75(2)	Prairie Dogs	0.71	0.46
Lindbo75NIR(1)	Prairie Dogs	0.73	0.47
Lindbo90(1)	Prairie Dogs	0.69	0.41
BeefCorral75(1)	Prairie Dogs	0.71	0.52
BeefCorral75(2)	Prairie Dogs	0.76	0.44

## OBIA

Talkington75(1)	Vegetation	0.75	0.66
Talkington75(2)	Vegetation	0.79	0.67
Talkington75NIR(1)	Vegetation	0.50	0.35
Talkington75NIR(2)	Vegetation	0.61	0.43
Talkington90(1)	Vegetation	0.56	0.36
Lindbo75(1)	Prairie Dogs	0.83	0.69
Lindbo75(2)	Prairie Dogs	0.84	0.66
Lindbo75NIR(1)	Prairie Dogs	0.71	0.41
Lindbo90(1)	Prairie Dogs	0.70	0.44
BeefCorral75(1)	Prairie Dogs	0.85	0.74
BeefCorral75(2)	Prairie Dogs	0.84	0.62

---

Notes: All UAS images are R-G-B unless otherwise stated in the image name

## DISCUSSION

Overall, RGB images obtained via a low-flying UAS and processed using OBIA in eCognition showed the highest accuracies for landscape and vegetation community classifications. Both pixel-based classifiers performed similarly and only displayed moderate accuracy. Between the two NAIP classifications, the classes with the highest accuracy were trees, grasses, and sagebrush. Park road produced many errors of commission and therefore mis-identified many other features in the image, which lowered overall accuracy. Maximum likelihood was only moderately accurate when classifying NAIP images, so future work should incorporate classifications using nearest

neighbor information in eCognition as well. Additionally, eCognition would likely increase accuracy for the park road class since vector layers can be added as an additional information source used in the classification. “Vegetation of interest” was described in Chapter 2 but was not sufficiently precise as created here to be useful for its intended purpose (classifying leafy spurge). Without a more distinctive signal derived from known patches of flowering spurge, it appears to be synonymous with “vegetation with a slightly different shade of green”, which potentially included many different types of vegetation. Given the low overall accuracies and relatively low Kappa coefficients, this classification would not be considered reliable as a basis for management. If pursued in eCognition and with appropriate reference spectra (even derived from UAS imagery) to improve accuracy, NAIP may be useful for creating new forage allocation models or managing the vegetation for large herbivores since it produces broad scale classifications. UAS, although it produced more accurate results, will not achieve the spatial extent requirements needed for informing managers about vegetation availability for large herbivores. However, it can serve as a reliable source for identifying vegetation categories and mapping those onto concordant portions of NAIP imagery to create training data for classifiers.

Images produced from flights that occurred over prairie dog colonies yielded higher accuracy than those that primarily featured vegetation. This could be because of the grazing behaviors of prairie dogs, since they clip vegetation and keep it short. The classifications therefore may be more accurate because of the short grass that dominates the image.

This work confirms previous findings that OBIA is better suited for classifying imagery than pixel-based methods (Yu et al. 2006, Hussain et al. 2013). In addition, some of the same classes that have been previously delineated for TRNP – specifically by Norland (1984) and Irby et al. (2002) were successfully classified in the UAS imagery. These classes include sagebrush, prairie dog colonies, grasses, and trees.

Previous studies have determined that a data fusion approach is most ideal for producing accurate studies of natural systems (Marvin et al. 2016), and the same can be applied for increasing accuracy when mapping vegetation communities as outlined in this chapter. Additional work could look at including LiDAR (light detection and ranging) to aid in detecting features of interest. LiDAR has been successful at identifying sagebrush (Streutker and Glenn 2006), forest canopy (Simard et al. 2011), and mapping general rangeland vegetation communities (Bork and Su 2007). This may aid in identifying trees and taller vegetation, which were often confused with other features of interest. Also, future work will incorporate using a multispectral Micasense camera that is capable of capturing 5-band images (R-G-B-RE-NIR).

This research has demonstrated that classification of UAS imagery via eCognition is a viable strategy for mapping vegetation communities. Pixel-based strategies produced more error than object-based classification methods but provided a useful baseline for park-wide vegetation mapping. A logical next step would be to also classify NAIP using OBIA, using UAS imagery to identify training data in the NAIP imagery. Despite error, managers can use these classifications to gain insight on vegetation communities within TRNP to update forage allocation models or compliment previous work.

## LITERATURE CITED

- Bork, E. W. and J. G. Su (2007). "Integrating LIDAR data and multispectral imagery for enhanced classification of rangeland vegetation: A meta analysis." *Remote Sensing of Environment* 111(1): 11-24.
- Congalton, R. G. and K. Green (1999). *Assessing the Accuracy of Remotely Sensed Data: Principles and Practices*. Boca Raton, FL, Lewis Publishers.
- Congalton, R. G. and R. A. Mead (1983). "A quantitative method to test for consistency and correctness in photointerpretation." *Photogrammetric engineering and remote sensing* 49(1): 69-74.
- Cortes, C. and V. Vapnik (1995). "Support-vector networks." *Machine learning* 20(3): 273-297.
- Dandois, J. P. and E. C. Ellis (2013). "High spatial resolution three-dimensional mapping of vegetation spectral dynamics using computer vision." *Remote Sensing of Environment* 136: 259-276.
- Daubenmire, Rexford. 1959. A Canopy-coverage method of vegetational analysis. *Northwest Science* 33:43-64.
- Daubenmire, R. and J. B. Daubenmire (1968). "Forest vegetation of eastern Washington and northern Idaho." *Technical Bulletin 60*. Pullman, WA: Washington State University, College of Agriculture, Washington Agricultural Experiment Station. 104 p.
- El-naggar, A. M. (2018). "Determination of optimum segmentation parameter values for extracting building from remote sensing images." *Alexandria engineering journal*.
- Erdas Inc. (1999). *ERDAS Field Guide*. Atlanta, Georgia. 672: 94.



- ESRI. ArcGIS Desktop: Release 10. Redlands, CA: Environmental Systems Research Institute.
- Hansen, P. L., G. R. Hoffman, et al. (1984). The Vegetation of Theodore Roosevelt National Park, North Dakota: A Habitat Type Classification. General Technical Report. RM-113.
- Howe, H. F. and L. C. Westley (1988). Ecological relationships of plants and animals, Oxford University Press.
- Hussain, M., D. Chen, et al. (2013). "Change detection from remotely sensed images: From pixel-based to object-based approaches." *ISPRS Journal of Photogrammetry and Remote Sensing* 80: 91-106.
- Irby, L. R., J. E. Norland, et al. (2002). "Evaluation of a forage allocation model for Theodore Roosevelt National Park." *Journal of Environmental Management* 64(2): 153-169.
- Jensen, J. R. (1996). *Introductory Digital Image Processing: A Remote Sensing Perspective*. Upper Saddle River, NJ, Prentice Hall.
- Kastens, J. H. and D. R. Legates (2002). "Time series remote sensing of landscape-vegetation interactions in the southern Great Plains." *Photogrammetric Engineering & Remote Sensing* 68(10): 1021-1030.
- Luscier, J. D., W. L. Thompson, et al. (2006). "Using Digital Photographs and Object-Based Image Analysis to Estimate Percent Ground Cover in Vegetation Plots." *Frontiers in Ecology and the Environment* 4(8).
- Marvin, D. C., L. P. Koh, et al. (2016). "Integrating technologies for scalable ecology and conservation." *Global Ecology and Conservation* 7: 262-275.

- Norland, J. E. (1984). Habitat use and distribution of bison in Theodore Roosevelt National Park. Range Science, Montana State University. Master of Science.
- Reddy, C. S., C. S. Jha, et al. (2015). "Nationwide classification of forest types of India using remote sensing and GIS." *Environ Monit Assess* 187(12): 777.
- Simard, M., N. Pinto, et al. (2011). "Mapping forest canopy height globally with spaceborne lidar." *Journal of Geophysical Research: Biogeosciences* 116(G4).
- Stehman, S. V. and G. M. Foody (2009). "Accuracy assessment." *The SAGE handbook of remote sensing*: 297-309.
- Streutker, D. R. and N. F. Glenn (2006). "LiDAR measurement of sagebrush steppe vegetation heights." *Remote Sensing of Environment* 102(1-2): 135-145.
- Trimble. (2015). *eCognition Developer: Release 9*. Sunnyville, CA: Trimble.
- Walton, K. M., D. E. Spalinger, et al. (2013). "High spatial resolution vegetation mapping for assessment of wildlife habitat." *Wildlife Society Bulletin* 37(4): 906-915.
- Yu, Q., P. Gong, et al. (2006). "Object-based Detailed Vegetation Classification with Airborne High Spatial Resolution Remote Sensing Imagery " *Photogrammetric Engineering & Remote Sensing* 72(7).

## CHAPTER IV

### BLACK-TAILED PRAIRIE DOG COLONY MAPPING IN THEODORE ROOSEVELT NATIONAL PARK

#### INTRODUCTION

Animals can have dramatic impacts on the environment and local ecosystems. In prairie landscapes such as the Northern Great Plains, prairie dogs are considered by many ecologists to be ecosystem engineers and a keystone species because they significantly alter the terrestrial realm around them (Miller et al. 2000, Detling 1998, Holland and Detling 1990, Detling and Whicker 1987). Black-tailed prairie dogs (*Cynomys ludovicianus*) are small, herbivorous rodents who live colonially in burrow systems, form strong social bonds, and exhibit an extensive communication network (Hoogland 1995). They are also the primary prey of a federally endangered species, the black footed ferret (*Mustela nigripes*), and their colonies are critical habitat for that species (Biggins et al. 1993). Because of their role in the function of prairie ecosystems, understanding their spatial distribution and dynamics is central to understanding the ecology of grasslands in areas where they are found. This understanding is important especially for natural areas such as Theodore Roosevelt National Park (TRNP), where prairie dogs are protected. Colony acreage in the park is constantly fluctuating, but has shown a gradual increase since the 1980s (Milne 2004). Managers need accurate, reliable, and cost-effective solutions for mapping prairie dog colonies, but accomplishing this by ground surveys is time-consuming and labor intensive. Advances in technology such as remote sensing (Jensen 1996) may help solve this problem if these methods prove sufficiently accurate

and affordable. My goal in this chapter is to test the efficacy of remotely sensed data collected using unmanned aircraft systems (UAS) and classified computationally for mapping prairie dog colonies.

In the beginning of the 20<sup>th</sup> century, there was an estimated 40 million hectares of prairies available for prairie dog habitat. However, after a nearly 98.5% decline by the 1960s, this was reduced to only 600,000 hectares (Miller et al. 2000). Anthropogenic activities are largely to blame for this reduction. Prairie dogs were considered – and still are by some – to be a nuisance or pest species. Their burrows traversed potential farm- and rangeland and there were fears that prairie dogs would decrease available forage for livestock, a claim that has been hotly contested for years (Miller et al. 2007). Although prairie dogs consume the same forage species as cattle, cattle weights were not found to differ between on- and off-colony grazing (Uresk 1987). Despite an apparent lack of competition with domestic grazers, prairie dog burrows were feared to be hazardous to livestock health, should an animal step in one. Additionally, colonies interfered with the placement of structures such as railroads (Wuerthner 1997). Declines in prairie dog numbers were also brought about by Sylvatic plague (*Yersinia pestis*) (Pauli and Buskirk 2006), which can decimate entire colonies and make it difficult for populations to persist (Antolin et al. 2002).

In places trying to protect this species such as Theodore Roosevelt National Park (TRNP), mapping colonies and their potential expansion is essential. By monitoring colony boundaries over multiple years, managers can gauge whether colonies are expanding, remaining the same, or declining. For other national parks such as Wind Cave National Park and Badlands National Park, colony size and expansion is crucial for the

prospect of reintroducing the critically endangered black-footed ferret, since prairie dogs are their primary food source and must be abundant enough to sustain a population. Additionally, colony size and expansion information can be useful when trying to manage for other species on the landscape such as bison who may benefit from the increased forage biomass available on prairie dog towns (Coppock et al. 1983, Archer et al. 1987).

Current methods of mapping prairie dog colonies require sending personnel into the field to walk the colony boundaries on foot and mark active peripheral burrows with a handheld Global Positioning System (GPS). General guidelines for considering a burrow as “active” include finding fecal pellets, tracks, freshly disturbed dirt, or lack of vegetation around the mound (Milne 2004). However, ground mapping is suspected to be inaccurate because perimeter mounds are often hard to identify. Outermost entrances to the colony are usually smaller mounds, exhibit no mound at all, or are surrounded by taller vegetation and are therefore missed on ground observations (Hoogland 2013).

With increasing availability of high-resolution imagery and continued advances in technology, remote sensing has the potential to be a useful tool for mapping prairie dog colonies. Managers are looking for mapping methods to be informative, reliable, cost-effective, and accurate, and remote sensing using unmanned aircraft systems (UAS) may provide these advantages (Alvarez-Taboada et al. 2017). UAS have been used to collect imagery for a wide variety of ecological objectives such as counting hippos (Linchant et al. 2018), measuring habitat quality for least bitterns (Chabot et al. 2014), and locating chimpanzee nests and trees (VanAndel et al. 2015). Hasan (2019) used UAS to collect imagery of a prairie dog colony to understand burrow spatial structuring, but they relied

on human visual detection for counting burrows in the imagery and found similar results to ground surveys. My study aims to test the effectiveness of computer-based classification to detect and map prairie dog burrows.

Two methods for computational analysis of remotely sensed data are pixel-based and object-based classifications. Pixel-based methods include maximum likelihood (Erdas 1999) and support vector machines (SVM) (Cortes and Vapnik 1995). Both of these methods are available in geographic information systems (GIS) software, in addition to a variety of other software tools. Object-based image analysis (OBIA) is implemented in specialized software, such as Trimble's eCognition (version 9.1.2, Trimble 2015). GIS is readily available as a commercial application such as ESRI ArcGIS (version 10.6, ESRI) which is used by many higher education institutions, state and federal agencies, and in open source formats such as QGIS (QGIS Development Team) available to anyone at no cost. Trimble's eCognition is less commonly used and available only as a commercial product.

In this chapter I will evaluate the use of remotely sensed data collected via a small UAS for prairie dog colony mapping. I will classify prairie dog mounds using standard pixel-based statistical methods available in most GIS software and using object-based methods in eCognition software, then determine which method of computational analysis yields better accuracy.

## METHODS

### *Study Area*

This research was conducted over the summer of 2018 in TRNP, which is located in the semi-arid region of southwestern North Dakota. TRNP is comprised of three

geographically separate units, two of which were included in this study. The larger South Unit (18,756 hectares) is located in Billings County, while the smaller North Unit (9,741 hectares) is located about 80 km to the north in McKenzie County. Two prairie dog colonies of interest in the South Unit were identified: Beef Corral and Lindbo Flats. The Beef Corral prairie dog colony is bounded by the Little Missouri River on the west and the paved park road cuts directly through the colony. The Lindbo Flats prairie dog colony is larger in size and occupies a relatively flat plain with the park boundary fence running through it.

#### *Data Acquisition*

In the summer of 2018, a University of North Dakota (UND) research crew from the Department of Biology flew a fixed-wing Trimble UX5. Flights followed preprogrammed parallel line transects that permitted adequate overlapping photography of ground survey areas. Image overlap was 80%. Flights were conducted at 75m and then 90m for each site. Unmanned aircraft systems flight operations for this research were approved by the National Park Service (Study #THRO-00099, Permit #THRO-2018-SCI-0010). All remotely sensed data used in this research are listed in Table 6.

**Table 6: Images used for classification and their temporal, spatial, and spectral characteristics. Only portions of the full extent produced by each flight were classified.**

<b>Image</b>	<b>Temporal Resolution</b>	<b>Spatial Resolution</b>	<b>Spatial Extent</b>	<b>Spectral Bands</b>
BeefCorral75(1)	June 2018	2.26 cm	612 m <sup>2</sup>	R-G-B
BeefCorral75(2)	June 2018	2.26 cm	662 m <sup>2</sup>	R-G-B
Lindbo75(1)	June 2018	2.24 cm	134 m <sup>2</sup>	R-G-B
Lindbo75(2)	June 2018	2.24 cm	105 m <sup>2</sup>	R-G-B
Lindbo75NIR(1)	June 2018	2.18 cm	134 m <sup>2</sup>	R-G-NIR
Lindbo90(1)	June 2018	2.7 cm	134 m <sup>2</sup>	R-G-B



## *Image Classification*

The overall image classification workflow was structured in three main parts: data pre-processing, classification, and validation (Chapter 2, Figure 3). This is true for classifications performed in ArcGIS as well as eCognition. The workflow is described in more detail in Chapter 2. I subset each image into two smaller portions to increase processing time: Beef Corral subsets are depicted in Figure 13 and Lindbo Flats subsets are in Figure 14.

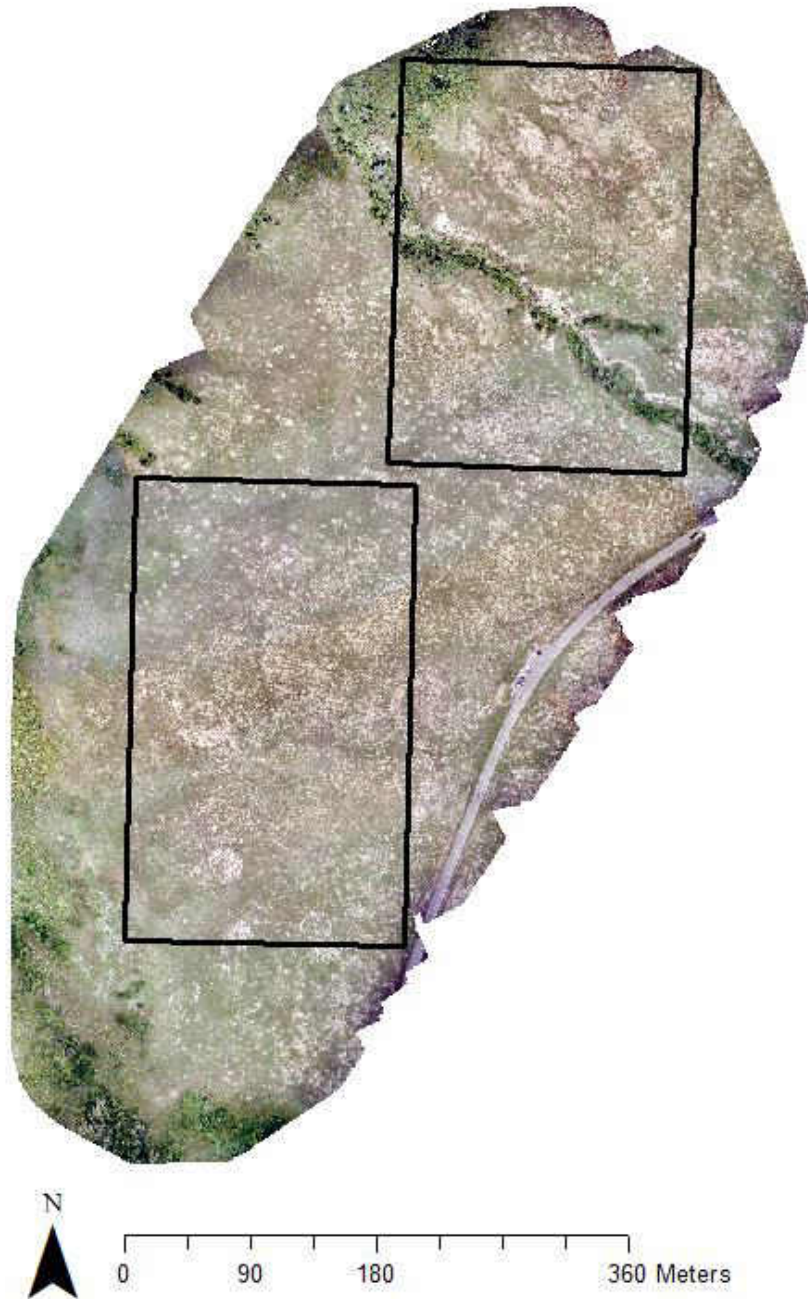


**Figure 13:** Beef Corral prairie dog colony mosaic image collected from low-flying UAS. Each box represents a small subset that was used for classification via pixel-based and object-based methods. The box on top corresponds to the BeefCorral75(1) classifications and the box on the bottom corresponds to the BeefCorral75(2) classifications.

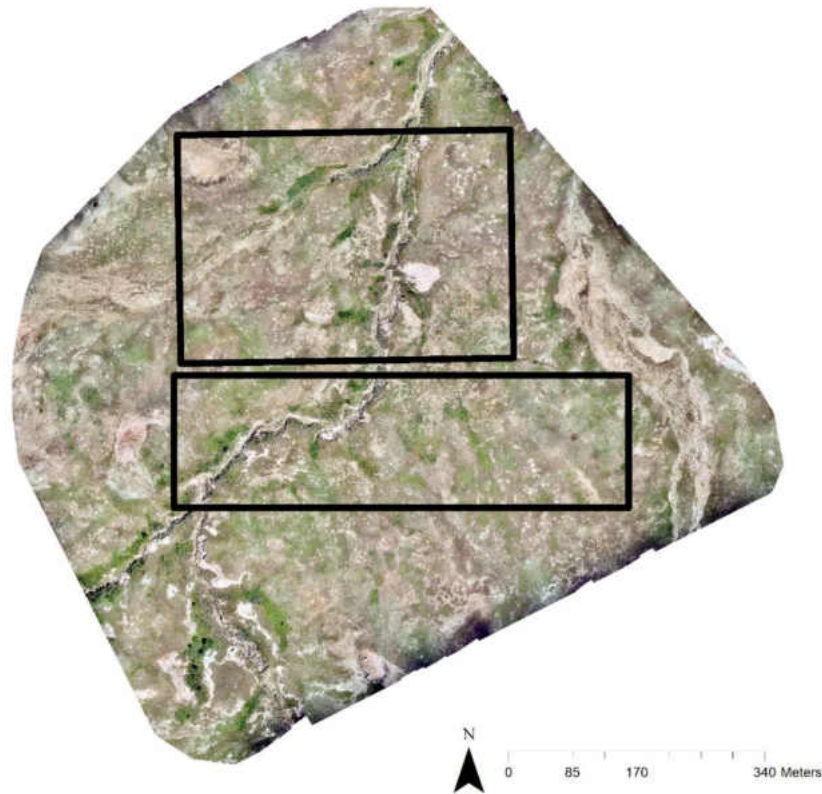


**Figure 14:** Lindbo Flats prairie dog colony mosaic image collected via low-flying UAS. Each box represents a small subset that was used for classification via pixel-based and object-based methods. The box on top corresponds to the Lindbo75(1) classifications and the box on the bottom corresponds to the Lindbo75(2) classifications.

I used ArcGIS (version 10.6, ESRI) to perform pixel-based classifications of the imagery using the following supervised methods: maximum likelihood and SVM. The maximum likelihood classifier is the best-known algorithms for supervised image classification (Erdas 1999). The SVM classifier groups similar pixels based on spectral values and creates pseudo-objects in n-dimensional space (segmentation), which are then used to create training samples (Cortes and Vapnik 1995). A series of segmentations were tested by adjusting the parameters of spectral detail and spatial detail. Spectral detail refers to the level of importance given to spectral features in the image, whereas spatial detail refers to the level of importance given to the proximity between features. The final image segmentations parameters were achieved using spectral detail of 15, spatial detail of 15, minimum segment size of 20, and band indexes 1, 2, and 3. Multiple training samples were created for each class then merged to form a reliable sample for the whole image. These training samples were then used by the classifier to identify classes that I delineated and assign pixels to the appropriate classes.

I performed object-based image analysis (OBIA) using eCognition Developer (version 9.1.2, Trimble 2015). Then I tested a series of segmentations by adjusting the parameters of scale, shape, and image weighting. Scale adjusts how large or small the desired image objects will be, shape adjusts the relationship between color and shape criteria for the resulting segments, compactness adjusts the overall area of the resulting segments, and image weighting refers to the importance given to each spectral band (El-naggar 2018). The final image segmentations were achieved using a scale of 40, image layer weights of 1, 1, and 1, shape of 0.2, and compactness of 0.6. I used the Nearest Neighbor (NN) classifier to classify objects based on training samples I created.

Classification parameters included mean color, brightness, standard deviation, maximum difference, area, shape, and mathematical band indices. After initial classification, I created rules and tested them until a ruleset was developed. This process is described in more detail in Chapter 2.

I performed error and accuracy assessments in the ArcGIS environment for both pixel based and OBIA classification techniques. I created confusion matrices where omission (false negatives) and commission (false positives) errors were quantified and examined. ArcGIS calculated a  $K_{HAT}$  (Kappa) statistic for each matrix, which gives an estimate for the measure of actual agreement within a confusion matrix (Congalton and Mead 1983). The Kappa statistic can be used to show how your classification performs against a completely random classification ( $Kappa = 0$ ) (Congalton and Green 1999). Since I am attempting to determine the accuracy of a small feature of interest (prairie dog mounds), I performed equalized accuracy assessments with a minimum of 100 sample points per class. I used this approach because rare-class sample sizes are often small when using stratified random sampling (Stehman and Foody 2009) and therefore results in a sampling deficiency for prairie dog mounds. For equalized accuracy assessments, overall accuracy for the entire classification and Kappa are less informative. Instead, producer's and user's accuracy for prairie dog mounds specifically are better at showing how the classifier performed. Producer's accuracy is a measure of errors of omission (i.e. X% of prairie dog mounds correctly classified as prairie dog mounds), while user's accuracy is a measure of errors of commission (i.e. Y% of objects classified as prairie dog mounds that were not actually prairie dog mounds).

### *Perimeter Delineation*

I converted objects classified as prairie dog mounds for the entire raster to point features using the *Feature to Point* tool in ArcGIS. I then input the point data into the *ConcaveHull* (Fairhurst 2012) tool to create a perimeter polygon for the colony. None of the UAS imagery used in this study contains the true perimeter of the colonies, but one small area in BeefCorral75 can be compared with ground-data for testing this method. I used the *Select by Attributes* function in ArcGIS to remove mounds from the image that were located to the east of the park road, to the northeast of the stream that cuts through the image, and to the south of the southernmost line of trees. This minor digitization allowed for the comparison of ground-data from 2016 and 2018 with the *ConcaveHull* output.

## RESULTS

SVM classifications in ArcGIS yielded highly inaccurate results for detecting prairie dog mounds. Errors of omission ranged from 74% to 88%, while errors of commission ranged from 87% to 97%. The maximum likelihood classifier in ArcGIS produced images that were more accurate than the SVM approach, but only modestly so. Classifications produced by pixel-based methods in ArcGIS exhibited large areas of land that were incorrectly classified as prairie dog mounds (Figure 15C and 15D). Each mound is only around one meter across and therefore should appear as small dots on the image, just as they do in the base imagery (Figure 15A). Images processed using the OBIA approach in eCognition produced much higher accuracies for detecting prairie dog mounds. Errors of omission for prairie dog mounds ranged from 4% to 35%, while errors of commission ranged from 49% to 79% (Table 7). The decrease in errors can be seen by

looking at the image; prairie dog mounds have been correctly classified as small, round objects (Figure 15B). This much more closely reflects what the human eye can see in the base imagery.

The ruleset I created in eCognition was developed for the BeefCorral image. That ruleset was used to classify all other images – including those taken at Lindbo Flats, an entirely different prairie dog colony that exhibits different landscape characteristics – to test for the transferability of these rulesets. By all classification modes, images that contained R-G-B bands performed better than images with R-G-NIR.

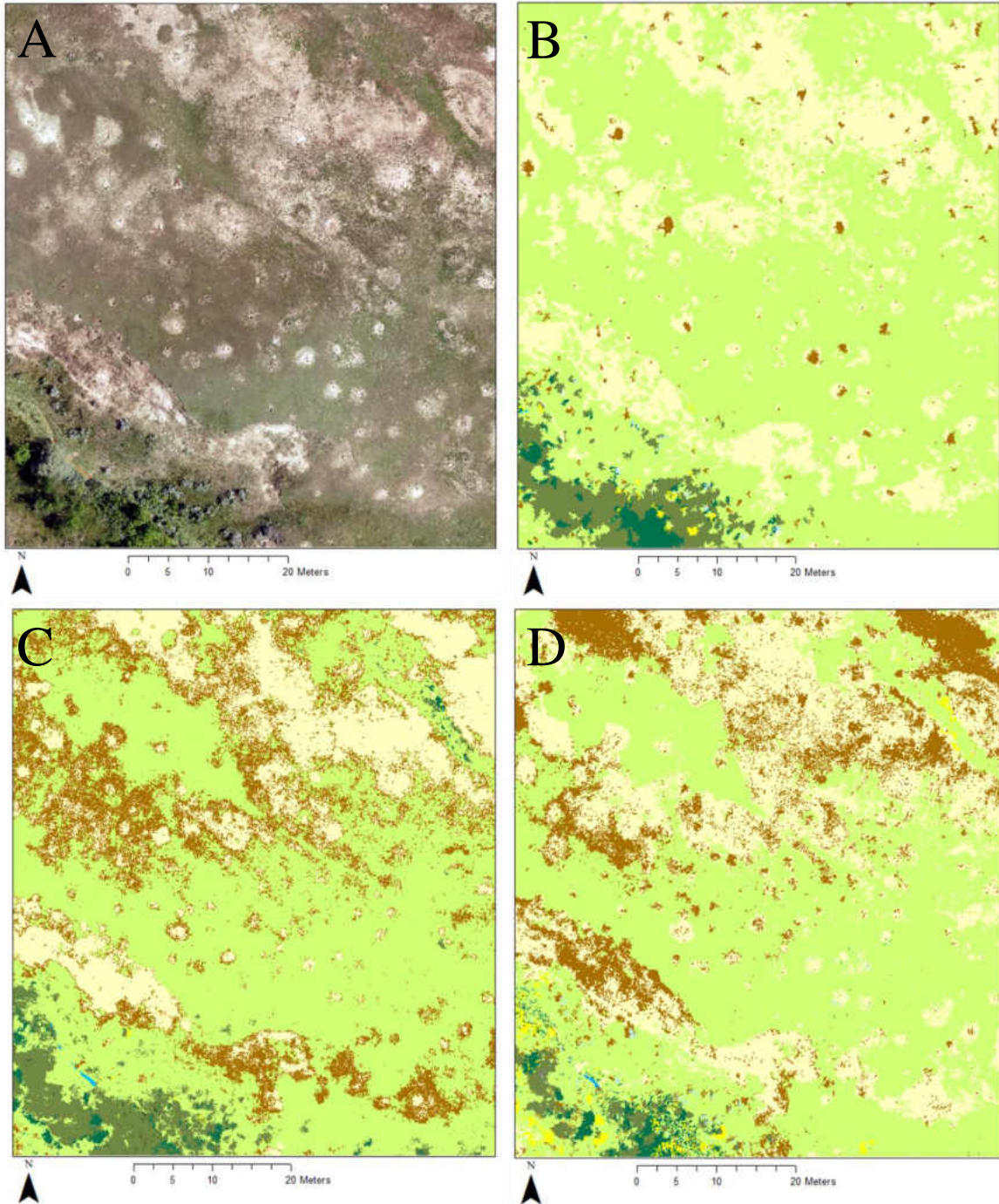


**Figure 15:** A) BeefCorral75(1) base image used for classification B) Classification produced using OBIA in eCognition C) Classification produced using maximum likelihood in ArcGIS D) Classification produced using SVM in ArcGIS. The brown color in the classification corresponds to prairie dog mounds, the off-white corresponds to bare ground, and the light green corresponds to short grasses.



**Table 7: Percent omission and commission error for prairie dog mounds for each classification of Beef Corral and Lindbo Flats taken via UAS**

<b>Classification Method</b>	<b>No. Accuracy Points</b>	<b>Percent Omission Error</b>	<b>Percent Commission Error</b>
<b>SVM</b>			
BeefCorral75(1)	100	74%	87%
BeefCorral75(2)	113	88%	97%
<b>MAXL</b>			
BeefCorral75(1)	111	67%	94%
BeefCorral75(2)	111	87%	97%
Lindbo75(1)	125	65%	92%
Lindbo75(2)	125	50%	89%
Lindbo75NIR(1)	114	67%	92%
Lindbo90(1)	107	59%	89%
<b>OBIA</b>			
BeefCorral75(1)	100	4%	49%
BeefCorral75(2)	100	27%	50%
Lindbo75(1)	110	20%	59%
Lindbo75(2)	111	21%	58%
Lindbo75NIR(1)	106	35%	79%
Lindbo90(1)	106	14%	65%

Notes: All UAS images are R-G-B unless otherwise stated in the image name. The higher the percentage, the more errors the classifier made.

The resulting perimeter based on all input points surrounded the entire image mosaic except for a few small sections of trees (Figure 16). This is expected since the colony extends past the boundaries of the UAS image and therefore prairie dog mounds can be seen even at the image edge. The isolation of the center portion of the colony (bounded by the park road and trees) allowed for adequate comparison between years (Figure 17). The boundary for that portion of the colony was larger in size in classified imagery than was mapped on foot: the perimeter from the 2016 ground data was 17.82 hectares, the perimeter from the 2018 ground data was 17.36 hectares, and the perimeter from the 2018 classification was 19.89 hectares. This means that in 2018, 13.58% of the colony was undetected on foot.

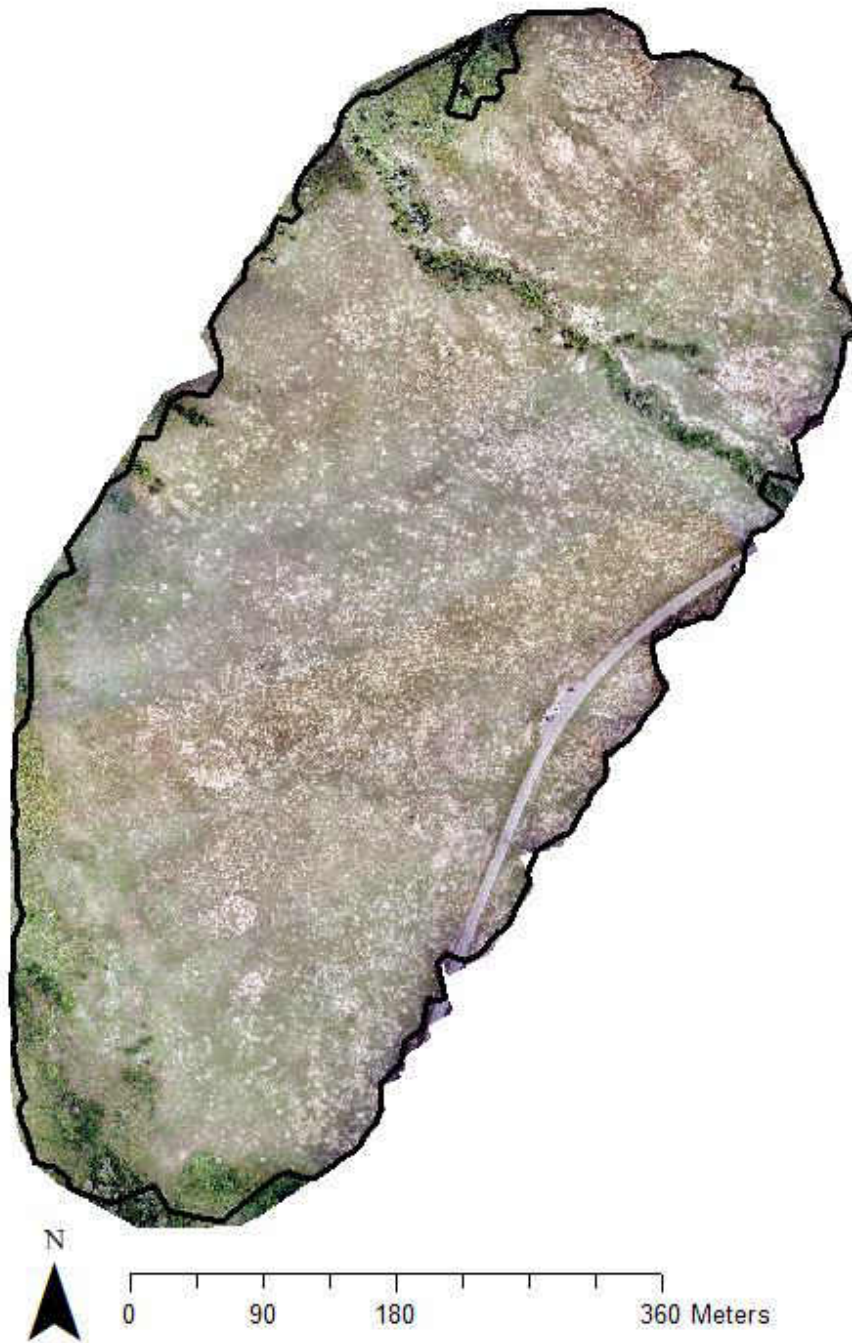


**Figure 16:** Beef Corral colony perimeter (black line) as mapped by the *ConcaveHull* tool in ArcGIS. This perimeter accurately follows the edge of the image mosaic and correctly excludes small sections of trees where there were no prairie dog mounds. The perimeter was estimated from the classified map but displayed over the original mosaic to visualize the relationship.

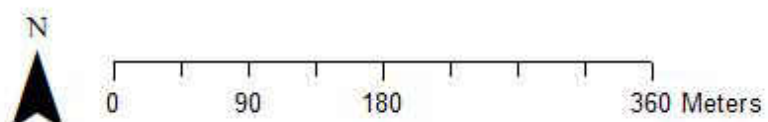
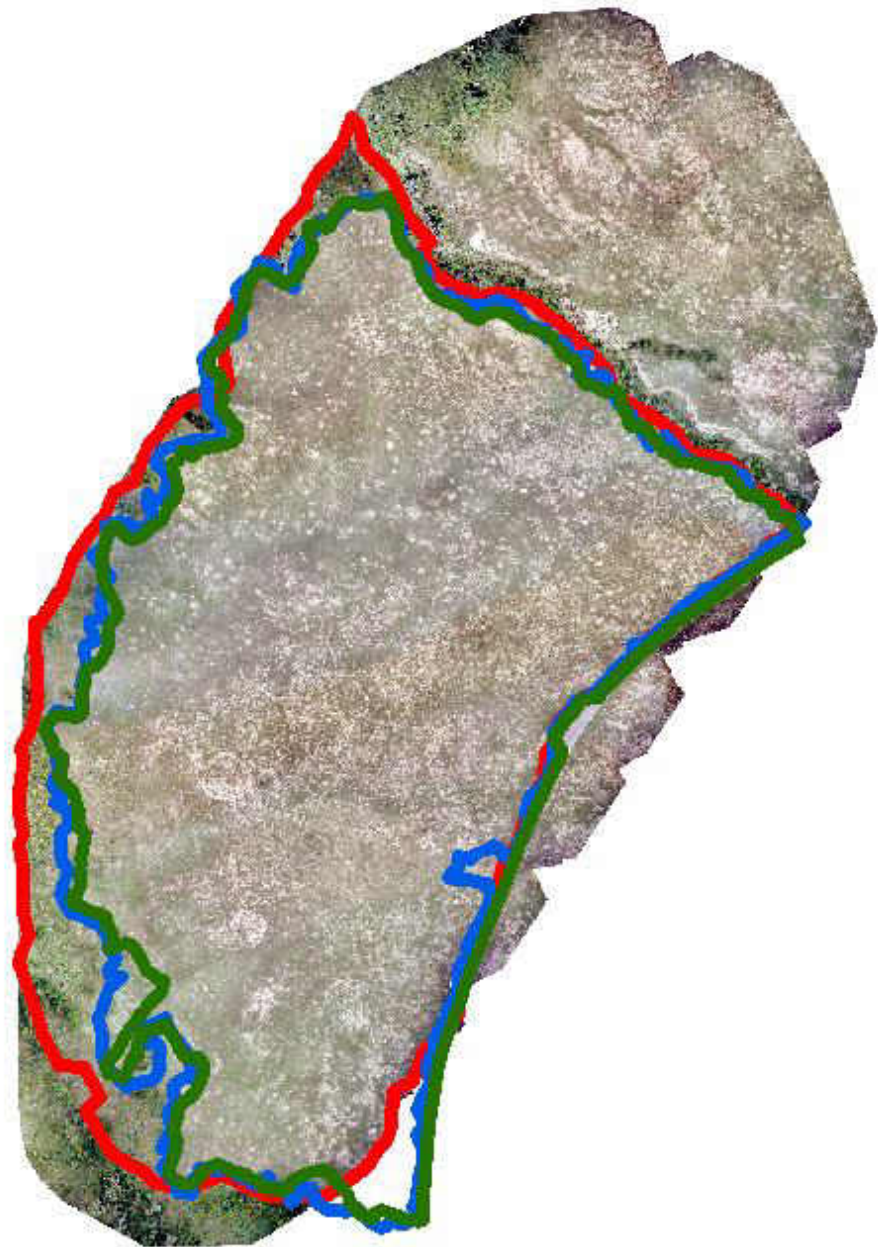


**Figure 17:** Colony perimeters for a central piece of the Beef Corral prairie dog colony. Ground data collected in 2016 is shown in blue, ground data collected in 2018 is shown in green, and the perimeter based on the image classification for 2018 is shown in red.

## DISCUSSION

R-G-B images obtained by low-flying small UAS and processed using OBIA achieved the highest accuracy among the methods I tested for detecting prairie dog mounds in TRNP. The best pixel-based classifier was maximum likelihood, but it only detected prairie dog mounds half of the time. In all classifications of all modes, user's accuracy was lower than producer's accuracy. This means that errors of commission were more frequent than errors of omission. Although the maps produced here may be accurate, they may not be as reliable for field use (i.e. locating individual mounds on foot using the classified imagery as a map). The classes most commonly confused with prairie dog mounds were bare ground and short/clipped grasses. This intuitively makes sense as prairie dog mounds essentially are bare ground.

Individual prairie dogs can sometimes be identified with the naked eye in the imagery but were not segmented as separate objects in eCognition. Decreasing the segmentation parameter or obtaining even higher resolution imagery (< 2cm) may be able to delineate prairie dogs as individual objects, but this would drastically increase processing time and therefore was not tested in this work. However, future work may look at this and use classified prairie dogs in the imagery as another parameter for identifying mounds. It remains to be seen if individual prairie dogs can be reliably and consistently discerned in images.

The classifications achieved using eCognition in this research were performed using the same ruleset for every image. This shows the transferability of rulesets from one image to another. Of note is that the paved park road cuts through the Beef Corral prairie dog colony but cannot be seen in the Lindbo Flats colony. Since the ruleset was

developed for an image with a park road in it, some objects in the Lindbo Flats classifications were misclassified as park road when that class should not have been exhibited at all. However, this did not drastically impact overall accuracy for detecting prairie dog mounds. Individual image accuracy could be increased by creating a new ruleset specific to each image, but that is inefficient. This work demonstrates that rulesets can be transferred between images with relatively high success, especially between images of the same spectral resolution (i.e. R-G-B to R-G-B).

Although the UAS images taken in 2018 did not capture any prairie dog colony boundaries, the methods presented in this study demonstrate a possible workflow for doing this work. Since no colony edge was present in the imagery, the image mosaic boundary was treated as a pseudo-perimeter for methods testing. The *ConcaveHull* tool accurately delineated the image mosaic based on burrow locations. I did minor digitization that took approximately 10 minutes. This step was necessary to remove mounds to the north-east of the northern tree line, mounds to the east of the park road, and erroneous mounds south of the southern tree line; this allowed for comparison of just the center piece of the colony since that was mapped as a separate piece in the ground truthed data. In a mosaicked photo of the entire colony, this type of minor digitization would not be needed. The boundary for the center portion of Beef Corral covered more area than the ground data and incorporated more taller vegetation within the colony boundary. By reviewing the imagery by eye, mounds can be seen in the taller vegetation that were likely missed on foot. This shows promise for using remote sensing for prairie dog colony mapping.

For high resolution imagery, such as that derived from low altitude UAS flights, computational limitations of object-based classifications on single workstations remain a concern. A computer with dual processors and 128 GB of RAM was not able to handle entire UAS images in a single analysis (files of 1 to 3 GB in size). This is a common problem with a simple solution: tiling the large image into manageable rectangles and processing each separately. The resulting rasters can then be reassembled to produce a complete map. For the purpose of my thesis, I had to subset the UAS images for faster processing. Cloud or cluster computing is a potential option for this work in the future as it will drastically speed up processing times, however that increases the cost since extra software licenses will have to be purchased.

Previous studies have determined that a data fusion approach is most ideal for producing accurate studies of natural systems (Marvin et al. 2016), and the same can be applied for increasing accuracy in detecting prairie dog mounds via the methods described in this paper. In addition, texture may be able to aid in mound identification because of prairie dogs disrupting surface soil outside of their burrows.

This research has demonstrated that classification of UAS imagery via eCognition is a viable strategy for detecting and mapping prairie dog colonies. Classified images captured more of the colony that was missed in ground observations. The knowledge gained from these types of analyses can be used to analyze colony growth and assess colony health.

## LITERATURE CITED

- Alvarez-Taboada, F., C. Paredes, et al. (2017). "Mapping of the Invasive Species *Hakea sericea* Using Unmanned Aerial Vehicle (UAV) and WorldView-2 Imagery and an Object-Oriented Approach." *Remote Sensing* 9(9): 913.
- Antolin, M. F., P. Gober, et al. (2002). "Influence of Sylvatic Plague on North American Wildlife at the Landscape Level, with Special Emphasis on Black-footed Ferret and Prairie Dog Conservation." *Transactions of the Sixty-Seventh North American Wildlife and Natural Resources Conference*.
- Archer, S., M. Garrett, et al. (1987). "Rates of vegetation change associated with prairie dog (*Cynomys ludovicianus*) grazing in North American mixed-grass prairie." *Vegetatio* 72(3): 159-166.
- Biggins, D. E., B. J. Miller, et al. (1993). "A technique for evaluating black-footed ferret habitat." *Management of prairie dog complexes for the reintroduction of the black-footed ferret*. US Fish and Wildlife Service Biological Report 13: 73-88.
- Chabot, D., V. Carignan, et al. (2014). "Measuring habitat quality for least bitterns in a created wetland with use of a small unmanned aircraft." *Wetlands* 34(3): 527-533.
- Congalton, R. G. and K. Green (1999). *Assessing the Accuracy of Remotely Sensed Data: Principles and Practices*. Boca Raton, FL, Lewis Publishers.
- Congalton, R. G. and R. A. Mead (1983). "A quantitative method to test for consistency and correctness in photointerpretation." *Photogrammetric engineering and remote sensing* 49(1): 69-74.



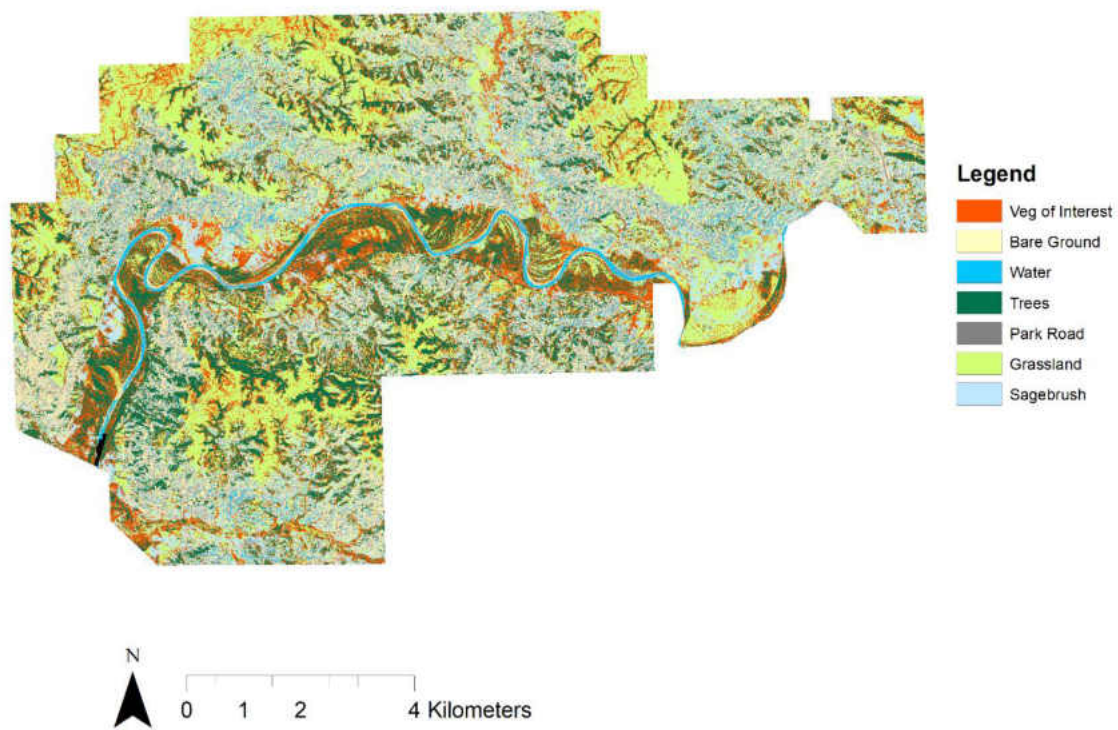
- Coppock, D. L., J. Detling, et al. (1983). "Plant-herbivore interactions in a North American mixed-grass prairie. I. Effects of black-tailed prairie dogs on intraseasonal aboveground plant biomass and nutrient dynamics and plant species diversity." *Oecologia* 56(1): 1-9.
- Cortes, C. and V. Vapnik (1995). "Support-vector networks." *Machine learning* 20(3): 273-297.
- Detling, J. K. (1998). "Mammalian herbivores: ecosystem-level effects in two grassland national parks." *Wildlife Society Bulletin* 26(3).
- Detling, J. K. and A. D. Whicker (1987). Control of ecosystem processes by prairie dogs and other grassland herbivores. Great Plains Wildlife Damage Control Workshop Proceedings.
- El-naggar, A. M. (2018). "Determination of optimum segmentation parameter values for extracting building from remote sensing images." *Alexandria engineering journal*.
- Erdas Inc. (1999). *ERDAS Field Guide*. Atlanta, Georgia. 672: 94.
- ESRI. *ArcGIS Desktop: Release 10*. Redlands, CA: Environmental Systems Research Institute.
- Fairhurst, R. (2012). *ConcaveHull Tool for ArcGIS*.
- Hasan, E. (2019). Comparative analysis of prairie dog colony spatial structure. *Ecology and Evolutionary Biology*. Boulder, Colorado, University of Colorado, Boulder.
- Holland, E. A. and J. K. Detling (1990). "Plant response to herbivory and belowground nitrogen cycling." *Ecology* 71(3): 1040-1049.

- Hoogland, J. (2013). Conservation of the black-tailed prairie dog: saving North America's western grasslands, Island Press.
- Hoogland, J. L. (1995). The black-tailed prairie dog: social life of a burrowing mammal, University of Chicago Press.
- Jensen, J. R. (1996). Introductory Digital Image Processing: A Remote Sensing Perspective. Upper Saddle River, NJ, Prentice Hall.
- Li, H., H. Gu, et al. (2006). Fusion of High-Resolution Aerial Imagery and Lidar Data for Object-Oriented Urban Land-Cover Classification Based on SVM. ISPRS Workshop on Updating Geo-spatial Databases with Imagery & The 5th ISPRS Workshop on DMGISs.
- Linchant, J., S. Lhoest, et al. (2018). "UAS imagery reveals new survey opportunities for counting hippos." PLoS One 13(11): e0206413.
- Marvin, D. C., L. P. Koh, et al. (2016). "Integrating technologies for scalable ecology and conservation." Global Ecology and Conservation 7: 262-275.
- Miller, B. J., R. P. Reading, et al. (2007). "Prairie Dogs: An Ecological Review and Current Biopolitics." Journal of Wildlife Management 71(8): 2801-2810.
- Miller, B., R. Reading, et al. (2000). "The role of prairie dogs as a keystone species: response to Stapp." Conservation Biology 14(1): 318-321.
- Milne, S. (2004). Population Ecology and Expansion Dynamics of Black-Tailed Prairie Dogs in Western North Dakota. Department of Biology. Grand Forks, North Dakota, University of North Dakota. Master of Science.

- Pauli, J. N. and S. W. Buskirk (2006). "A Plague Epizootic in the Black-Tailed Prairie Dog (*Cynomys ludovicianus*)." *Journal of Wildlife Diseases* 42(1).
- QGIS Development Team. (2019). QGIS Geographic Information System. Open Source Geospatial Foundation Project. <http://qgis.osgeo.org>
- Stehman, S. V. and G. M. Foody (2009). "Accuracy assessment." *The SAGE handbook of remote sensing*: 297-309.
- Trimble. (2015). *eCognition Developer: Release 9*. Sunnyville, CA: Trimble.
- Uresk, D. W. (1987). "Relation of black-tailed prairie dogs and control programs to vegetation, livestock, and wildlife."
- van Andel, A. C., S. A. Wich, et al. (2015). "Locating chimpanzee nests and identifying fruiting trees with an unmanned aerial vehicle." *Am J Primatol* 77(10): 1122-1134.
- Wuerthner, G. (1997). "Viewpoint: The black-tailed prairie dog - headed for extinction?" *Journal of Range Management* 50.

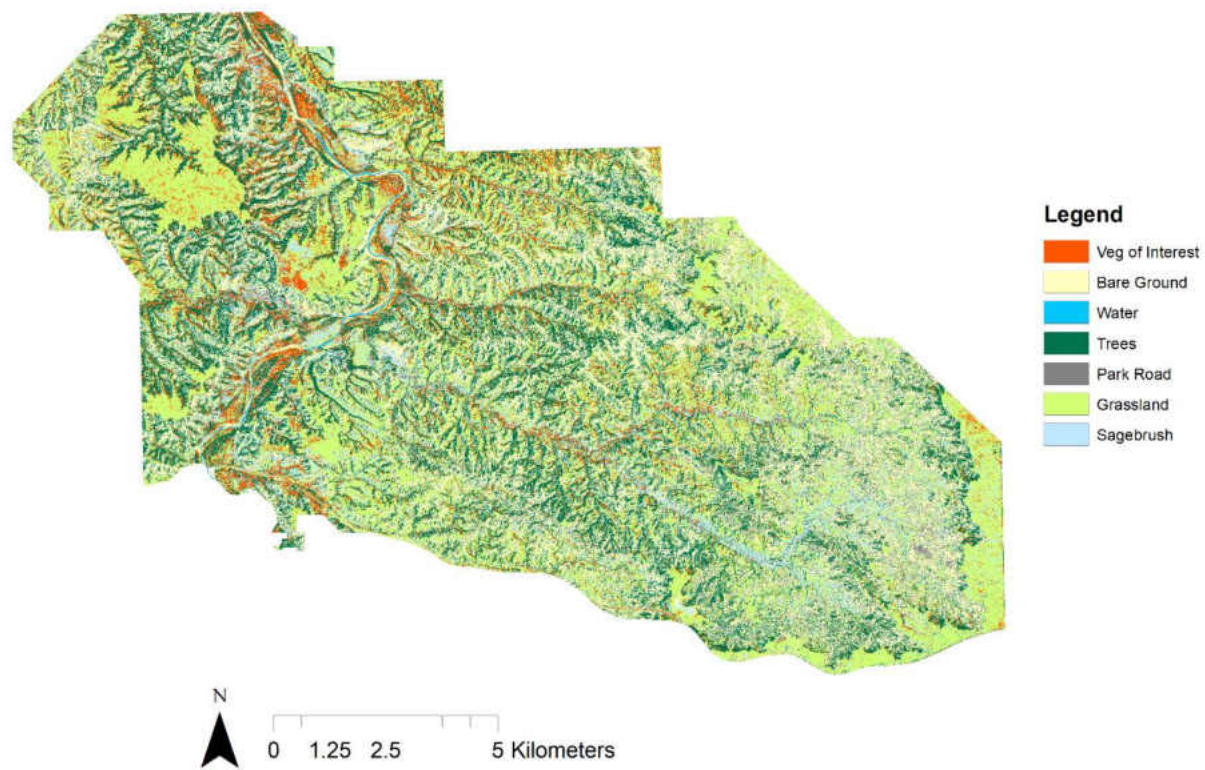
**APPENDIX A:**  
**CLASSIFICATION FIGURES**

Maximum Likelihood Classification of NUMosaic



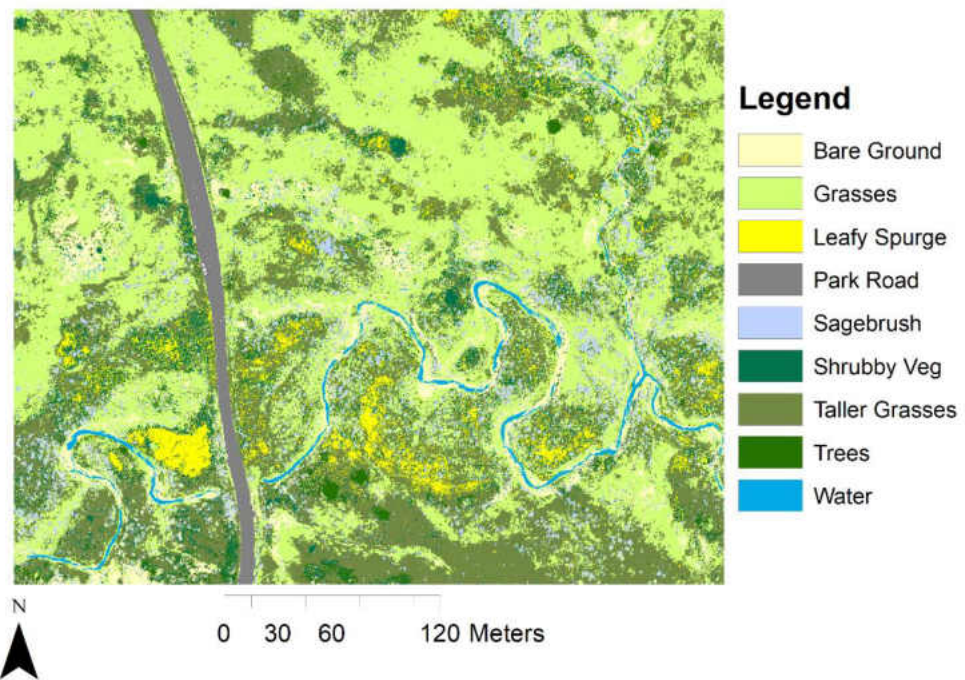
**Appendix A: Figure 1.** Maximum likelihood classification of the north unit of Theodore Roosevelt National Park from NAIP imagery.

Maximum Likelihood Classification of SUMosaic



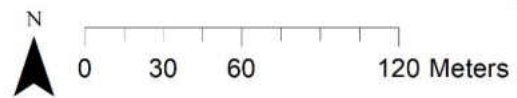
**Appendix A: Figure 2.** Maximum likelihood classification of the south unit of Theodore Roosevelt National Park from NAIP imagery.

### Object-based Classification of Talkington75(1)



**Appendix A: Figure 3.** Object-based classification performed on a subset of a UAS image.

### Object-based Classification of Talkington75(2)



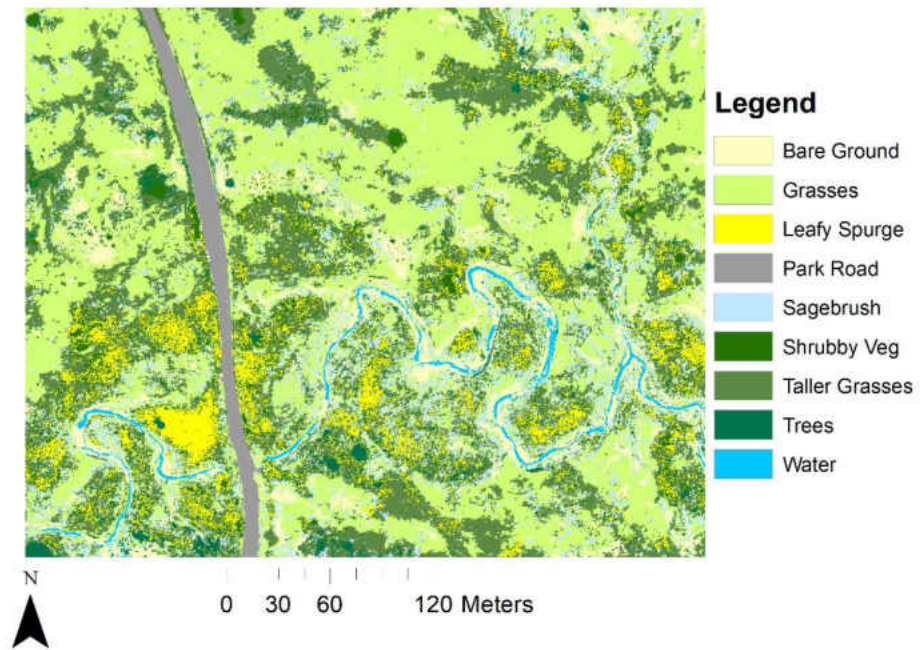
#### Legend



**Appendix A: Figure 4.** Object-based classification performed on a subset of a UAS image.

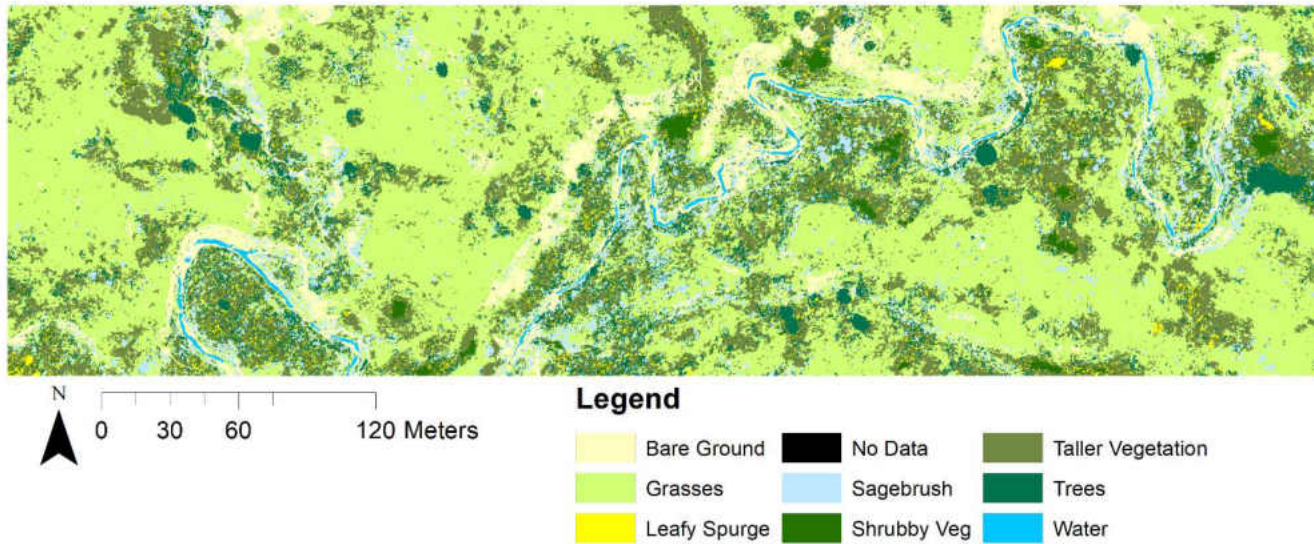


### Object-based Classification of Talkington75NIR(1)



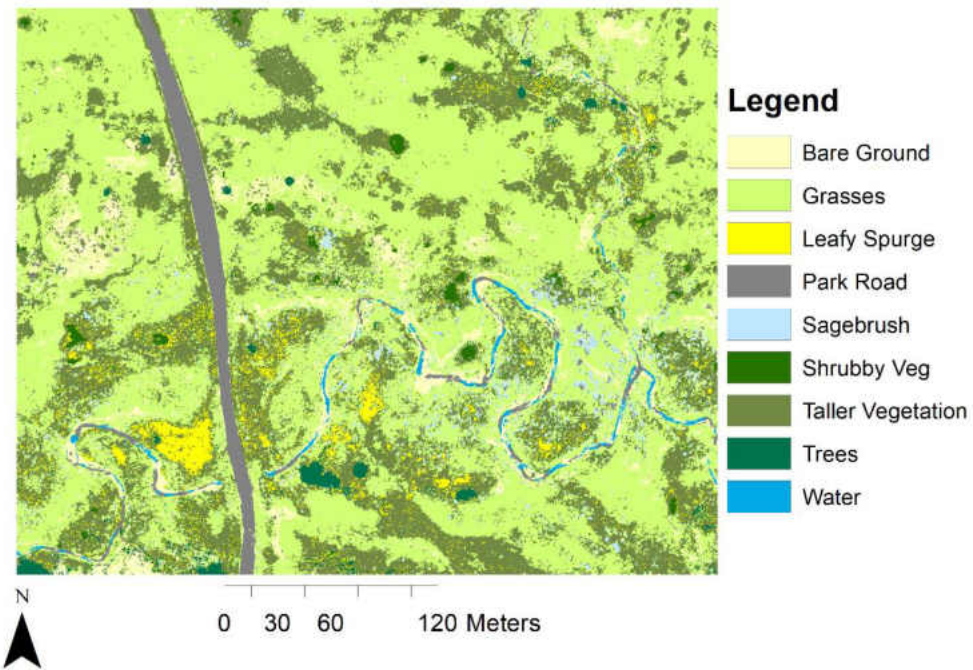
**Appendix A: Figure 5.** Object-based classification performed on a subset of a UAS image.

### Object-based Classification of Talkington75NIR(2)



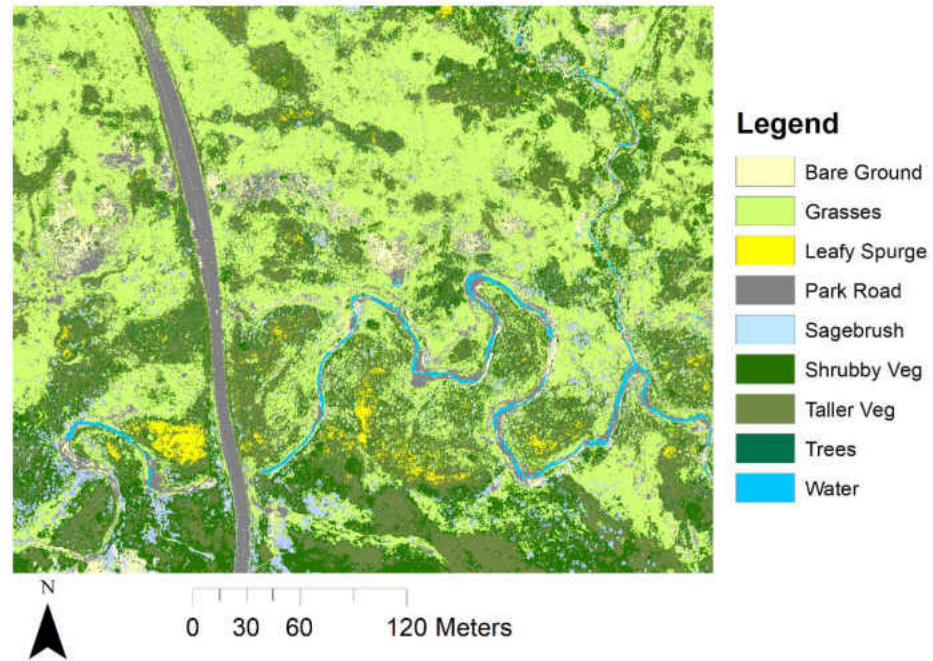
**Appendix A: Figure 6.** Object-based classification performed on a subset of a UAS image.

### Object-based Classification of Talkington90(1)



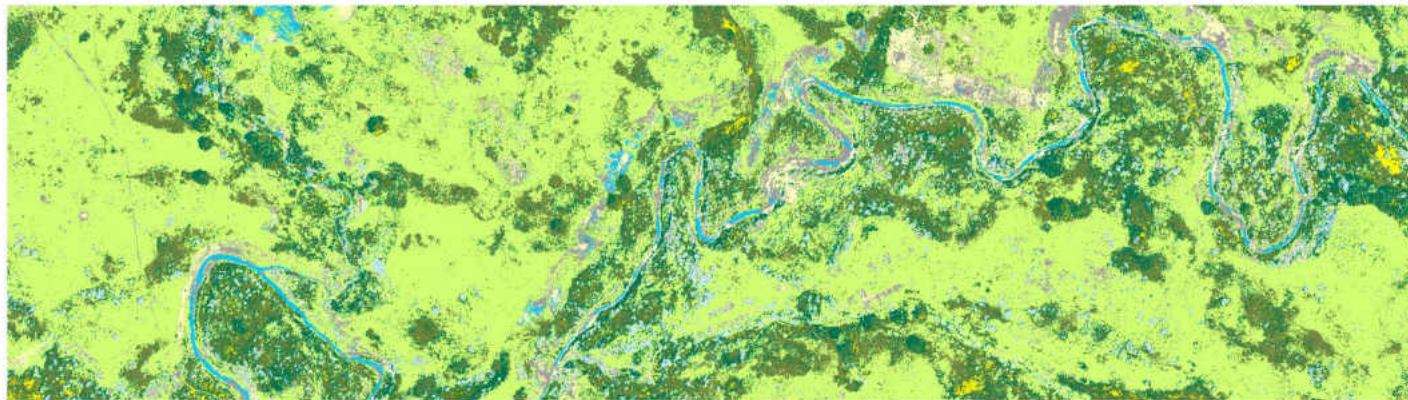
**Appendix A: Figure 7.** Object-based classification performed on a subset of a UAS image.

### Maximum Likelihood Classification of Talkington75(1)



**Appendix A: Figure 8.** Maximum likelihood classification performed on a subset of a UAS image.

### Maximum Likelihood Classification of Talkington75(2)

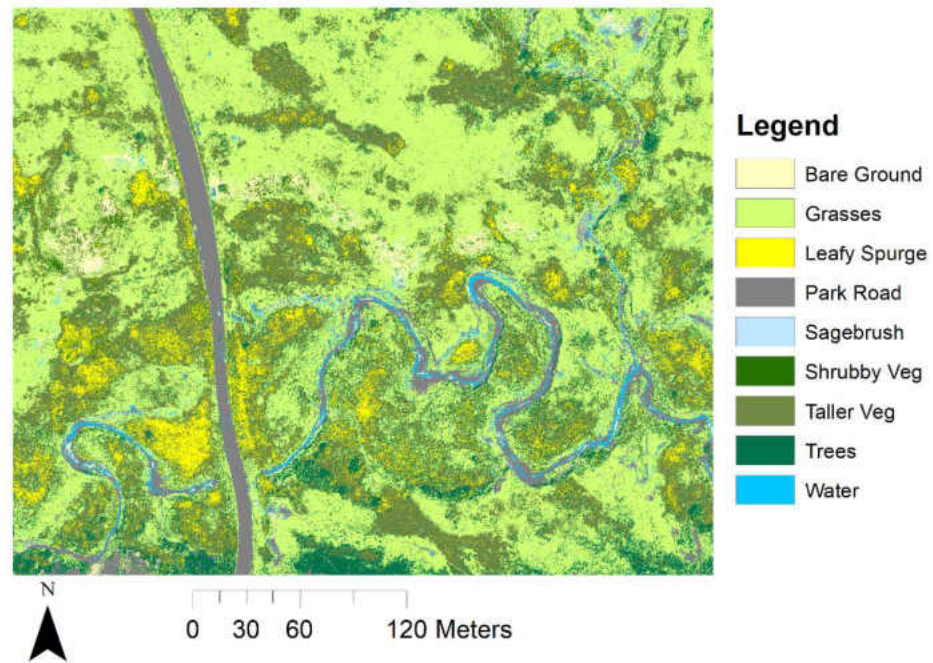


#### Legend

Bare Ground	Park Road	Taller Veg
Grasses	Sagebrush	Trees
Leafy Spurge	Shrubby Veg	Water

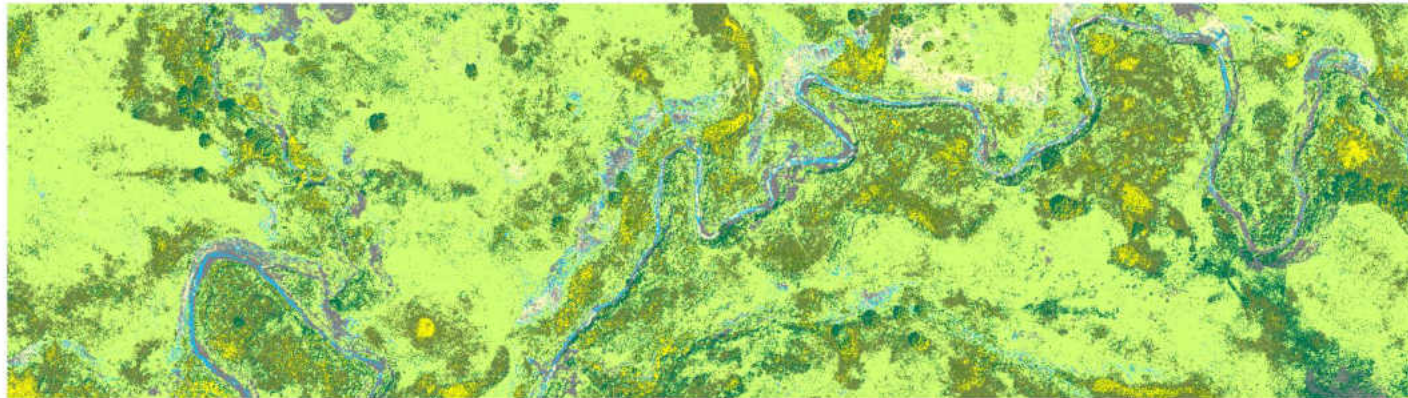
**Appendix A: Figure 9.** Maximum likelihood classification performed on a subset of a UAS image.

### Maximum Likelihood Classification of Talkington75NIR(1)



**Appendix A: Figure 10.** Maximum likelihood classification performed on a subset of a UAS image.

### Maximum Likelihood Classification of Talkington75NIR(2)

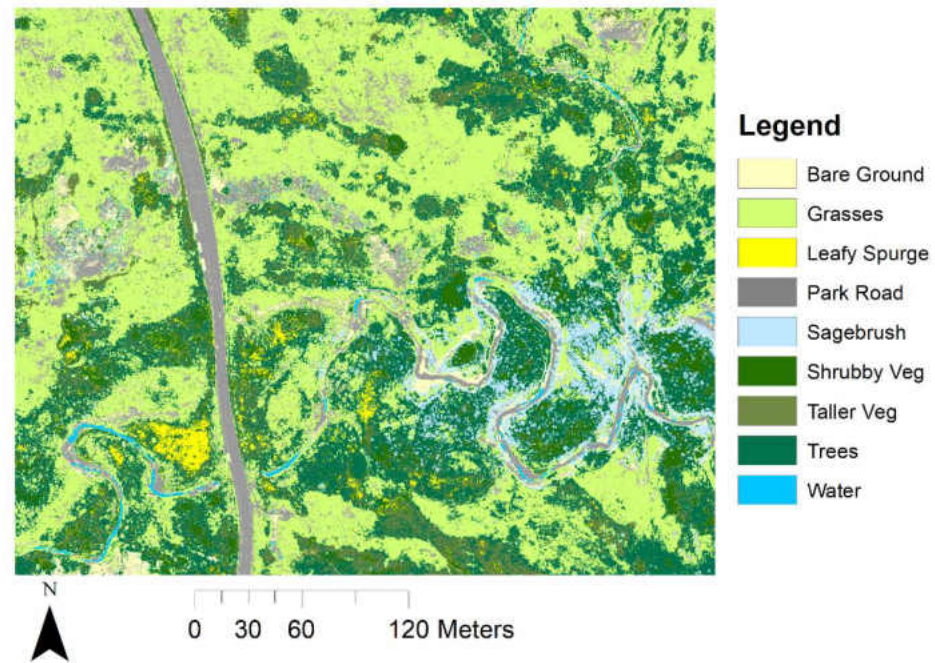


#### Legend

Bare Ground	Park Road	Taller Veg
Grasses	Sagebrush	Trees
Leafy Spurge	Shrubby Veg	Water

**Appendix A: Figure 11.** Maximum likelihood classification performed on a subset of a UAS image.

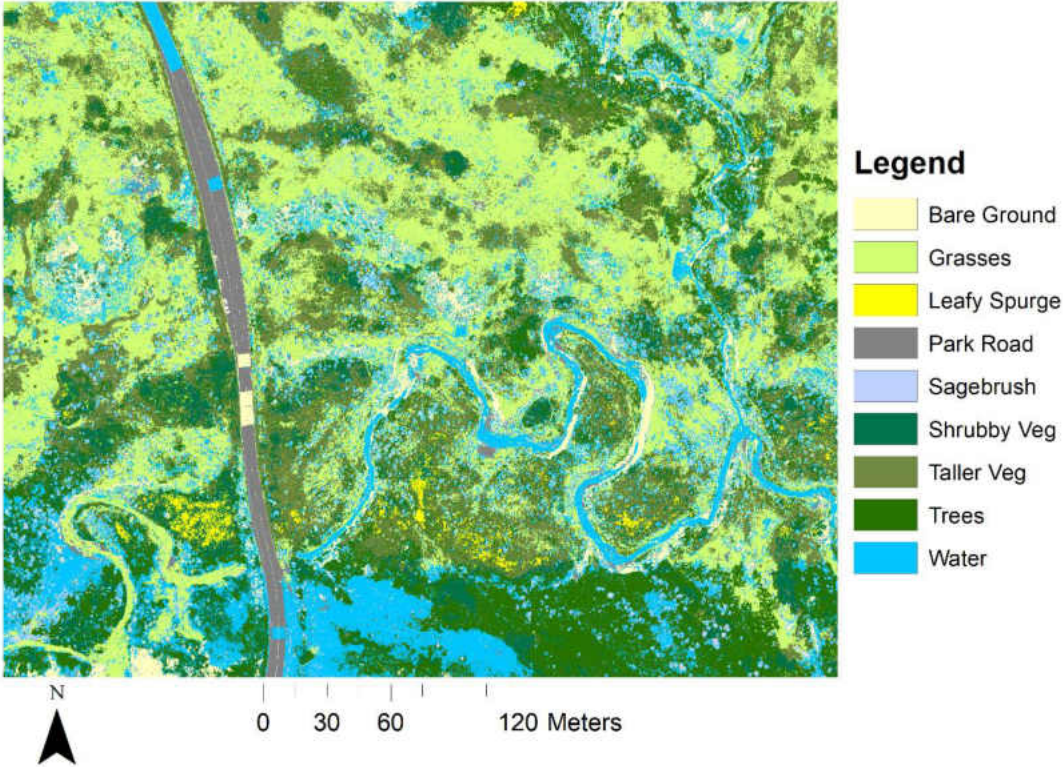
### Maximum Likelihood Classification of Talkington90(1)



**Appendix A: Figure 12.** Maximum likelihood classification performed on a subset of a UAS image.

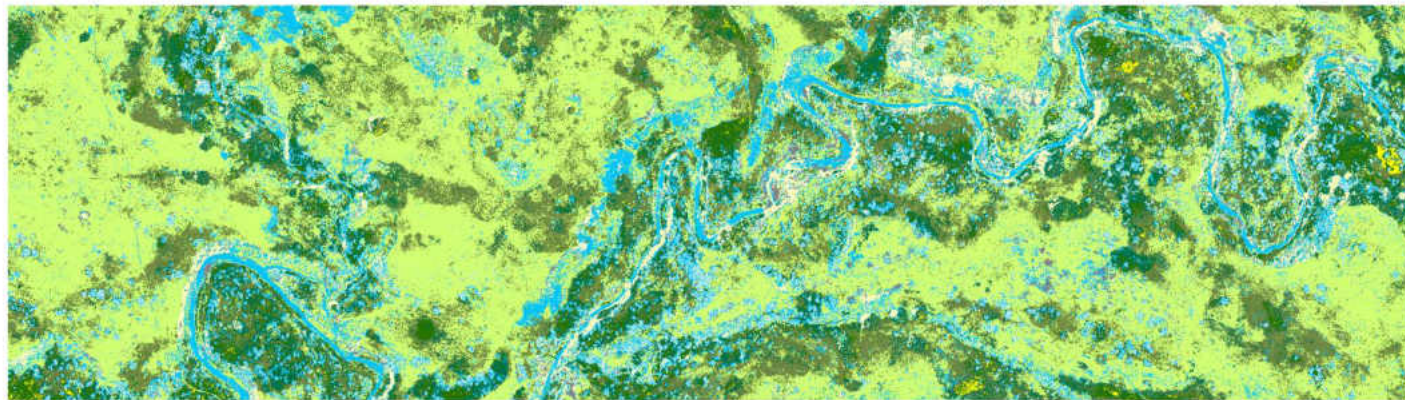


### Support Vector Machines Classification of Talkington75(1)



Appendix A: Figure 13. Support vector machines classification performed on a subset of a UAS image.

### Support Vector Machines Classification of Talkington75(2)

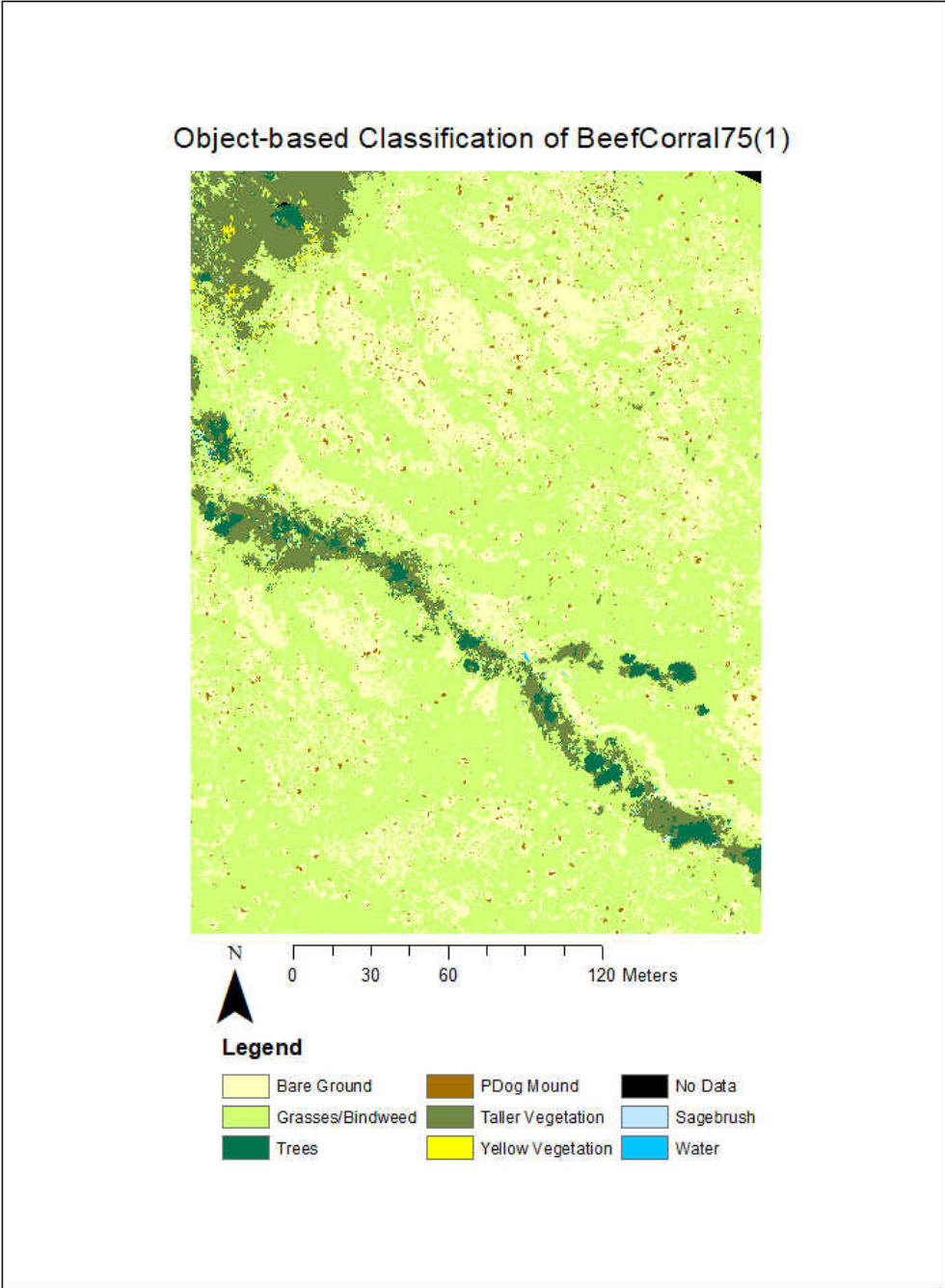


0 30 60 120 Meters

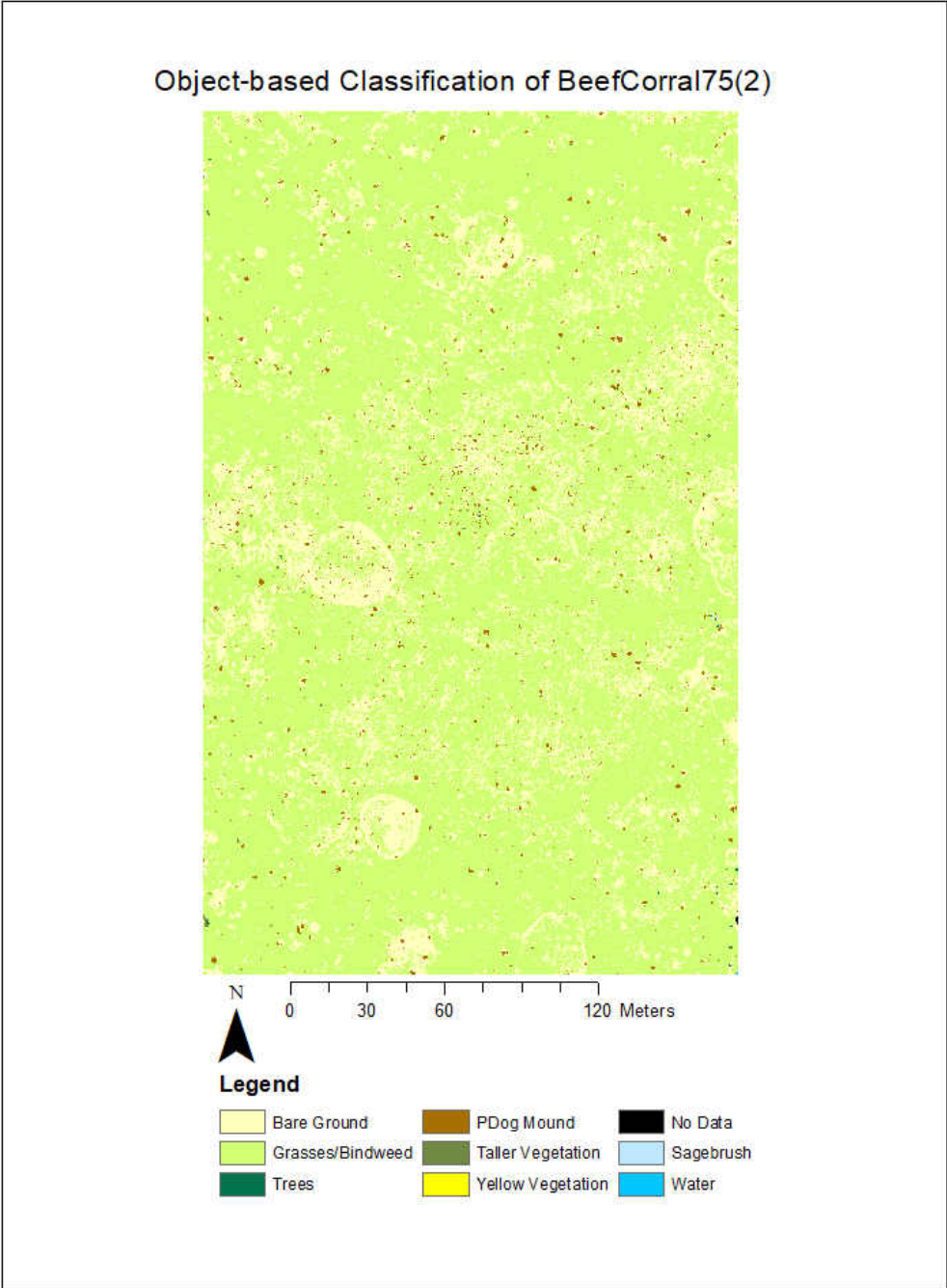
#### Legend

Bare Ground	Park Road	Taller Veg
Grasses	Sagebrush	Trees
Leafy Spurge	Shrubby Veg	Water

**Appendix A: Figure 14.** Support vector machines classification performed on a subset of a UAS image.

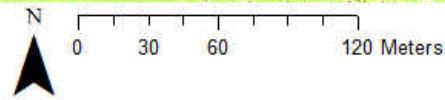
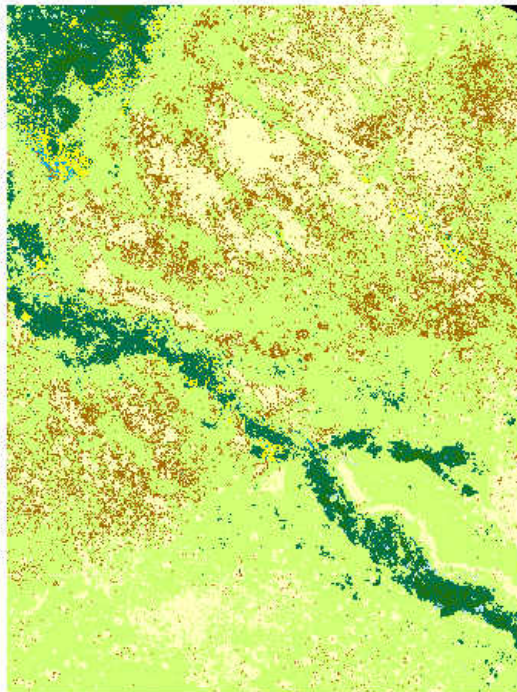


**Appendix A: Figure 15.** Object-based classification performed on a subset of a UAS image.



**Appendix A: Figure 16.** Object-based classification performed on a subset of a UAS image.

Maximum Likelihood Classification of BeefCorral75(1)

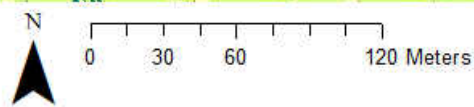
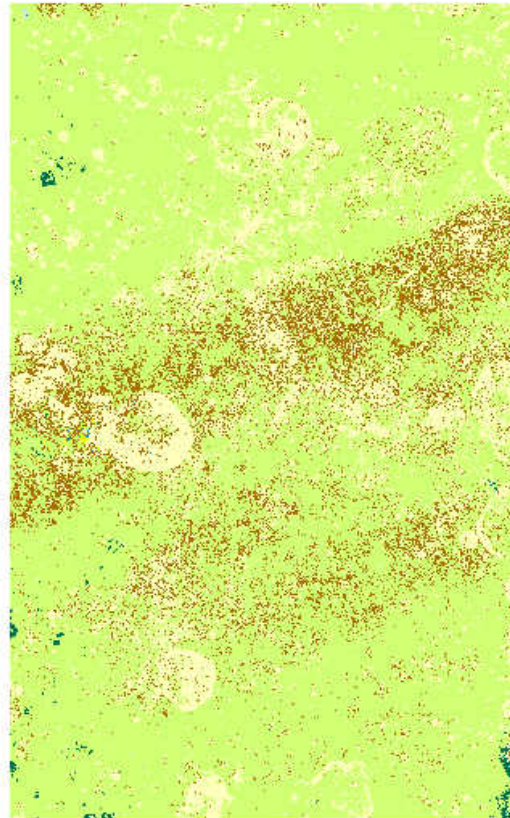


Legend

Bare Ground	PDog Mound	Taller Veg
Grasses	No Data	Trees
Leafy Spurge	Sagebrush	Water

Appendix A: Figure 17. Maximum likelihood classification performed on a subset of a UAS image.

### Maximum Likelihood Classification of BeefCorral75(2)

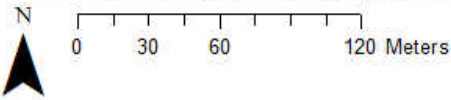
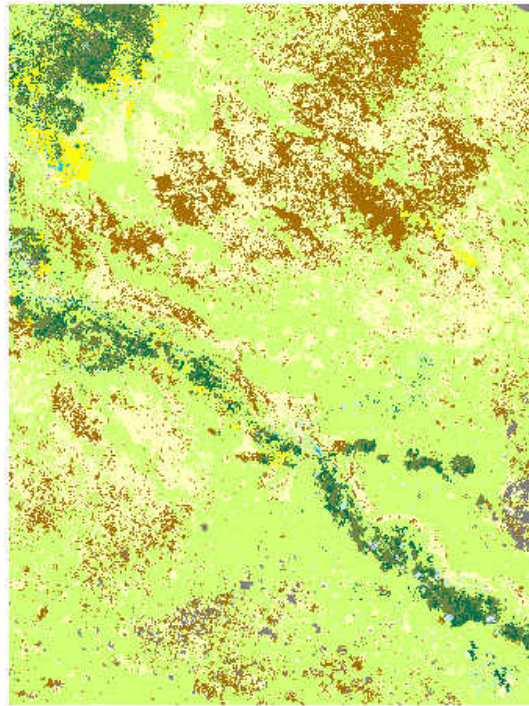


#### Legend

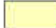


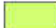





Bare Ground	PDog Mound	Taller Veg
Grasses	No Data	Trees
Leafy Spurge	Sagebrush	Water

**Appendix A: Figure 18.** Maximum likelihood classification performed on a subset of a UAS image.

### Support Vector Machines Classification of BeefCorral75(1)

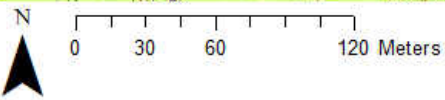
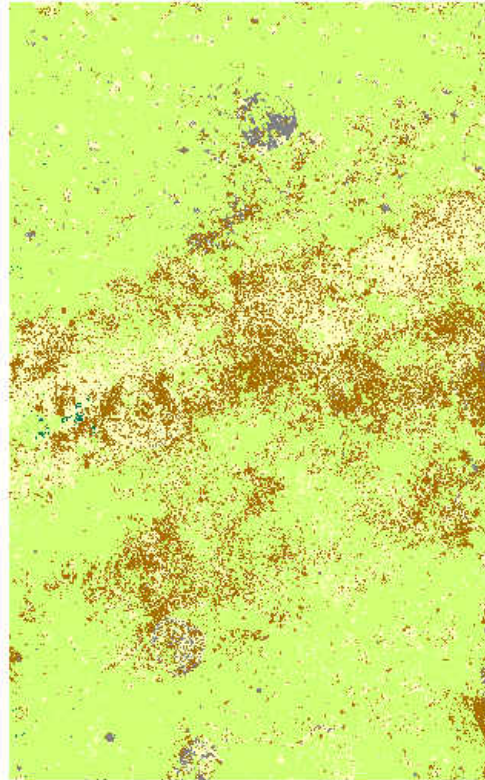


#### Legend

 Bare Ground	 P-Dog Mound	 Sagebrush
 Grasses/Bindweed	 Taller Vegetation	 Water
 Trees	 Yellow Vegetation	 Park Road

**Appendix A: Figure 19.** Support vector machines classification performed on a subset of a UAS image.

### Support Vector Machines Classification of BeefCorral75(2)



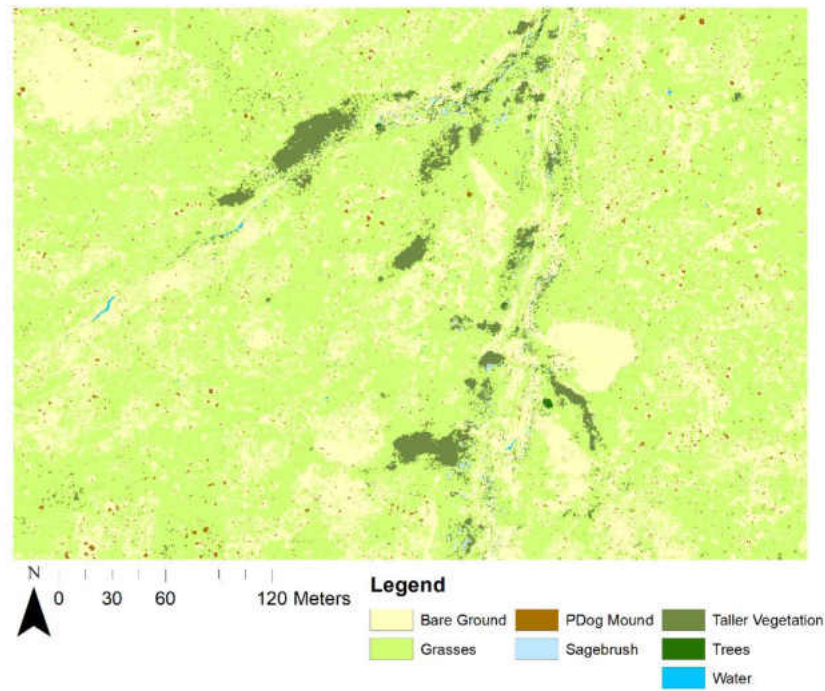
#### Legend

Bare Ground	PDog Mound	Water
Grasses/Bindweed	Taller Vegetation	Park Road
Trees	Sagebrush	

**Appendix A: Figure 20.** Support vector machines classification performed on a subset of a UAS image.

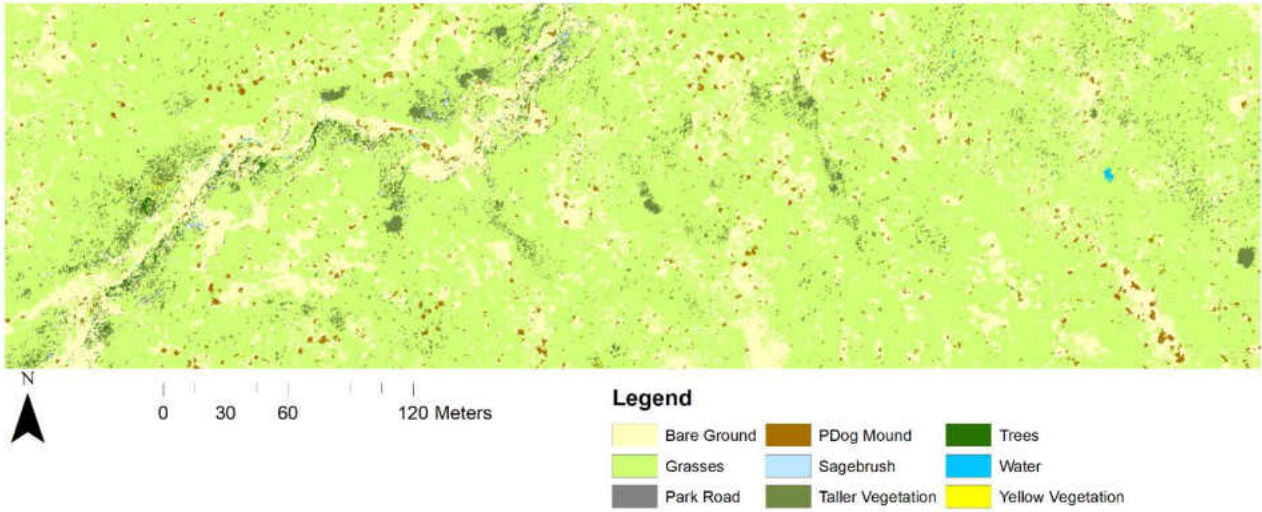


Object-based Classification of Lindbo75(1)



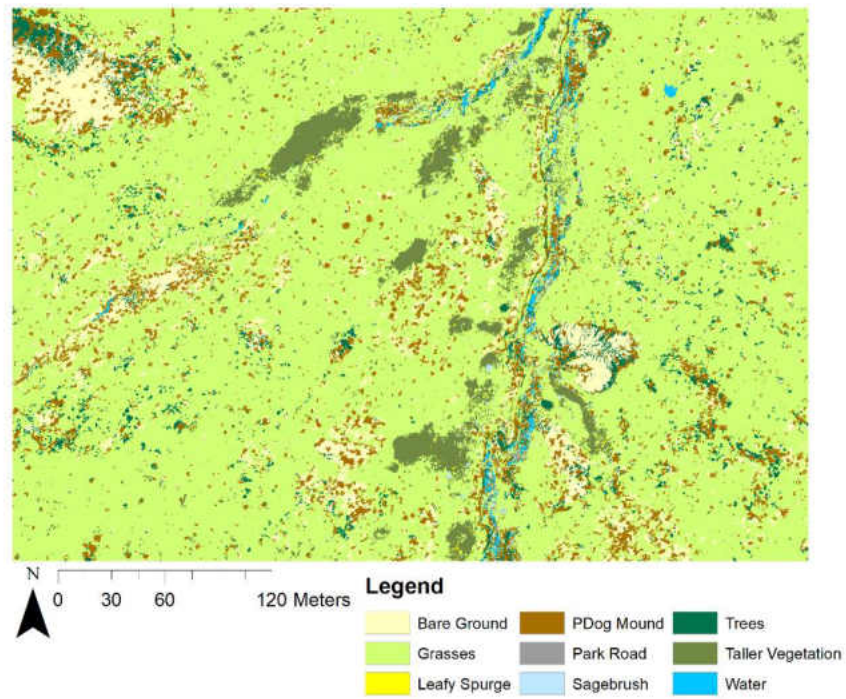
**Appendix A: Figure 21.** Object-based classification performed on a subset of a UAS image.

Object-based Classification of Lindbo75(2)



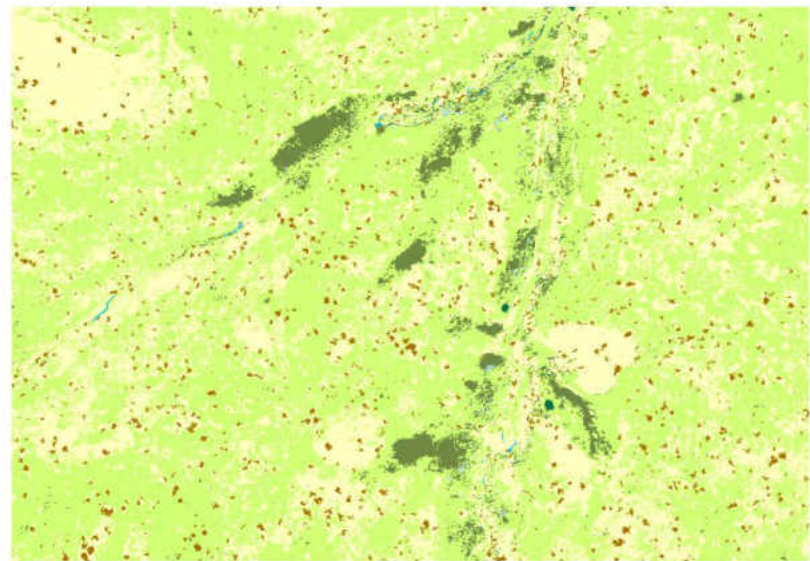
Appendix A: Figure 22. Object-based classification performed on a subset of a UAS image.

Object-based Classification of Lindbo75NIR(1)



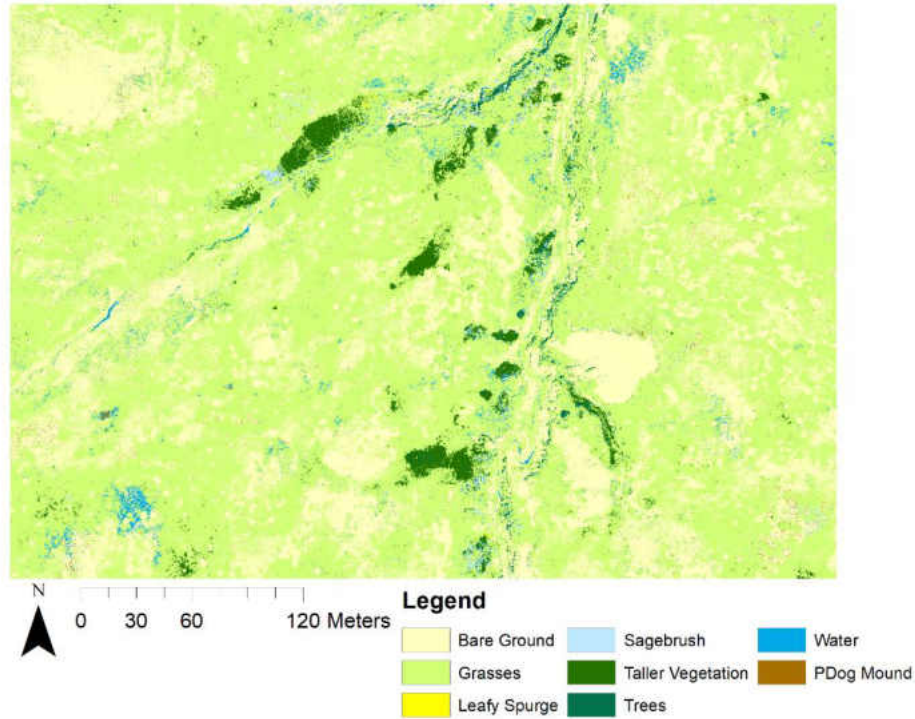
**Appendix A: Figure 23.** Object-based classification performed on a subset of a UAS image.

Object-based Classification of Lindbo90(1)



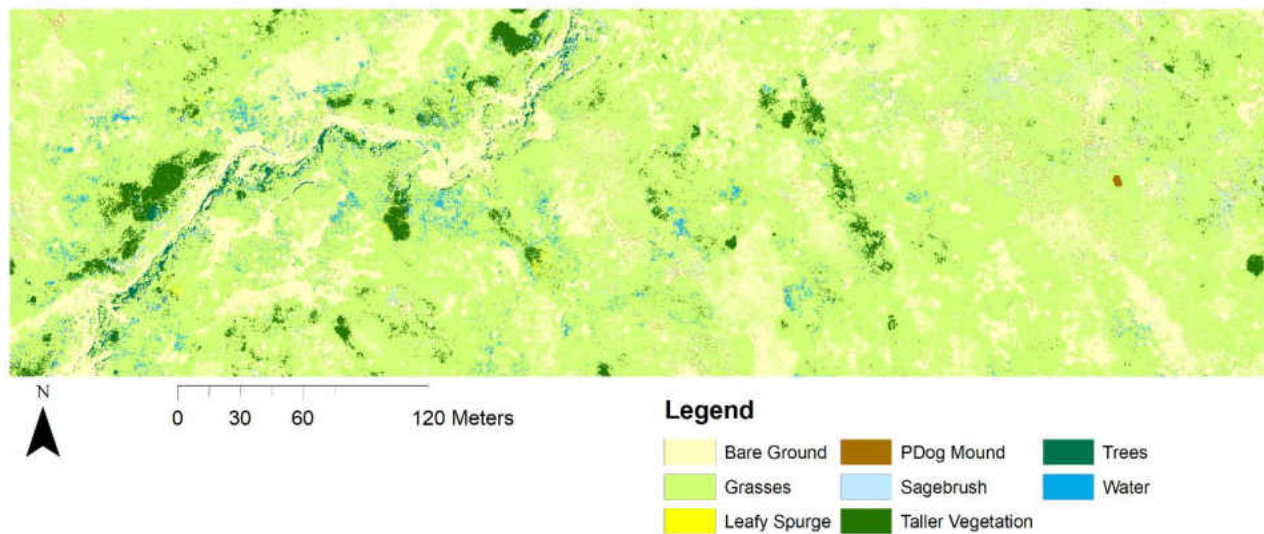
**Appendix A: Figure 24.** Object-based classification performed on a subset of a UAS image.

Maximum Likelihood Classification of Lindbo75(1)



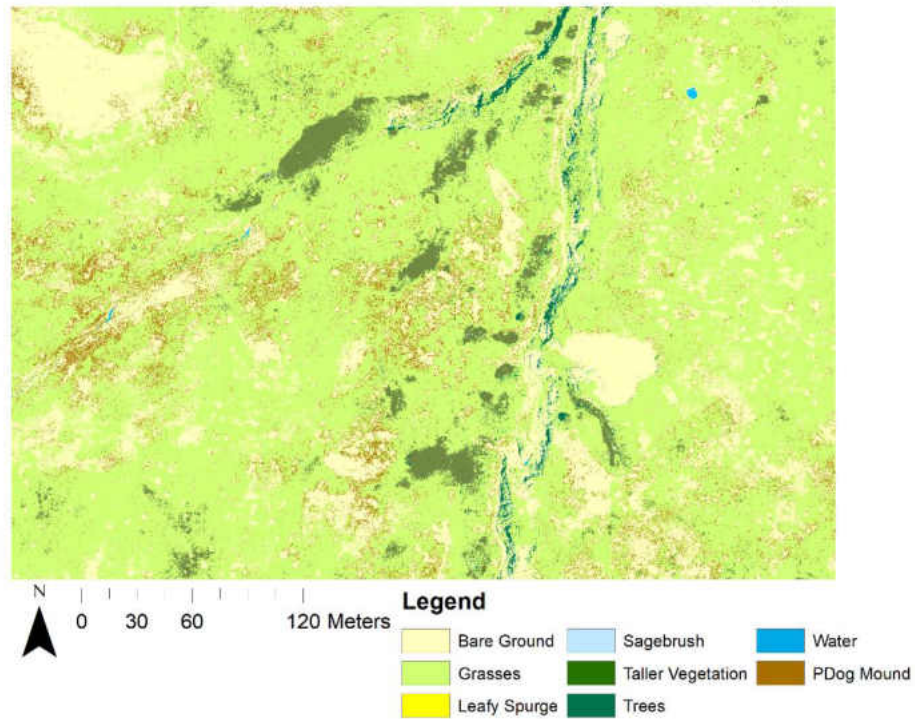
Appendix A: Figure 25. Maximum likelihood classification performed on a subset of a UAS image.

### Maximum Likelihood Classification of Lindbo75(2)



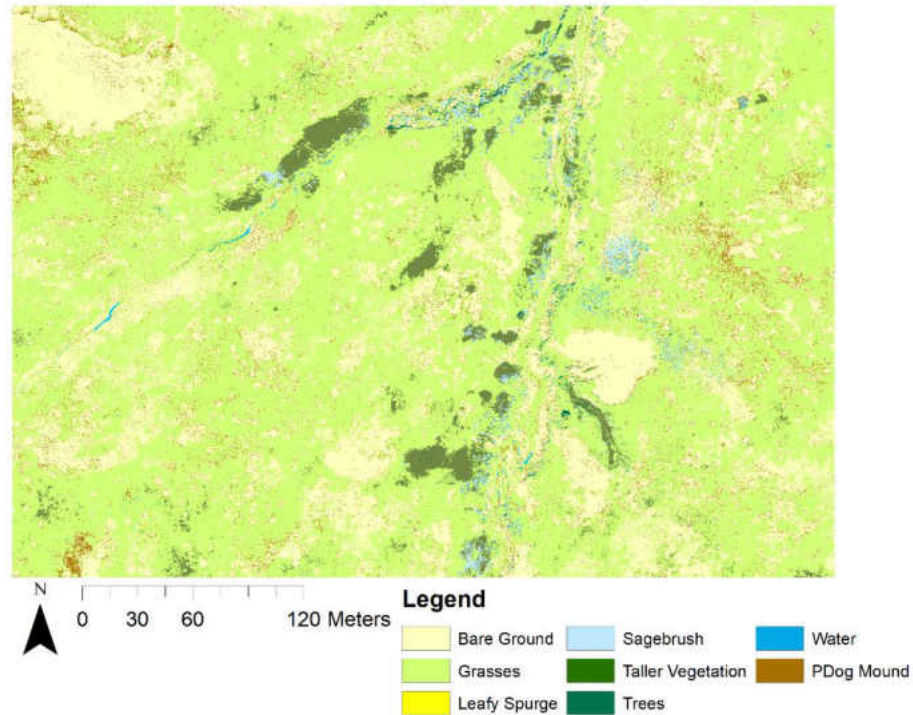
**Appendix A: Figure 26.** Maximum likelihood classification performed on a subset of a UAS image.

Maximum Likelihood Classification of Lindbo75NIR(1)



**Appendix A: Figure 27.** Maximum likelihood classification performed on a subset of a UAS image.

Maximum Likelihood Classification of Lindbo90(1)



Appendix A: Figure 28. Maximum likelihood classification performed on a subset of a UAS image.



**APPENDIX B:**  
**CONFUSION MATRICES**

**Appendix B: Table 1.** Ecognition UAS Talkington75(1) Stratified Random Accuracy Confusion Matrix

<b>Class</b>	<b>Bare Ground</b>	<b>Grasses</b>	<b>Leafy Spurge</b>	<b>Park Road</b>	<b>Sagebrush</b>	<b>Shrubby Veg</b>	<b>Taller Veg</b>	<b>Trees</b>	<b>Water</b>	<b>Total</b>	<b>Users Accuracy</b>	<b>Kappa</b>
<b>Bare Ground</b>	35	5	0	0	11	0	0	0	3	54	0.648148	0
<b>Grasses</b>	27	270	1	0	24	0	7	4	0	333	0.810811	0
<b>Leafy Spurge</b>	0	1	17	0	1	1	10	0	0	30	0.566667	0
<b>Park Road</b>	0	1	0	17	0	0	0	0	0	18	0.944444	0
<b>Sagebrush</b>	0	1	0	0	36	0	0	3	0	40	0.9	0
<b>Shrubby Veg</b>	1	3	3	0	8	14	5	1	0	35	0.4	0
<b>Taller Veg</b>	1	20	7	0	15	4	180	2	0	229	0.786026	0
<b>Trees</b>	2	3	0	0	2	5	4	5	0	21	0.238095	0
<b>Water</b>	3	1	0	0	0	0	0	0	6	10	0.6	0
<b>Total</b>	69	305	28	17	97	24	206	15	9	770	0	0
<b>Producers Accuracy</b>	0.507246	0.885246	0.607143	1	0.371134	0.583333	0.873786	0.333333	0.666667	0	0.753247	0
<b>Kappa</b>	0	0	0	0	0	0	0	0	0	0	0	0.663031

**Appendix B: Table 2.** Ecognition UAS Talkington75(2) Stratified Random Confusion Matrix

<b>Class</b>	<b>Bare Ground</b>	<b>Grasses</b>	<b>Leafy Spurge</b>	<b>Sagebrush</b>	<b>Shrubby Veg</b>	<b>Taller Veg</b>	<b>Trees</b>	<b>Water</b>	<b>Total</b>	<b>Users Accuracy</b>	<b>Kappa</b>
<b>Bare Ground</b>	39	4	0	3	0	0	0	2	48	0.8125	0
<b>Grasses</b>	23	376	0	26	2	15	5	0	447	0.841163	0
<b>Leafy Spurge</b>	0	1	3	0	4	2	0	0	10	0.3	0
<b>Sagebrush</b>	0	1	0	35	0	0	2	0	38	0.921053	0
<b>Shrubby Veg</b>	0	1	0	3	11	2	1	0	18	0.611111	0
<b>Taller Veg</b>	3	12	1	9	9	129	5	0	168	0.767857	0
<b>Trees</b>	1	3	0	6	5	8	13	1	37	0.351351	0
<b>Water</b>	2	0	0	0	0	0	0	8	10	0.8	0
<b>Total</b>	68	398	4	82	31	156	26	11	776	0	0
<b>Producers Accuracy</b>	0.573529	0.944724	0.75	0.426829	0.354839	0.826923	0.5	0.727273	0	0.791237	0
<b>Kappa</b>	0	0	0	0	0	0	0	0	0	0	0.677671

**Appendix B: Table 3.** Ecognition UAS Talkington75NIR(1) Stratified Random Accuracy Confusion Matrix

<b>Class</b>	<b>Bare Ground</b>	<b>Grasses</b>	<b>Leafy Spurge</b>	<b>Park Road</b>	<b>Sagebrush</b>	<b>Shrubby Veg</b>	<b>Taller Veg</b>	<b>Trees</b>	<b>Water</b>	<b>Total</b>	<b>Users Accuracy</b>	<b>Kappa</b>
<b>Bare Ground</b>	31	15	0	0	9	2	8	1	5	71	0.43662	0
<b>Grasses</b>	21	190	2	1	21	0	27	0	0	262	0.725191	0
<b>Leafy Spurge</b>	0	3	14	0	10	7	21	2	0	57	0.245614	0
<b>Park Road</b>	1	1	0	15	0	0	1	0	0	18	0.833333	0
<b>Sagebrush</b>	7	32	0	0	26	1	28	3	0	97	0.268041	0
<b>Shrubby Veg</b>	0	2	1	0	5	9	11	2	0	30	0.3	0
<b>Taller Veg</b>	6	57	8	1	22	4	101	5	2	206	0.490291	0
<b>Trees</b>	0	5	3	0	4	1	9	2	0	24	0.083333	0
<b>Water</b>	3	0	0	0	0	0	0	0	2	5	0.4	0
<b>Total</b>	69	305	28	17	97	24	206	15	9	770	0	0
<b>Producers Accuracy</b>	0.449275	0.622951	0.5	0.882353	0.268041	0.375	0.490291	0.133333	0.222222	0	0.506494	0
<b>Kappa</b>	0	0	0	0	0	0	0	0	0	0	0	0.354396

**Appendix B: Table 4.** Ecognition UAS Talkington75(2) Stratified Random Confusion Matrix

<b>Class</b>	<b>Bare Ground</b>	<b>Grasses</b>	<b>Leafy Spurge</b>	<b>Sagebrush</b>	<b>Shrubby Veg</b>	<b>Taller Veg</b>	<b>Trees</b>	<b>Water</b>	<b>Total</b>	<b>Users Accuracy</b>	<b>Kappa</b>
<b>Bare Ground</b>	51	8	0	6	1	1	0	4	71	0.71831	0
<b>Grasses</b>	8	307	1	19	3	49	3	1	391	0.785166	0
<b>Leafy Spurge</b>	0	1	1	0	1	6	1	0	10	0.1	0
<b>Sagebrush</b>	5	19	0	21	0	5	3	0	53	0.396226	0
<b>Shrubby Veg</b>	0	2	0	2	3	5	0	0	12	0.25	0
<b>Taller Veg</b>	1	51	2	16	12	73	4	0	159	0.459119	0
<b>Trees</b>	2	10	0	18	11	17	15	1	74	0.202703	0
<b>Water</b>	1	0	0	0	0	0	0	5	6	0.833333	0
<b>Total</b>	68	398	4	82	31	156	26	11	776	0	0
<b>Producers Accuracy</b>	0.75	0.771357	0.25	0.256098	0.096774	0.467949	0.576923	0.454545	0	0.613402	0
<b>Kappa</b>	0	0	0	0	0	0	0	0	0	0	0.432442

**Appendix B: Table 5.** Ecognition UAS Talkington90(1) Stratified Random Accuracy Confusion Matrix

<b>Class</b>	<b>Bare Ground</b>	<b>Grasses</b>	<b>Leafy Spurge</b>	<b>Park Road</b>	<b>Sagebrush</b>	<b>Shrubby Veg</b>	<b>Taller Veg</b>	<b>Trees</b>	<b>Water</b>	<b>Total</b>	<b>Users Accuracy</b>	<b>Kappa</b>
<b>Bare Ground</b>	21	14	1	0	5	1	5	2	3	52	0.403846	0
<b>Grasses</b>	40	252	4	0	57	2	74	2	1	432	0.583333	0
<b>Leafy Spurge</b>	0	1	9	0	2	1	4	0	0	17	0.529412	0
<b>Park Road</b>	0	0	0	17	2	0	1	0	3	23	0.73913	0
<b>Sagebrush</b>	0	2	2	0	5	1	3	0	0	13	0.384615	0
<b>Shrubby Veg</b>	0	0	0	0	0	5	2	0	0	7	0.714286	0
<b>Taller Veg</b>	5	34	12	0	22	13	116	6	0	208	0.557692	0
<b>Trees</b>	1	1	0	0	1	1	0	5	0	9	0.555556	0
<b>Water</b>	2	1	0	0	3	0	0	0	2	8	0.25	0
<b>Total</b>	69	305	28	17	97	24	205	15	9	769	0	0
<b>Producers Accuracy</b>	0.304348	0.82623	0.321429	1	0.051546	0.208333	0.565854	0.333333	0.222222	0	0.561769	0
<b>Kappa</b>	0	0	0	0	0	0	0	0	0	0	0	0.369258

**Appendix B: Table 6.** Ecognition UAS Talkington75(1) Equalized Random Accuracy Confusion Matrix

<b>Class</b>	<b>Bare Ground</b>	<b>Grasses</b>	<b>Leafy Spurge</b>	<b>Park Road</b>	<b>Sagebrush</b>	<b>Shrubby Veg</b>	<b>Taller Veg</b>	<b>Trees</b>	<b>Water</b>	<b>Total</b>	<b>Users Accuracy</b>	<b>Kappa</b>
<b>Bare Ground</b>	88	8	0	0	10	1	0	1	3	111	0.792793	0
<b>Grasses</b>	4	96	0	0	11	0	0	0	0	111	0.864865	0
<b>Leafy Spurge</b>	1	3	61	0	3	19	21	3	0	111	0.54955	0
<b>Park Road</b>	1	0	0	110	0	0	0	0	0	111	0.990991	0
<b>Sagebrush</b>	5	4	0	0	95	1	3	3	0	111	0.855856	0
<b>Shrubby Veg</b>	2	0	6	0	7	84	12	0	0	111	0.756757	0
<b>Taller Veg</b>	0	2	4	0	1	5	97	2	0	111	0.873874	0
<b>Trees</b>	3	2	2	0	4	22	52	26	0	111	0.234234	0
<b>Water</b>	15	1	0	0	0	0	1	0	94	111	0.846847	0
<b>Total</b>	119	116	73	110	131	132	186	35	97	999	0	0
<b>Producers Accuracy</b>	0.739496	0.827586	0.835616	1	0.725191	0.636364	0.521505	0.742857	0.969072	0	0.751752	0
<b>Kappa</b>	0	0	0	0	0	0	0	0	0	0	0	0.720721

**Appendix B: Table 7.** Ecognition UAS Talkington75(2) Equalized Random Confusion Matrix

<b>Class</b>	<b>Bare Ground</b>	<b>Grasses</b>	<b>Leafy Spurge</b>	<b>Sagebrush</b>	<b>Shrubby Veg</b>	<b>Taller Veg</b>	<b>Trees</b>	<b>Water</b>	<b>Total</b>	<b>Users Accuracy</b>	<b>Kappa</b>
<b>Bare Ground</b>	103	6	0	5	0	4	0	7	125	0.824	0
<b>Grasses</b>	3	114	0	3	0	4	1	0	125	0.912	0
<b>Leafy Spurge</b>	0	0	58	0	39	19	9	0	125	0.464	0
<b>Sagebrush</b>	2	3	0	111	1	5	3	0	125	0.888	0
<b>Shrubby Veg</b>	2	0	4	22	61	34	2	0	125	0.488	0
<b>Taller Veg</b>	0	2	2	3	6	111	1	0	125	0.888	0
<b>Trees</b>	4	0	4	26	20	37	33	1	125	0.264	0
<b>Water</b>	11	0	0	0	0	1	0	113	125	0.904	0
<b>Total</b>	125	125	68	170	127	215	49	121	1000	0	0
<b>Producers Accuracy</b>	0.824	0.912	0.852941	0.652941	0.480315	0.516279	0.673469	0.933884	0	0.704	0
<b>Kappa</b>	0	0	0	0	0	0	0	0	0	0	0.661714



**Appendix B: Table 8.** Ecognition UAS Talkington75NIR(1) Equalized Random Accuracy Confusion Matrix

<b>Class</b>	<b>Bare Ground</b>	<b>Grasses</b>	<b>Leafy Spurge</b>	<b>Park Road</b>	<b>Sagebrush</b>	<b>Shrubby Veg</b>	<b>Taller Veg</b>	<b>Trees</b>	<b>Water</b>	<b>Total</b>	<b>Users Accuracy</b>	<b>Kappa</b>
<b>Bare Ground</b>	55	34	1	0	8	0	7	1	5	111	0.495495	0
<b>Grasses</b>	5	94	1	1	7	0	3	0	0	111	0.846847	0
<b>Leafy Spurge</b>	1	14	33	0	17	23	20	3	0	111	0.297297	0
<b>Park Road</b>	3	10	0	92	0	0	6	0	0	111	0.828829	0
<b>Sagebrush</b>	8	41	1	1	39	6	15	0	0	111	0.351351	0
<b>Shrubby Veg</b>	2	9	5	0	14	64	15	1	1	111	0.576577	0
<b>Taller Veg</b>	1	9	5	2	10	1	79	4	0	111	0.711712	0
<b>Trees</b>	4	13	10	1	13	12	30	27	1	111	0.243243	0
<b>Water</b>	45	13	0	0	5	0	4	1	43	111	0.387387	0
<b>Total</b>	124	237	56	97	113	106	179	37	50	999	0	0
<b>Producers Accuracy</b>	0.443548	0.396624	0.589286	0.948454	0.345133	0.603774	0.441341	0.72973	0.86	0	0.526527	0
<b>Kappa</b>	0	0	0	0	0	0	0	0	0	0	0	0.467342

**Appendix B: Table 9.** Ecognition UAS Talkington75NIR(2) Equalized Random Accuracy Confusion Matrix

<b>Class</b>	<b>Bare Ground</b>	<b>Grasses</b>	<b>Leafy Spurge</b>	<b>No Data</b>	<b>Sagebrush</b>	<b>Shrubby Veg</b>	<b>Taller Veg</b>	<b>Trees</b>	<b>Water</b>	<b>Total</b>	<b>Users Accuracy</b>	<b>Kappa</b>
<b>Bare Ground</b>	76	21	0	0	5	0	2	1	6	111	0.684685	0
<b>Grasses</b>	2	96	1	0	2	1	9	0	0	111	0.864865	0
<b>Leafy Spurge</b>	0	10	17	0	5	28	45	6	0	111	0.153153	0
<b>No Data</b>	0	86	0	0	20	0	5	0	0	111	0	0
<b>Sagebrush</b>	9	21	0	0	64	3	13	1	0	111	0.576577	0
<b>Shrubby Veg</b>	0	0	9	0	7	75	17	3	0	111	0.675676	0
<b>Taller Veg</b>	0	11	3	0	8	7	82	0	0	111	0.738739	0
<b>Trees</b>	6	14	3	0	20	8	30	28	2	111	0.252252	0
<b>Water</b>	11	0	0	0	0	0	1	1	98	111	0.882883	0
<b>Total</b>	104	259	33	0	131	122	204	40	106	999	0	0
<b>Producers Accuracy</b>	0.730769	0.370656	0.515152	0	0.48855	0.614754	0.401961	0.7	0.924528	0	0.536537	0
<b>Kappa</b>	0	0	0	0	0	0	0	0	0	0	0	0.478604

**Appendix B: Table 10.** Ecognition UAS Talkington90(1) Equalized Random Accuracy Confusion Matrix

<b>Class</b>	<b>Bare Ground</b>	<b>Grasses</b>	<b>Leafy Spurge</b>	<b>Park Road</b>	<b>Sagebrush</b>	<b>Shrubby Veg</b>	<b>Taller Veg</b>	<b>Trees</b>	<b>Water</b>	<b>Total</b>	<b>Users Accuracy</b>	<b>Kappa</b>
<b>Bare Ground</b>	85	12	1	0	9	1	1	2	0	111	0.765766	0
<b>Grasses</b>	5	95	0	0	9	0	2	0	0	111	0.855856	0
<b>Leafy Spurge</b>	1	2	68	0	1	14	22	3	0	111	0.612613	0
<b>Park Road</b>	9	2	0	77	6	2	1	2	12	111	0.693694	0
<b>Sagebrush</b>	0	5	0	0	101	0	4	1	0	111	0.90991	0
<b>Shrubby Veg</b>	2	1	10	1	7	85	3	2	0	111	0.765766	0
<b>Taller Veg</b>	0	5	5	0	4	9	87	1	0	111	0.783784	0
<b>Trees</b>	2	2	5	0	4	14	16	68	0	111	0.612613	0
<b>Water</b>	24	6	0	0	4	0	0	0	77	111	0.693694	0
<b>Total</b>	128	130	89	78	145	125	136	79	89	999	0	0
<b>Producers Accuracy</b>	0.664063	0.730769	0.764045	0.987179	0.696552	0.68	0.639706	0.860759	0.865169	0	0.743744	0
<b>Kappa</b>	0	0	0	0	0	0	0	0	0	0	0	0.711712

**Appendix B: Table 11.** Maximum Likelihood UAS Talkington75(1) Stratified Random Accuracy Confusion Matrix

<b>Class</b>	<b>Bare Ground</b>	<b>Grasses</b>	<b>Leafy Spurge</b>	<b>Park Road</b>	<b>Sagebrush</b>	<b>Shrubby Veg</b>	<b>Taller Veg</b>	<b>Trees</b>	<b>Water</b>	<b>Total</b>	<b>Users Accuracy</b>	<b>Kappa</b>
<b>Bare Ground</b>	20	7	0	0	1	0	0	1	0	29	0.689655	0
<b>Grasses</b>	17	225	0	0	42	2	32	2	1	321	0.700935	0
<b>Leafy Spurge</b>	0	0	10	0	0	1	3	0	0	14	0.714286	0
<b>Park Road</b>	25	8	0	16	3	0	1	0	1	54	0.296296	0
<b>Sagebrush</b>	2	10	1	0	28	1	0	0	0	42	0.666667	0
<b>Shrubby Veg</b>	0	1	0	0	0	1	2	1	0	5	0.2	0
<b>Taller Veg</b>	0	18	9	0	1	25	112	4	1	170	0.658824	0
<b>Trees</b>	4	40	3	0	18	12	48	8	0	133	0.06015	0
<b>Water</b>	0	0	0	0	0	0	0	0	2	2	1	0
<b>Total</b>	68	309	23	16	93	42	198	16	5	770	0	0
<b>Producers Accuracy</b>	0.294118	0.728155	0.434783	1	0.301075	0.02381	0.565657	0.5	0.4	0	0.548052	0
<b>Kappa</b>	0	0	0	0	0	0	0	0	0	0	0	0.405378

**Appendix B: Table 12.** Maximum Likelihood UAS Talkington75(2) Stratified Random Accuracy Confusion Matrix

<b>Class</b>	<b>Bare Ground</b>	<b>Grasses</b>	<b>Leafy Spurge</b>	<b>Park Road</b>	<b>Sagebrush</b>	<b>Shrubby Veg</b>	<b>Taller Veg</b>	<b>Trees</b>	<b>Water</b>	<b>Total</b>	<b>Users Accuracy</b>	<b>Kappa</b>
<b>Bare Ground</b>	13	0	0	0	4	0	1	0	2	20	0.65	0
<b>Grasses</b>	25	357	0	0	30	2	38	2	1	455	0.784615	0
<b>Leafy Spurge</b>	0	0	2	0	0	1	2	1	0	6	0.333333	0
<b>Park Road</b>	21	5	0	0	6	0	0	0	1	33	0	0
<b>Sagebrush</b>	2	1	0	0	22	0	0	2	0	27	0.814815	0
<b>Shrubby Veg</b>	0	0	1	0	0	0	2	0	0	3	0	0
<b>Taller Veg</b>	0	16	1	0	2	19	71	1	1	111	0.63964	0
<b>Trees</b>	1	19	0	0	18	9	42	20	0	109	0.183486	0
<b>Water</b>	6	0	0	0	0	0	0	0	6	12	0.5	0
<b>Total</b>	68	398	4	0	82	31	156	26	11	776	0	0
<b>Producers Accuracy</b>	0.191176	0.896985	0.5	0	0.268293	0	0.455128	0.769231	0.545455	0	0.632732	0
<b>Kappa</b>	0	0	0	0	0	0	0	0	0	0	0	0.44308

**Appendix B: Table 13.** Maximum Likelihood UAS Talkington75NIR(1) Stratified Random Accuracy Confusion Matrix

<b>Class</b>	<b>Bare Ground</b>	<b>Grasses</b>	<b>Leafy Spurge</b>	<b>Park Road</b>	<b>Sagebrush</b>	<b>Shrubby Veg</b>	<b>Taller Veg</b>	<b>Trees</b>	<b>Water</b>	<b>Total</b>	<b>Users Accuracy</b>	<b>Kappa</b>
<b>Bare Ground</b>	9	5	0	0	3	0	2	0	0	19	0.473684	0
<b>Grasses</b>	30	217	2	2	36	1	52	2	1	343	0.632653	0
<b>Leafy Spurge</b>	0	4	10	0	6	8	13	0	0	41	0.243902	0
<b>Park Road</b>	17	5	0	14	5	1	2	1	4	49	0.285714	0
<b>Sagebrush</b>	1	0	0	0	0	0	0	0	0	1	0	0
<b>Shrubby Veg</b>	1	1	1	0	1	0	6	0	0	10	0	0
<b>Taller Veg</b>	4	49	12	1	31	11	98	6	1	213	0.460094	0
<b>Trees</b>	2	24	3	0	15	3	32	6	1	86	0.069767	0
<b>Water</b>	5	0	0	0	0	0	1	0	2	8	0.25	0
<b>Total</b>	69	305	28	17	97	24	206	15	9	770	0	0
<b>Producers Accuracy</b>	0.130435	0.711475	0.357143	0.823529	0	0	0.475728	0.4	0.222222	0	0.462338	0
<b>Kappa</b>	0	0	0	0	0	0	0	0	0	0	0	0.274537

**Appendix B: Table 14.** Maximum Likelihood UAS Talkington75NIR(2) Stratified Random Accuracy Confusion Matrix

<b>Class</b>	<b>Bare Ground</b>	<b>Grasses</b>	<b>Leafy Spurge</b>	<b>Park Road</b>	<b>Sagebrush</b>	<b>Shrubby Veg</b>	<b>Taller Veg</b>	<b>Trees</b>	<b>Water</b>	<b>Total</b>	<b>Users Accuracy</b>	<b>Kappa</b>
<b>Bare Ground</b>	17	2	0	0	0	0	0	1	3	23	0.73913	0
<b>Grasses</b>	10	317	0	0	39	1	53	5	0	425	0.745882	0
<b>Leafy Spurge</b>	0	0	3	0	2	6	8	1	0	20	0.15	0
<b>Park Road</b>	28	6	0	0	8	1	0	0	2	45	0	0
<b>Sagebrush</b>	0	0	0	0	1	0	0	1	0	2	0.5	0
<b>Shrubby Veg</b>	1	2	0	0	0	1	1	0	0	5	0.2	0
<b>Taller Veg</b>	0	37	0	0	12	11	68	6	0	134	0.507463	0
<b>Trees</b>	4	30	1	0	20	11	26	12	3	107	0.11215	0
<b>Water</b>	8	4	0	0	2	0	0	0	3	15	0.2	0
<b>Total</b>	68	398	4	0	82	31	156	26	11	776	0	0
<b>Producers Accuracy</b>	0.25	0.796482	0.75	0	0.012195	0.032258	0.435897	0.461538	0.272727	0	0.543814	0
<b>Kappa</b>	0	0	0	0	0	0	0	0	0	0	0	0.325403

**Appendix B: Table 15.** Maximum Likelihood UAS Talkington90(1) Stratified Random Accuracy Confusion Matrix

<b>Class</b>	<b>Bare Ground</b>	<b>Grasses</b>	<b>Leafy Spurge</b>	<b>Park Road</b>	<b>Sagebrush</b>	<b>Shrubby Veg</b>	<b>Taller Veg</b>	<b>Trees</b>	<b>Water</b>	<b>Total</b>	<b>Users Accuracy</b>	<b>Kappa</b>
<b>Bare Ground</b>	17	4	0	1	0	1	1	0	0	24	0.708333	0
<b>Grasses</b>	18	224	1	0	48	2	48	3	1	345	0.649275	0
<b>Leafy Spurge</b>	0	0	3	0	0	5	5	1	0	14	0.214286	0
<b>Park Road</b>	21	13	0	15	3	1	1	0	2	56	0.267857	0
<b>Sagebrush</b>	3	9	0	0	12	2	3	0	1	30	0.4	0
<b>Shrubby Veg</b>	1	0	6	0	0	10	7	1	0	25	0.4	0
<b>Taller Veg</b>	2	6	4	0	7	6	41	2	0	68	0.602941	0
<b>Trees</b>	4	53	9	0	23	15	90	9	0	203	0.044335	0
<b>Water</b>	2	0	0	0	0	0	2	0	1	5	0.2	0
<b>Total</b>	68	309	23	16	93	42	198	16	5	770	0	0
<b>Producers Accuracy</b>	0.25	0.724919	0.130435	0.9375	0.129032	0.238095	0.207071	0.5625	0.2	0	0.431169	0
<b>Kappa</b>	0	0	0	0	0	0	0	0	0	0	0	0.271369



**Appendix B: Table 16.** Maximum Likelihood UAS Talkington75(1) Equalized Random Accuracy Confusion Matrix

<b>Class</b>	<b>Bare Ground</b>	<b>Grasses</b>	<b>Leafy Spurge</b>	<b>Park Road</b>	<b>Sagebrush</b>	<b>Shrubby Veg</b>	<b>Taller Veg</b>	<b>Trees</b>	<b>Water</b>	<b>Total</b>	<b>Users Accuracy</b>	<b>Kappa</b>
<b>Bare Ground</b>	79	15	0	3	11	0	0	1	2	111	0.711712	0
<b>Grasses</b>	4	94	0	0	10	0	1	1	1	111	0.846847	0
<b>Leafy Spurge</b>	0	1	83	0	0	5	22	0	0	111	0.747748	0
<b>Park Road</b>	47	21	0	35	4	0	0	0	4	111	0.315315	0
<b>Sagebrush</b>	5	18	1	0	80	2	3	2	0	111	0.720721	0
<b>Shrubby Veg</b>	1	2	27	0	1	29	49	2	0	111	0.261261	0
<b>Taller Veg</b>	0	8	22	0	1	7	73	0	0	111	0.657658	0
<b>Trees</b>	2	21	14	0	18	6	41	9	0	111	0.081081	0
<b>Water</b>	13	4	0	0	0	0	0	0	94	111	0.846847	0
<b>Total</b>	151	184	147	38	125	49	189	15	101	999	0	0
<b>Producers Accuracy</b>	0.523179	0.51087	0.564626	0.921053	0.64	0.591837	0.386243	0.6	0.930693	0	0.576577	0
<b>Kappa</b>	0	0	0	0	0	0	0	0	0	0	0	0.523649

**Appendix B: Table 17.** Maximum Likelihood UAS Talkington75(2) Equalized Random Accuracy Confusion Matrix

<b>Class</b>	<b>Bare Ground</b>	<b>Grasses</b>	<b>Leafy Spurge</b>	<b>Park Road</b>	<b>Sagebrush</b>	<b>Shrubby Veg</b>	<b>Taller Veg</b>	<b>Trees</b>	<b>Water</b>	<b>Total</b>	<b>Users Accuracy</b>	<b>Kappa</b>
<b>Bare Ground</b>	69	13	0	0	21	1	0	2	5	111	0.621622	0
<b>Grasses</b>	2	97	0	0	9	1	2	0	0	111	0.873874	0
<b>Leafy Spurge</b>	0	0	23	0	0	33	42	13	0	111	0.207207	0
<b>Park Road</b>	66	21	1	0	20	0	0	0	3	111	0	0
<b>Sagebrush</b>	4	9	0	0	84	2	5	7	0	111	0.756757	0
<b>Shrubby Veg</b>	1	4	13	0	1	43	44	5	0	111	0.387387	0
<b>Taller Veg</b>	0	8	3	0	0	10	87	2	1	111	0.783784	0
<b>Trees</b>	3	9	2	0	13	24	53	7	0	111	0.063063	0
<b>Water</b>	41	3	0	0	0	0	0	0	67	111	0.603604	0
<b>Total</b>	186	164	42	0	148	114	233	36	76	999	0	0
<b>Producers Accuracy</b>	0.370968	0.591463	0.547619	0	0.567568	0.377193	0.373391	0.194444	0.881579	0	0.477477	0
<b>Kappa</b>	0	0	0	0	0	0	0	0	0	0	0	0.412162

**Appendix B: Table 18.** Maximum Likelihood UAS Talkington75NIR(1) Equalized Random Accuracy Confusion Matrix

<b>Class</b>	<b>Bare Ground</b>	<b>Grasses</b>	<b>Leafy Spurge</b>	<b>Park Road</b>	<b>Sagebrush</b>	<b>Shrubby Veg</b>	<b>Taller Veg</b>	<b>Trees</b>	<b>Water</b>	<b>Total</b>	<b>Users Accuracy</b>	<b>Kappa</b>
<b>Bare Ground</b>	67	21	0	0	5	4	10	0	4	111	0.603604	0
<b>Grasses</b>	7	71	5	0	11	0	16	1	0	111	0.63964	0
<b>Leafy Spurge</b>	4	7	35	1	9	25	30	0	0	111	0.315315	0
<b>Park Road</b>	35	12	1	37	10	0	6	3	7	111	0.333333	0
<b>Sagebrush</b>	6	41	13	2	20	0	26	1	2	111	0.18018	0
<b>Shrubby Veg</b>	25	17	9	0	9	10	39	2	0	111	0.09009	0
<b>Taller Veg</b>	3	14	14	1	15	5	59	0	0	111	0.531532	0
<b>Trees</b>	6	27	10	1	20	4	32	10	1	111	0.09009	0
<b>Water</b>	47	20	0	4	16	0	2	0	22	111	0.198198	0
<b>Total</b>	200	230	87	46	115	48	220	17	36	999	0	0
<b>Producers Accuracy</b>	0.335	0.308696	0.402299	0.804348	0.173913	0.208333	0.268182	0.588235	0.611111	0	0.331331	0
<b>Kappa</b>	0	0	0	0	0	0	0	0	0	0	0	0.247748

**Appendix B: Table 19.** Maximum Likelihood UAS Talkington75NIR(2) Equalized Random Accuracy Confusion Matrix

<b>Class</b>	<b>Bare Ground</b>	<b>Grasses</b>	<b>Leafy Spurge</b>	<b>Park Road</b>	<b>Sagebrush</b>	<b>Shrubby Veg</b>	<b>Taller Veg</b>	<b>Trees</b>	<b>Water</b>	<b>Total</b>	<b>Users Accuracy</b>	<b>Kappa</b>
<b>Bare Ground</b>	80	17	0	0	4	2	1	0	7	111	0.720721	0
<b>Grasses</b>	4	84	1	0	11	2	8	1	0	111	0.756757	0
<b>Leafy Spurge</b>	1	5	20	0	2	53	23	7	0	111	0.18018	0
<b>Park Road</b>	80	8	0	0	10	0	5	0	8	111	0	0
<b>Sagebrush</b>	12	25	4	0	21	6	35	8	0	111	0.189189	0
<b>Shrubby Veg</b>	2	9	12	0	8	35	40	5	0	111	0.315315	0
<b>Taller Veg</b>	1	8	8	0	4	18	67	4	1	111	0.603604	0
<b>Trees</b>	5	19	6	0	20	13	36	12	0	111	0.108108	0
<b>Water</b>	51	25	0	0	4	1	2	0	28	111	0.252252	0
<b>Total</b>	236	200	51	0	84	130	217	37	44	999	0	0
<b>Producers Accuracy</b>	0.338983	0.42	0.392157	0	0.25	0.269231	0.308756	0.324324	0.636364	0	0.347347	0
<b>Kappa</b>	0	0	0	0	0	0	0	0	0	0	0	0.265766

**Appendix B: Table 20.** Maximum Likelihood UAS Talkington90(1) Equalized Random Accuracy Confusion Matrix

<b>Class</b>	<b>Bare Ground</b>	<b>Grasses</b>	<b>Leafy Spurge</b>	<b>Park Road</b>	<b>Sagebrush</b>	<b>Shrubby Veg</b>	<b>Taller Veg</b>	<b>Trees</b>	<b>Water</b>	<b>Total</b>	<b>Users Accuracy</b>	<b>Kappa</b>
<b>Bare Ground</b>	83	4	0	4	12	0	1	4	3	111	0.747748	0
<b>Grasses</b>	7	88	1	0	5	0	9	0	1	111	0.792793	0
<b>Leafy Spurge</b>	0	0	57	0	0	31	22	1	0	111	0.513514	0
<b>Park Road</b>	48	22	0	30	1	0	2	0	8	111	0.27027	0
<b>Sagebrush</b>	17	20	0	0	73	0	0	1	0	111	0.657658	0
<b>Shrubby Veg</b>	0	0	19	0	0	81	7	4	0	111	0.72973	0
<b>Taller Veg</b>	0	2	9	0	0	27	68	5	0	111	0.612613	0
<b>Trees</b>	0	14	13	0	6	14	61	3	0	111	0.027027	0
<b>Water</b>	46	10	0	0	0	0	0	0	55	111	0.495495	0
<b>Total</b>	201	160	99	34	97	153	170	18	67	999	0	0
<b>Producers Accuracy</b>	0.412935	0.55	0.575758	0.882353	0.752577	0.529412	0.4	0.166667	0.820896	0	0.538539	0
<b>Kappa</b>	0	0	0	0	0	0	0	0	0	0	0	0.480856

**Appendix B: Table 21.** Support Vector Machines UAS Talkington75(1) Stratified Random Accuracy Confusion Matrix

<b>Class</b>	<b>Bare Ground</b>	<b>Grasses</b>	<b>Leafy Spurge</b>	<b>Park Road</b>	<b>Sagebrush</b>	<b>Shrubby Veg</b>	<b>Taller Veg</b>	<b>Trees</b>	<b>Water</b>	<b>Total</b>	<b>Users Accuracy</b>	<b>Kappa</b>
<b>Bare Ground</b>	19	3	0	1	12	0	3	3	1	42	0.452381	0
<b>Grasses</b>	17	194	0	0	9	0	14	1	3	238	0.815126	0
<b>Leafy Spurge</b>	0	0	7	0	0	0	2	0	0	9	0.777778	0
<b>Park Road</b>	9	5	0	13	1	0	0	1	0	29	0.448276	0
<b>Sagebrush</b>	1	6	0	0	20	0	1	0	0	28	0.714286	0
<b>Shrubby Veg</b>	0	4	6	0	2	8	13	2	0	35	0.228571	0
<b>Taller Veg</b>	1	35	8	0	4	4	94	2	0	148	0.635135	0
<b>Trees</b>	0	24	7	0	14	11	61	4	0	121	0.033058	0
<b>Water</b>	22	34	0	3	35	1	18	3	5	120	0.041667	0
<b>Total</b>	69	305	28	17	97	24	206	15	9	770	0	0
<b>Producers Accuracy</b>	0.275362	0.636066	0.25	0.764706	0.206186	0.333333	0.456311	0.266667	0.555556	0	0.472727	0
<b>Kappa</b>	0	0	0	0	0	0	0	0	0	0	0	0.348339

**Appendix B: Table 22.** Support Vector Machines UAS Talkington75(2) Stratified Random Accuracy Confusion Matrix

<b>Class</b>	<b>Bare Ground</b>	<b>Grasses</b>	<b>Leafy Spurge</b>	<b>Park Road</b>	<b>Sagebrush</b>	<b>Shrubby Veg</b>	<b>Taller Veg</b>	<b>Trees</b>	<b>Water</b>	<b>Total</b>	<b>Users Accuracy</b>	<b>Kappa</b>
<b>Bare Ground</b>	20	3	0	0	15	0	1	5	2	46	0.434783	0
<b>Grasses</b>	15	316	0	0	10	0	17	1	0	359	0.880223	0
<b>Leafy Spurge</b>	0	0	2	0	0	1	1	1	0	5	0.4	0
<b>Park Road</b>	5	1	0	0	3	0	0	0	0	9	0	0
<b>Sagebrush</b>	0	2	0	0	18	0	0	2	0	22	0.818182	0
<b>Shrubby Veg</b>	0	2	2	0	1	8	17	1	0	31	0.258065	0
<b>Taller Veg</b>	0	45	0	0	1	7	88	4	0	145	0.606897	0
<b>Trees</b>	0	11	0	0	8	13	27	9	0	68	0.132353	0
<b>Water</b>	28	18	0	0	26	2	5	3	9	91	0.098901	0
<b>Total</b>	68	398	4	0	82	31	156	26	11	776	0	0
<b>Producers Accuracy</b>	0.294118	0.79397	0.5	0	0.219512	0.258065	0.564103	0.346154	0.818182	0	0.60567	0
<b>Kappa</b>	0	0	0	0	0	0	0	0	0	0	0	0.445186

**Appendix B: Table 23.** Support Vector Machines UAS Talkington75(2) Equalized Random Accuracy Confusion Matrix

<b>Class</b>	<b>Bare Ground</b>	<b>Grasses</b>	<b>Leafy Spurge</b>	<b>Park Road</b>	<b>Sagebrush</b>	<b>Shrubby Veg</b>	<b>Taller Veg</b>	<b>Trees</b>	<b>Water</b>	<b>Total</b>	<b>Users Accuracy</b>	<b>Kappa</b>
<b>Bare Ground</b>	52	24	2	5	18	4	0	4	2	111	0.468468	0
<b>Grasses</b>	5	101	1	0	2	1	1	0	0	111	0.90991	0
<b>Leafy Spurge</b>	0	0	88	0	1	13	8	1	0	111	0.792793	0
<b>Park Road</b>	15	22	1	65	6	0	0	2	0	111	0.585586	0
<b>Sagebrush</b>	4	10	1	0	90	0	5	0	1	111	0.810811	0
<b>Shrubby Veg</b>	0	9	19	0	1	50	29	3	0	111	0.45045	0
<b>Taller Veg</b>	0	9	16	0	5	6	74	1	0	111	0.666667	0
<b>Trees</b>	0	15	17	0	18	15	42	4	0	111	0.036036	0
<b>Water</b>	16	40	4	1	27	4	10	1	8	111	0.072072	0
<b>Total</b>	92	230	149	71	168	93	169	16	11	999	0	0
<b>Producers Accuracy</b>	0.565217	0.43913	0.590604	0.915493	0.535714	0.537634	0.43787	0.25	0.727273	0	0.532533	0
<b>Kappa</b>	0	0	0	0	0	0	0	0	0	0	0	0.474099



**Appendix B: Table 24.** Support Vector Machines UAS Talkington75(2) Equalized Random Accuracy Confusion Matrix

<b>Class</b>	<b>Bare Ground</b>	<b>Grasses</b>	<b>Leafy Spurge</b>	<b>Park Road</b>	<b>Sagebrush</b>	<b>Shrubby Veg</b>	<b>Taller Veg</b>	<b>Trees</b>	<b>Water</b>	<b>Total</b>	<b>Users Accuracy</b>	<b>Kappa</b>
<b>Bare Ground</b>	52	15	0	0	34	4	1	3	2	111	0.468468	0
<b>Grasses</b>	7	98	0	0	1	1	4	0	0	111	0.882883	0
<b>Leafy Spurge</b>	0	0	23	0	0	38	32	18	0	111	0.207207	0
<b>Park Road</b>	54	33	0	0	22	1	1	0	0	111	0	0
<b>Sagebrush</b>	6	18	0	0	73	2	7	5	0	111	0.657658	0
<b>Shrubby Veg</b>	0	4	16	0	0	60	26	5	0	111	0.540541	0
<b>Taller Veg</b>	0	13	4	0	1	11	81	1	0	111	0.72973	0
<b>Trees</b>	1	11	6	0	8	35	39	11	0	111	0.099099	0
<b>Water</b>	33	21	1	0	27	5	9	3	12	111	0.108108	0
<b>Total</b>	153	213	50	0	166	157	200	46	14	999	0	0
<b>Producers Accuracy</b>	0.339869	0.460094	0.46	0	0.439759	0.382166	0.405	0.23913	0.857143	0	0.41041	0
<b>Kappa</b>	0	0	0	0	0	0	0	0	0	0	0	0.336712

**Appendix B: Table 25.** Ecognition UAS BeefCorral75(1) Stratified Random Accuracy Confusion Matrix

<b>Class</b>	<b>Bare Ground</b>	<b>Grasses</b>	<b>Trees</b>	<b>Pdog Mound</b>	<b>Taller Veg</b>	<b>Yellow Veg</b>	<b>No Data</b>	<b>Sagebrush</b>	<b>Water</b>	<b>Total</b>	<b>Users Accuracy</b>	<b>Kappa</b>
<b>Bare Ground</b>	163	31	0	9	0	0	0	0	0	203	0.802956	0
<b>Grasses</b>	25	450	4	5	0	0	0	3	0	487	0.924025	0
<b>Trees</b>	0	0	15	0	0	0	0	0	0	15	1	0
<b>Pdog Mound</b>	3	3	0	3	0	0	0	1	0	10	0.3	0
<b>Taller Veg</b>	0	4	16	0	31	1	0	0	0	52	0.596154	0
<b>Yellow Veg</b>	0	3	1	0	2	4	0	0	0	10	0.4	0
<b>No Data</b>	0	0	0	0	0	0	10	0	0	10	1	0
<b>Sagebrush</b>	0	2	1	1	0	0	0	6	0	10	0.6	0
<b>Water</b>	0	2	0	0	0	0	0	0	8	10	0.8	0
<b>Total</b>	191	495	37	18	33	5	10	10	8	807	0	0
<b>Producers Accuracy</b>	0.853403	0.909091	0.405405	0.166667	0.939394	0.8	1	0.6	1	0	0.855019	0
<b>Kappa</b>	0	0	0	0	0	0	0	0	0	0	0	0.743865

**Appendix B: Table 26.** Ecognition UAS BeefCorral75(2) Stratified Random Accuracy Confusion Matrix

<b>Class</b>	<b>Bare Ground</b>	<b>Grasses</b>	<b>Trees</b>	<b>Pdog Mound</b>	<b>Taller Veg</b>	<b>Yellow Veg</b>	<b>No Data</b>	<b>Sagebrush</b>	<b>Water</b>	<b>Total</b>	<b>Users Accuracy</b>	<b>Kappa</b>
<b>Bare Ground</b>	117	38	0	5	0	0	0	0	0	160	0.73125	0
<b>Grasses</b>	26	573	0	3	0	0	0	0	0	602	0.951827	0
<b>Trees</b>	3	6	0	1	0	0	0	0	0	10	0	0
<b>Pdog Mound</b>	4	1	0	5	0	0	0	0	0	10	0.5	0
<b>Taller Veg</b>	0	10	0	0	0	0	0	0	0	10	0	0
<b>Yellow Veg</b>	4	6	0	0	0	0	0	0	0	10	0	0
<b>No Data</b>	0	0	0	0	0	0	10	0	0	10	1	0
<b>Sagebrush</b>	3	7	0	0	0	0	0	0	0	10	0	0
<b>Water</b>	10	0	0	0	0	0	0	0	0	10	0	0
<b>Total</b>	167	641	0	14	0	0	10	0	0	832	0	0
<b>Producers Accuracy</b>	0.700599	0.893916	0	0.357143	0	0	1	0	0	0	0.847356	0
<b>Kappa</b>	0	0	0	0	0	0	0	0	0	0	0	0.621794

**Appendix B: Table 27.** Ecognition UAS BeefCorral75(1) Equalized Random Accuracy Confusion Matrix

<b>Class</b>	<b>Bare Ground</b>	<b>Grasses</b>	<b>Trees</b>	<b>Pdog Mound</b>	<b>Taller Veg</b>	<b>Yellow Veg</b>	<b>No Data</b>	<b>Sagebrush</b>	<b>Water</b>	<b>Total</b>	<b>Users Accuracy</b>	<b>Kappa</b>
<b>Bare Ground</b>	87	11	0	2	0	0	0	0	0	100	0.87	0
<b>Grasses</b>	1	96	2	0	0	0	0	1	0	100	0.96	0
<b>Trees</b>	0	2	86	0	4	0	0	8	0	100	0.86	0
<b>Pdog Mound</b>	17	22	1	51	3	0	0	6	0	100	0.51	0
<b>Taller Veg</b>	0	7	16	0	75	1	0	1	0	100	0.75	0
<b>Yellow Veg</b>	0	23	15	0	29	29	0	4	0	100	0.29	0
<b>No Data</b>	0	0	0	0	0	0	100	0	0	100	1	0
<b>Sagebrush</b>	3	7	23	0	0	0	0	67	0	100	0.67	0
<b>Water</b>	0	18	0	0	0	1	0	0	81	100	0.81	0
<b>Total</b>	108	186	143	53	111	31	100	87	81	900	0	0
<b>Producers Accuracy</b>	0.805556	0.516129	0.601399	0.962264	0.675676	0.935484	1	0.770115	1	0	0.746667	0
<b>Kappa</b>	0	0	0	0	0	0	0	0	0	0	0	0.715

**Appendix B: Table 28.** Ecognition UAS BeefCorral75(2) Equalized Random Accuracy Confusion Matrix

<b>Class</b>	<b>Bare Ground</b>	<b>Grasses</b>	<b>Trees</b>	<b>Pdog Mound</b>	<b>Taller Veg</b>	<b>Yellow Veg</b>	<b>No Data</b>	<b>Sagebrush</b>	<b>Water</b>	<b>Total</b>	<b>Users Accuracy</b>	<b>Kappa</b>
<b>Bare Ground</b>	72	24	0	4	0	0	0	0	0	100	0.72	0
<b>Grasses</b>	3	97	0	0	0	0	0	0	0	100	0.97	0
<b>Trees</b>	14	83	0	3	0	0	0	0	0	100	0	0
<b>Pdog Mound</b>	15	35	0	50	0	0	0	0	0	100	0.5	0
<b>Taller Veg</b>	6	84	0	10	0	0	0	0	0	100	0	0
<b>Yellow Veg</b>	10	89	0	1	0	0	0	0	0	100	0	0
<b>No Data</b>	0	0	0	0	0	0	100	0	0	100	1	0
<b>Sagebrush</b>	2	96	0	0	0	0	0	2	0	100	0.2	0
<b>Water</b>	100	0	0	0	0	0	0	0	0	100	0	0
<b>Total</b>	222	508	0	68	0	0	100	2	0	900	0	0
<b>Producers Accuracy</b>	0.324324	0.190945	0	0.735294	0	0	1	1	0	0	0.356667	0
<b>Kappa</b>	0	0	0	0	0	0	0	0	0	0	0	0.27625

**Appendix B: Table 29.** Maximum likelihood UAS BeefCorral75(1) Stratified Random Accuracy Confusion Matrix

<b>Class</b>	<b>Bare Ground</b>	<b>Grasses</b>	<b>Yellow Veg</b>	<b>Pdog Mound</b>	<b>No Data</b>	<b>Sagebrush</b>	<b>Taller Veg</b>	<b>Trees</b>	<b>Water</b>	<b>Total</b>	<b>Users Accuracy</b>	<b>Kappa</b>
<b>Bare Ground</b>	127	29	1	10	0	0	0	1	0	168	0.755952	0
<b>Grasses</b>	26	400	2	7	5	1	0	7	0	448	0.892857	0
<b>Yellow Veg</b>	0	15	25	0	22	3	2	2	0	69	0.362319	0
<b>Pdog Mound</b>	38	46	0	1	0	0	0	0	0	85	0.011765	0
<b>No Data</b>	0	0	8	0	4	0	0	0	0	12	0.333333	0
<b>Sagebrush</b>	0	3	1	0	2	1	0	0	0	7	0.142857	0
<b>Taller Veg</b>	0	0	0	0	0	0	8	0	0	8	1	0
<b>Trees</b>	0	0	0	0	0	0	0	0	0	0	0	0
<b>Water</b>	0	2	0	0	0	0	0	0	8	10	0.8	0
<b>Total</b>	191	495	37	18	33	5	10	10	8	807	0	0
<b>Producers Accuracy</b>	0.664921	0.808081	0.675676	0.055556	0.121212	0.2	0.8	0	1	0	0.711276	0
<b>Kappa</b>	0	0	0	0	0	0	0	0	0	0	0	0.521217

**Appendix B: Table 30.** Maximum likelihood UAS BeefCorral75(2) Stratified Random Accuracy Confusion Matrix

<b>Class</b>	<b>Bare Ground</b>	<b>Grasses</b>	<b>Pdog Mound</b>	<b>No Data</b>	<b>Sagebrush</b>	<b>Taller Veg</b>	<b>Trees</b>	<b>Total</b>	<b>Users Accuracy</b>	<b>Kappa</b>
<b>Bare Ground</b>	96	45	10	0	0	0	0	151	0.635762	0
<b>Grasses</b>	33	536	3	0	0	0	0	572	0.937063	0
<b>Pdog Mound</b>	28	54	1	0	0	0	0	83	0.012048	0
<b>No Data</b>	0	0	0	0	0	10	0	10	0	0
<b>Sagebrush</b>	1	0	0	0	0	0	0	1	0	0
<b>Taller Veg</b>	0	0	0	0	0	0	0	0	0	0
<b>Trees</b>	9	4	0	0	0	0	0	13	0	0
<b>Total</b>	167	639	14	0	0	10	0	830	0	0
<b>Producers Accuracy</b>	0.57485	0.838811	0.071429	0	0	0	0	0	0.762651	0
<b>Kappa</b>	0	0	0	0	0	0	0	0	0	0.449485

**Appendix B: Table 31.** Maximum likelihood UAS BeefCorral75(1) Equalized Random Accuracy Confusion Matrix

<b>Class</b>	<b>Bare Ground</b>	<b>Grasses</b>	<b>Yellow Veg</b>	<b>Pdog Mound</b>	<b>No Data</b>	<b>Sagebrush</b>	<b>Taller Veg</b>	<b>Trees</b>	<b>Water</b>	<b>Total</b>	<b>Users Accuracy</b>	<b>Kappa</b>
<b>Bare Ground</b>	82	15	0	14	0	0	0	0	0	111	0.738739	0
<b>Grasses</b>	1	103	0	0	0	4	3	0	0	111	0.927928	0
<b>Yellow Veg</b>	0	65	10	0	0	1	15	20	0	111	0.09009	0
<b>Pdog Mound</b>	36	68	0	7	0	0	0	0	0	111	0.063063	0
<b>No Data</b>	0	0	0	0	111	0	0	0	0	111	1	0
<b>Sagebrush</b>	1	2	1	0	0	68	1	38	0	111	0.612613	0
<b>Taller Veg</b>	0	2	0	0	0	0	67	42	0	111	0.603604	0
<b>Trees</b>	0	17	2	0	0	4	49	39	0	111	0.351351	0
<b>Water</b>	0	83	0	0	0	0	1	0	27	111	0.243243	0
<b>Total</b>	120	355	13	21	111	77	136	139	27	999	0	0
<b>Producers Accuracy</b>	0.683333	0.290141	0.769231	0.333333	1	0.883117	0.492647	0.280576	1	0	0.514515	0
<b>Kappa</b>	0	0	0	0	0	0	0	0	0	0	0	0.453829



**Appendix B: Table 32.** Maximum likelihood UAS BeefCorral75(2) Equalized Random Accuracy Confusion Matrix

<b>Class</b>	<b>Bare Ground</b>	<b>Grasses</b>	<b>Yellow Veg</b>	<b>Pdog Mound</b>	<b>No Data</b>	<b>Sagebrush</b>	<b>Taller Veg</b>	<b>Trees</b>	<b>Water</b>	<b>Total</b>	<b>Users Accuracy</b>	<b>Kappa</b>
<b>Bare Ground</b>	62	35	0	14	0	0	0	0	0	111	0.558559	0
<b>Grasses</b>	2	109	0	0	0	0	0	0	0	111	0.981982	0
<b>Yellow Veg</b>	3	108	0	0	0	0	0	0	0	111	0	0
<b>Pdog Mound</b>	31	75	0	4	0	0	0	0	0	111	0.036036	0
<b>No Data</b>	0	0	0	0	111	0	0	0	0	111	1	0
<b>Sagebrush</b>	88	23	0	0	0	0	0	0	0	111	0	0
<b>Taller Veg</b>	0	103	0	8	0	0	0	0	0	111	0	0
<b>Trees</b>	1	107	0	3	0	0	0	0	0	111	0	0
<b>Water</b>	16	94	0	1	0	0	0	0	0	111	0	0
<b>Total</b>	204	654	0	30	111	0	0	0	0	999	0	0
<b>Producers Accuracy</b>	0.303922	0.166667	0	0.133333	1	0	0	0	0	0	0.286286	0
<b>Kappa</b>	0	0	0	0	0	0	0	0	0	0	0	0.197072

**Appendix B: Table 33.** Support Vector Machines UAS BeefCorral75(1) Stratified Random Accuracy Confusion Matrix

Class	Bare Ground	Grasses	Trees	Pdog Mound	Taller Veg	Yellow Veg	No Data	Sagebrush	Water	Park Road	Total	Users Accuracy	Kappa
<b>Bare Ground</b>	119	58	0	7	0	0	0	0	3	0	187	0.636364	0
<b>Grasses</b>	26	375	6	6	14	3	0	7	0	0	437	0.858124	0
<b>Trees</b>	0	0	11	0	2	2	0	1	0	0	16	0.6875	0
<b>Pdog Mound</b>	39	49	1	5	0	0	0	0	0	0	94	0.053191	0
<b>Taller Veg</b>	0	1	16	0	15	0	0	0	0	0	32	0.46875	0
<b>Yellow Veg</b>	0	10	1	0	1	0	0	0	0	0	12	0	0
<b>No Data</b>	0	0	0	0	0	0	0	0	0	0	0	0	0
<b>Sagebrush</b>	0	1	2	0	1	0	0	2	0	0	6	0.333333	0
<b>Water</b>	0	1	0	0	0	0	0	0	5	0	6	0.833333	0
<b>Park Road</b>	7	0	0	0	0	0	10	0	0	0	17	0	0
<b>Total</b>	191	495	37	18	33	5	10	10	8	0	807	0	0
<b>Producers Accuracy</b>	0.623037	0.757576	0.297297	0.277778	0.454545	0	0	0.2	0.625	0	0	0.659232	0
<b>Kappa</b>	0	0	0	0	0	0	0	0	0	0	0	0	0.439171

---

**Appendix B: Table 34** Support Vector Machines UAS BeefCorral75(2) Stratified Random Accuracy Confusion Matrix

---

<b>Class</b>	<b>Bare Ground</b>	<b>Grasses</b>	<b>Pdog Mound</b>	<b>Taller Veg</b>	<b>Sagebrush</b>	<b>Park Road</b>	<b>Total</b>	<b>Users Accuracy</b>	<b>Kappa</b>
<b>Bare Ground</b>	94	59	4	0	0	0	157	0.598726	0
<b>Grasses</b>	32	500	3	0	0	0	535	0.934579	0
<b>Pdog Mound</b>	36	76	6	0	0	0	118	0.050847	0
<b>Taller Veg</b>	0	0	0	0	0	0	0	0	0
<b>Sagebrush</b>	1	1	0	0	0	0	2	0	0
<b>Park Road</b>	4	3	1	10	0	0	18	0	0
<b>Total</b>	167	639	14	10	0	0	830	0	0
<b>Producers Accuracy</b>	0.562874	0.782473	0.428571	0	0	0	0	0.722892	0
<b>Kappa</b>	0	0	0	0	0	0	0	0	0.401875

---

**Appendix B: Table 35.** Support Vector Machines UAS BeefCorral75(1) Equalized Random Accuracy Confusion Matrix

<b>Class</b>	<b>Bare Ground</b>	<b>Grasses</b>	<b>Trees</b>	<b>Pdog Mound</b>	<b>Taller Veg</b>	<b>Yellow Veg</b>	<b>Sagebrush</b>	<b>Water</b>	<b>Park Road</b>	<b>Total</b>	<b>Users Accuracy</b>	<b>Kappa</b>
<b>Bare Ground</b>	57	35	0	7	1	0	0	0	0	100	0.57	0
<b>Grasses</b>	7	82	5	0	5	1	0	0	0	100	0.82	0
<b>Trees</b>	0	13	45	0	40	2	0	0	0	100	0.45	0
<b>Pdog Mound</b>	37	47	1	13	0	0	2	0	0	100	0.13	0
<b>Taller Veg</b>	0	4	43	0	50	1	2	0	0	100	0.5	0
<b>Yellow Veg</b>	0	64	9	0	17	9	1	0	0	100	0.09	0
<b>Sagebrush</b>	10	38	17	2	3	1	29	0	0	100	0.29	0
<b>Water</b>	0	52	0	0	0	0	0	48	0	100	0.48	0
<b>Park Road</b>	57	7	7	27	0	0	0	0	2	100	0.02	0
<b>Total</b>	168	342	127	49	116	14	34	48	2	900	0	0
<b>Producers Accuracy</b>	0.339286	0.239766	0.354331	0.265306	0.431034	0.642857	0.852941	1	1	0	0.372222	0
<b>Kappa</b>	0	0	0	0	0	0	0	0	0	0	0	0.29375

**Appendix B: Table 36.** Support Vector Machines UAS BeefCorral75(2) Equalized Random Confusion Matrix

<b>Class</b>	<b>Bare Ground</b>	<b>Grasses</b>	<b>Trees</b>	<b>Pdog Mound</b>	<b>Taller Veg</b>	<b>Sagebrush</b>	<b>Water</b>	<b>Park Road</b>	<b>Total</b>	<b>Users Accuracy</b>	<b>Kappa</b>
<b>Bare Ground</b>	45	62	0	6	0	0	0	0	113	0.39823	0
<b>Grasses</b>	3	106	0	4	0	0	0	0	113	0.938053	0
<b>Trees</b>	5	106	0	2	0	0	0	0	113	0	0
<b>Pdog Mound</b>	29	80	0	4	0	0	0	0	113	0.035398	0
<b>Taller Veg</b>	0	110	0	3	0	0	0	0	113	0	0
<b>Sagebrush</b>	4	108	0	1	0	0	0	0	113	0	0
<b>Water</b>	113	0	0	0	0	0	0	0	113	0	0
<b>Park Road</b>	58	43	0	12	0	0	0	0	113	0	0
<b>Total</b>	257	615	0	32	0	0	0	0	904	0	0
<b>Producers Accuracy</b>	0.175097	0.172358	0	0.125	0	0	0	0	0	0.17146	0
<b>Kappa</b>	0	0	0	0	0	0	0	0	0	0	0.053097

**Appendix B: Table 37.** Ecognition UAS Lindbo75(1) Stratified Random Accuracy Confusion Matrix

<b>Class</b>	<b>Grasses</b>	<b>Bare Ground</b>	<b>Taller Veg</b>	<b>Pdog Mound</b>	<b>Trees</b>	<b>Water</b>	<b>Sagebrush</b>	<b>No Data</b>	<b>Thistle</b>	<b>Total</b>	<b>Users Accuracy</b>	<b>Kappa</b>
<b>Grasses</b>	461	27	1	1	0	0	2	0	0	492	0.936992	0
<b>Bare Ground</b>	49	184	0	6	0	0	1	0	0	240	0.766667	0
<b>Taller Veg</b>	3	0	20	0	0	0	1	0	0	24	0.833333	0
<b>Pdog Mound</b>	4	4	0	1	0	0	1	0	0	10	0.1	0
<b>Trees</b>	1	3	2	0	2	1	1	0	0	10	0.2	0
<b>Water</b>	2	1	0	0	0	7	0	0	0	10	0.7	0
<b>Sagebrush</b>	0	2	0	0	0	0	8	0	0	10	0.8	0
<b>No Data</b>	2	6	1	0	0	0	1	0	0	10	0	0
<b>Thistle</b>	0	9	0	0	0	1	0	0	0	10	0	0
<b>Total</b>	522	236	24	8	2	9	15	0	0	816	0	0
<b>Producers Accuracy</b>	0.883142	0.779661	0.833333	0.125	1	0.777778	0.533333	0	0	0	0.83701	0
<b>Kappa</b>	0	0	0	0	0	0	0	0	0	0	0	0.691222

**Appendix B: Table 38.** Ecognition UAS Lindbo75(2) lf75RGBClip2 Stratified Random Accuracy Confusion Matrix

<b>Class</b>	<b>Grasses</b>	<b>Bare Ground</b>	<b>Taller Veg</b>	<b>Pdog Mound</b>	<b>Trees</b>	<b>Water</b>	<b>Sagebrush</b>	<b>Yellow Veg</b>	<b>Park Road</b>	<b>Total</b>	<b>Users Accuracy</b>	<b>Kappa</b>
<b>Grasses</b>	521	37	1	6	1	1	0	0	0	567	0.918871	0
<b>Bare Ground</b>	21	125	8	0	0	5	0	0	0	159	0.786164	0
<b>Taller Veg</b>	1	7	5	0	0	0	0	0	0	13	0.384615	0
<b>Pdog Mound</b>	8	2	0	12	1	2	0	0	0	25	0.48	0
<b>Trees</b>	1	0	0	2	3	4	0	0	0	10	0.3	0
<b>Water</b>	3	0	0	0	0	7	0	0	0	10	0.7	0
<b>Sagebrush</b>	8	1	0	0	0	1	0	0	0	10	0	0
<b>Yellow Veg</b>	0	2	0	4	0	1	0	1	2	10	0.1	0
<b>Park Road</b>	0	0	0	0	0	0	0	0	10	10	1	0
<b>Total</b>	563	174	14	24	5	21	0	1	12	814	0	0
<b>Producers Accuracy</b>	0.9254	0.718391	0.357143	0.5	0.6	0.333333	0	1	0.833333	0	0.840295	0
<b>Kappa</b>	0	0	0	0	0	0	0	0	0	0	0	0.663569

**Appendix B: Table 39.** Ecognition UAS Lindbo75NIR(1) Stratified Random Accuracy Confusion Matrix

<b>Class</b>	<b>Bare Ground</b>	<b>Grasses</b>	<b>Yellow Veg</b>	<b>Pdog Mound</b>	<b>Park Road</b>	<b>Sagebrush</b>	<b>Trees</b>	<b>Taller Veg</b>	<b>Water</b>	<b>Total</b>	<b>Users Accuracy</b>	<b>Kappa</b>
<b>Bare Ground</b>	50	8	0	3	0	0	0	0	0	61	0.819672	0
<b>Grasses</b>	70	485	0	11	0	2	0	19	0	587	0.826235	0
<b>Yellow Veg</b>	0	2	0	0	0	2	0	6	0	10	0	0
<b>Pdog Mound</b>	33	9	0	13	0	0	0	0	0	55	0.236364	0
<b>Park Road</b>	8	2	0	0	0	0	0	0	0	10	0	0
<b>Sagebrush</b>	3	3	0	0	0	2	0	2	0	10	0.2	0
<b>Trees</b>	14	10	0	1	0	0	0	0	0	25	0	0
<b>Taller Veg</b>	4	7	0	0	0	1	2	20	0	34	0.588235	0
<b>Water</b>	5	2	0	0	0	1	0	1	1	10	0.1	0
<b>Total</b>	187	528	0	28	0	8	2	48	1	802	0	0
<b>Producers Accuracy</b>	0.26738	0.918561	0	0.464286	0	0.25	0	0.416667	1	0	0.71197	0
<b>Kappa</b>	0	0	0	0	0	0	0	0	0	0	0	0.418419



**Appendix B: Table 40.** Ecognition UAS Lindbo90(1) Stratified Random Accuracy Confusion Matrix

<b>Class</b>	<b>Bare Ground</b>	<b>Grasses</b>	<b>Pdog Mound</b>	<b>Sagebrush</b>	<b>Trees</b>	<b>Taller Veg</b>	<b>Water</b>	<b>Total</b>	<b>Users Accuracy</b>	<b>Kappa</b>
<b>Bare Ground</b>	137	113	16	0	0	1	0	267	0.513109	0
<b>Grasses</b>	34	402	8	4	1	24	1	474	0.848101	0
<b>Pdog Mound</b>	13	5	4	0	0	0	0	22	0.181818	0
<b>Sagebrush</b>	2	0	0	2	0	0	0	4	0.5	0
<b>Trees</b>	0	0	0	0	0	0	0	0	0	0
<b>Taller Veg</b>	1	8	0	1	1	23	0	34	0.676471	0
<b>Water</b>	0	0	0	1	0	0	0	1	0	0
<b>Total</b>	187	528	28	8	2	48	1	802	0	0
<b>Producers Accuracy</b>	0.73262	0.761364	0.142857	0.25	0	0.479167	0	0	0.708229	0
<b>Kappa</b>	0	0	0	0	0	0	0	0	0	0.449205

**Appendix B: Table 41.** Ecognition UAS Lindbo75(1) Equalized Random Accuracy Confusion Matrix

<b>Class</b>	<b>Grasses</b>	<b>Bare Ground</b>	<b>Taller Veg</b>	<b>Pdog Mound</b>	<b>Trees</b>	<b>Water</b>	<b>Sagebrush</b>	<b>No Data</b>	<b>Thistle</b>	<b>Total</b>	<b>Users Accuracy</b>	<b>Kappa</b>
<b>Grasses</b>	97	10	1	3	0	0	0	0	0	111	0.873874	0
<b>Bare Ground</b>	27	77	0	7	0	0	0	0	0	111	0.693694	0
<b>Taller Veg</b>	9	3	94	0	0	1	4	0	0	111	0.846847	0
<b>Pdog Mound</b>	26	28	10	46	0	0	0	0	0	111	0.418182	0
<b>Trees</b>	20	20	43	0	9	1	18	0	0	111	0.081081	0
<b>Water</b>	8	2	0	1	0	100	0	0	0	111	0.900901	0
<b>Sagebrush</b>	9	20	14	0	1	1	66	0	0	111	0.594595	0
<b>No Data</b>	11	49	24	0	0	7	19	0	0	111	0	0
<b>Thistle</b>	2	108	0	0	0	0	1	0	0	111	0	0
<b>Total</b>	209	317	186	57	10	110	108	0	0	997	0	0
<b>Producers Accuracy</b>	0.464115	0.242902	0.505376	0.807018	0.9	0.909091	0.611111	0	0	0	0.490471	0
<b>Kappa</b>	0	0	0	0	0	0	0	0	0	0	0	0.426674

**Appendix B: Table 42.** Ecognition UAS Lindbo75(2) Equalized Random Accuracy Confusion Matrix

Class	Grasses	Bare Ground	Taller Veg	Pdog Mound	Trees	Water	Sagebrush	Yellow Veg	Park Road	Total	Users Accuracy	Kappa
<b>Grasses</b>	95	7	1	8	0	0	0	0	0	111	0.855856	0
<b>Bare Ground</b>	22	77	9	1	0	2	0	0	0	111	0.693694	0
<b>Taller Veg</b>	11	52	47	1	0	0	0	0	0	111	0.423423	0
<b>Pdog Mound</b>	19	6	0	79	1	4	0	1	1	111	0.711712	0
<b>Trees</b>	5	32	0	47	9	15	0	1	2	111	0.081081	0
<b>Water</b>	21	7	1	8	1	73	0	0	0	111	0.657658	0
<b>Sagebrush</b>	87	4	1	7	0	11	0	0	1	111	0	0
<b>Yellow Veg</b>	8	15	0	61	3	3	0	18	3	111	0.162162	0
<b>Park Road</b>	8	1	0	2	0	0	0	0	100	111	0.900901	0
<b>Total</b>	276	201	59	214	14	108	0	20	107	999	0	0
<b>Producers Accuracy</b>	0.344203	0.383085	0.79661	0.369159	0.642857	0.675926	0	0.9	0.934579	0	0.498498	0
<b>Kappa</b>	0	0	0	0	0	0	0	0	0	0	0	0.435811

**Appendix B: Table 43.** Ecognition UAS Lindbo75NIR(1) Equalized Random Accuracy Confusion Matrix

<b>Class</b>	<b>Bare Ground</b>	<b>Grasses</b>	<b>Yellow Veg</b>	<b>Pdog Mound</b>	<b>Park Road</b>	<b>Sagebrush</b>	<b>Trees</b>	<b>Taller Veg</b>	<b>Water</b>	<b>Total</b>	<b>Users Accuracy</b>	<b>Kappa</b>
<b>Bare Ground</b>	93	9	0	4	0	0	0	0	0	106	0.877358	0
<b>Grasses</b>	13	85	0	4	0	0	0	4	0	106	0.801887	0
<b>Yellow Veg</b>	2	25	0	0	0	17	0	62	0	106	0	0
<b>Pdog Mound</b>	71	10	0	23	0	1	0	0	1	106	0.216981	0
<b>Park Road</b>	67	25	0	1	0	6	0	6	1	106	0	0
<b>Sagebrush</b>	37	23	0	0	0	31	1	14	0	106	0.292453	0
<b>Trees</b>	85	17	0	3	0	1	0	0	0	106	0	0
<b>Taller Veg</b>	2	12	0	0	0	5	0	87	0	106	0.820755	0
<b>Water</b>	63	19	0	0	0	3	0	4	17	106	0.160377	0
<b>Total</b>	433	225	0	35	0	64	1	177	19	954	0	0
<b>Producers Accuracy</b>	0.214781	0.377778	0	0.657143	0	0.484375	0	0.491525	0.894737	0	0.352201	0
<b>Kappa</b>	0	0	0	0	0	0	0	0	0	0	0	0.271226

**Appendix B: Table 44.** Ecognition UAS Lindbo90(1) Equalized Random Accuracy Confusion Matrix

<b>Class</b>	<b>Bare Ground</b>	<b>Grasses</b>	<b>Yellow Veg</b>	<b>Pdog Mound</b>	<b>Park Road</b>	<b>Sagebrush</b>	<b>Trees</b>	<b>Taller Veg</b>	<b>Water</b>	<b>Total</b>	<b>Users Accuracy</b>	<b>Kappa</b>
<b>Bare Ground</b>	74	26	0	6	0	0	0	0	0	106	0.698113	0
<b>Grasses</b>	7	94	0	0	0	0	0	5	0	106	0.886792	0
<b>Yellow Veg</b>	0	0	0	0	0	0	0	39	67	106	0	0
<b>Pdog Mound</b>	42	25	0	38	0	1	0	0	0	106	0.358491	0
<b>Park Road</b>	55	15	0	0	0	0	0	7	126	106	0	0
<b>Sagebrush</b>	16	10	0	0	0	73	0	6	1	106	0.688679	0
<b>Trees</b>	21	5	0	0	0	7	61	11	1	106	0.575472	0
<b>Taller Veg</b>	2	7	0	0	0	6	0	91	0	106	0.858491	0
<b>Water</b>	0	0	0	0	0	0	0	7	99	106	0.933962	0
<b>Total</b>	217	182	0	44	0	87	61	166	194	954	0	0
<b>Producers Accuracy</b>	0.341014	0.516484	0	0.863636	0	0.83908	1	0.548193	0.510309	0	0.555556	0
<b>Kappa</b>	0	0	0	0	0	0	0	0	0	0	0	0.5

**Appendix B: Table 45.** Maximum likelihood UAS Lindbo75(1) Stratified Random Accuracy Confusion Matrix

<b>Class</b>	<b>Bare Ground</b>	<b>Grasses</b>	<b>Yellow Veg</b>	<b>Pdog Mound</b>	<b>Sagebrush</b>	<b>Taller Veg</b>	<b>Trees</b>	<b>Water</b>	<b>Total</b>	<b>Users Accuracy</b>	<b>Kappa</b>
<b>Bare Ground</b>	137	79	0	22	0	0	0	0	238	0.57563	0
<b>Grasses</b>	44	425	0	6	5	1	27	1	509	0.834971	0
<b>Yellow Veg</b>	0	0	0	0	0	0	1	0	1	0	0
<b>Pdog Mound</b>	3	5	0	0	0	0	0	0	8	0	0
<b>Sagebrush</b>	1	6	0	0	1	0	2	0	10	0.1	0
<b>Taller Veg</b>	0	3	0	0	0	0	12	0	15	0	0
<b>Trees</b>	2	5	0	0	2	1	6	0	16	0.375	0
<b>Water</b>	0	5	0	0	0	0	0	0	5	0	0
<b>Total</b>	187	528	0	28	8	2	48	1	802	0	0
<b>Producers Accuracy</b>	0.73262	0.804924	0	0	0.125	0	0.125	0	0	0.709476	0
<b>Kappa</b>	0	0	0	0	0	0	0	0	0	0	0.43174

**Appendix B: Table 46.** Maximum likelihood UAS Lindbo75(2) Stratified Random Accuracy Confusion Matrix

<b>Class</b>	<b>Bare Ground</b>	<b>Grasses</b>	<b>Pdog Mound</b>	<b>Sagebrush</b>	<b>Taller Veg</b>	<b>Trees</b>	<b>Water</b>	<b>Total</b>	<b>Users Accuracy</b>	<b>Kappa</b>
<b>Bare Ground</b>	122	68	20	2	0	0	1	213	0.57277	0
<b>Grasses</b>	55	433	5	5	1	15	0	514	0.842412	0
<b>Pdog Mound</b>	1	2	0	0	0	0	5	8	0	0
<b>Sagebrush</b>	0	7	0	11	0	2	0	20	0.55	0
<b>Taller Veg</b>	0	2	0	0	0	25	0	27	0	0
<b>Trees</b>	3	1	0	6	0	9	0	19	0.473684	0
<b>Water</b>	0	7	0	0	0	1	5	13	0.364615	0
<b>Total</b>	181	520	25	24	1	52	11	814	0	0
<b>Producers Accuracy</b>	0.674033	0.832692	0	0.458333	0	0.173077	0.454545	0	0.712531	0
<b>Kappa</b>	0	0	0	0	0	0	0	0	0	0.463335

**Appendix B: Table 47.** Maximum likelihood UAS Lindbo75NIR(1) Stratified Random Accuracy Confusion Matrix

<b>Class</b>	<b>Bare Ground</b>	<b>Grasses</b>	<b>Pdog Mound</b>	<b>Sagebrush</b>	<b>Taller Veg</b>	<b>Trees</b>	<b>Water</b>	<b>Total</b>	<b>Users Accuracy</b>	<b>Kappa</b>
<b>Bare Ground</b>	108	39	15	0	0	1	0	163	0.662577	0
<b>Grasses</b>	49	454	9	4	2	23	0	541	0.839187	0
<b>Pdog Mound</b>	16	16	4	0	0	0	0	36	0.111111	0
<b>Sagebrush</b>	3	2	0	1	0	0	0	6	0.166667	0
<b>Taller Veg</b>	10	6	0	1	0	4	0	21	0	0
<b>Trees</b>	1	11	0	1	0	20	0	33	0.606061	0
<b>Water</b>	0	0	0	1	0	0	1	2	0.5	0
<b>Total</b>	187	528	28	8	2	48	1	802	0	0
<b>Producers Accuracy</b>	0.57754	0.859848	0.142857	0.125	0	0.416667	1	0	0.733167	0
<b>Kappa</b>	0	0	0	0	0	0	0	0	0	0.470922



**Appendix B: Table 48.** Maximum likelihood UAS Lindbo90(1) Stratified Random Accuracy Confusion Matrix

<b>Class</b>	<b>Bare Ground</b>	<b>Grasses</b>	<b>Pdog Mound</b>	<b>Sagebrush</b>	<b>Taller Veg</b>	<b>Trees</b>	<b>Water</b>	<b>Total</b>	<b>Users Accuracy</b>	<b>Kappa</b>
<b>Bare Ground</b>	126	84	16	0	0	1	0	227	0.555066	0
<b>Grasses</b>	47	410	10	2	0	25	1	495	0.828283	0
<b>Pdog Mound</b>	9	21	2	0	0	0	0	32	0.0625	0
<b>Sagebrush</b>	2	3	0	2	1	6	0	14	0.142857	0
<b>Taller Veg</b>	1	3	0	1	1	0	0	6	0.166667	0
<b>Trees</b>	0	6	0	2	0	16	0	24	0.666667	0
<b>Water</b>	2	1	0	1	0	0	0	4	0	0
<b>Total</b>	187	528	28	8	2	48	1	802	0	0
<b>Producers Accuracy</b>	0.673797	0.776515	0.071429	0.25	0.5	0.333333	0	0	0.694514	0
<b>Kappa</b>	0	0	0	0	0	0	0	0	0	0.417322

**Appendix B: Table 49.** Maximum likelihood UAS Lindbo75(1) Equalized Random Accuracy Confusion Matrix

<b>Class</b>	<b>Bare Ground</b>	<b>Grasses</b>	<b>Yellow Veg</b>	<b>Pdog Mound</b>	<b>Sagebrush</b>	<b>Taller Veg</b>	<b>Trees</b>	<b>Water</b>	<b>Total</b>	<b>Users Accuracy</b>	<b>Kappa</b>
<b>Bare Ground</b>	92	19	0	14	0	0	0	0	125	0.736	0
<b>Grasses</b>	18	104	0	1	0	2	0	0	125	0.832	0
<b>Yellow Veg</b>	2	71	0	3	0	49	0	0	125	0	0
<b>Pdog Mound</b>	58	50	0	11	3	1	0	2	125	0.088	0
<b>Sagebrush</b>	7	43	0	0	68	8	0	0	125	0.544	0
<b>Taller Veg</b>	0	23	0	0	0	102	0	0	125	0.826	0
<b>Trees</b>	27	19	0	1	32	43	0	3	125	0	0
<b>Water</b>	11	107	0	1	0	0	0	6	125	0.048	0
<b>Total</b>	215	435	0	31	103	205	0	11	1000	0	0
<b>Producers Accuracy</b>	0.427907	0.23908	0	0.354839	0.660194	0.497561	0	0.545455	0	0.383	0
<b>Kappa</b>	0	0	0	0	0	0	0	0	0	0	0.294857

**Appendix B: Table 50.** Maximum likelihood UAS Lindbo75(2) Equalized Random Accuracy Confusion Matrix

<b>Class</b>	<b>Bare Ground</b>	<b>Grasses</b>	<b>Yellow Veg</b>	<b>Pdog Mound</b>	<b>Sagebrush</b>	<b>Taller Veg</b>	<b>Trees</b>	<b>Water</b>	<b>Total</b>	<b>Users Accuracy</b>	<b>Kappa</b>
<b>Bare Ground</b>	103	11	0	11	0	0	0	0	125	0.824	0
<b>Grasses</b>	12	108	0	0	2	2	1	0	125	0.864	0
<b>Yellow Veg</b>	0	98	1	1	1	23	1	0	125	0.008	0
<b>Pdog Mound</b>	54	47	0	14	7	0	0	3	125	0.112	0
<b>Sagebrush</b>	13	74	0	2	35	1	0	0	125	0.28	0
<b>Taller Veg</b>	0	31	0	0	0	94	0	0	125	0.752	0
<b>Trees</b>	22	20	0	0	28	49	6	0	125	0.048	0
<b>Water</b>	8	113	0	0	0	0	0	4	125	0.032	0
<b>Total</b>	212	502	1	28	73	169	8	7	1000	0	0
<b>Producers Accuracy</b>	0.485849	0.215139	1	0.5	0.479452	0.556213	0.75	0.571429	0	0.365	0
<b>Kappa</b>	0	0	0	0	0	0	0	0	0	0	0.274286

**Appendix B: Table 51.** Maximum likelihood UAS Lindbo75NIR(1) Equalized Random Accuracy Confusion Matrix

<b>Class</b>	<b>Bare Ground</b>	<b>Grasses</b>	<b>Pdog Mound</b>	<b>Sagebrush</b>	<b>Taller Veg</b>	<b>Trees</b>	<b>Water</b>	<b>Total</b>	<b>Users Accuracy</b>	<b>Kappa</b>
<b>Bare Ground</b>	74	29	11	0	0	0	0	114	0.649123	0
<b>Grasses</b>	11	93	6	1	0	3	0	114	0.815789	0
<b>Pdog Mound</b>	40	63	10	1	0	0	0	114	0.087719	0
<b>Sagebrush</b>	51	26	1	19	2	15	0	114	0.166667	0
<b>Taller Veg</b>	44	30	0	24	2	14	0	114	0.017544	0
<b>Trees</b>	2	31	2	1	0	78	0	114	0.684211	0
<b>Water</b>	4	3	0	2	0	0	105	114	0.921053	0
<b>Total</b>	226	275	30	48	4	110	105	798	0	0
<b>Producers Accuracy</b>	0.327434	0.338182	0.333333	0.395833	0.5	0.709091	1	0	0.477444	0
<b>Kappa</b>	0	0	0	0	0	0	0	0	0	0.390351

**Appendix B: Table 52.** Maximum likelihood UAS Lindbo90(1) Equalized Random Accuracy Confusion Matrix

<b>Class</b>	<b>Bare Ground</b>	<b>Grasses</b>	<b>Pdog Mound</b>	<b>Sagebrush</b>	<b>Taller Veg</b>	<b>Trees</b>	<b>Water</b>	<b>Total</b>	<b>Users Accuracy</b>	<b>Kappa</b>
<b>Bare Ground</b>	60	37	10	0	0	0	0	107	0.560748	0
<b>Grasses</b>	6	95	2	0	0	4	0	107	0.88785	0
<b>Pdog Mound</b>	32	61	12	2	0	0	0	107	0.11215	0
<b>Sagebrush</b>	6	31	1	50	0	18	1	107	0.46729	0
<b>Taller Veg</b>	19	21	0	29	7	29	2	107	0.065421	0
<b>Trees</b>	1	23	1	3	0	79	0	107	0.738318	0
<b>Water</b>	15	45	3	11	0	5	28	107	0.261682	0
<b>Total</b>	139	313	29	95	7	135	31	749	0	0
<b>Producers Accuracy</b>	0.431655	0.303514	0.413793	0.526316	1	0.585185	0.903226	0	0.441923	0
<b>Kappa</b>	0	0	0	0	0	0	0	0	0	0.34891

**Appendix B: Table 53.** Maximum likelihood NUMosaic\_NAIP Stratified Random Accuracy Confusion Matrix

<b>Class</b>	<b>Bare Ground</b>	<b>Grasses</b>	<b>Veg of Interest</b>	<b>Park Road</b>	<b>Sagebrush</b>	<b>Trees</b>	<b>Water</b>	<b>No Data</b>	<b>Total</b>	<b>Users Accuracy</b>	<b>Kappa</b>
<b>Bare Ground</b>	95	12	0	1	3	5	2	0	118	0.805085	0
<b>Grasses</b>	2	165	2	0	11	7	1	0	188	0.87766	0
<b>Veg of Interest</b>	0	27	52	0	9	43	0	0	131	0.396947	0
<b>Park Road</b>	36	1	0	2	1	0	1	0	41	0.04878	0
<b>Sagebrush</b>	13	58	0	0	28	19	0	0	118	0.237288	0
<b>Trees</b>	0	7	18	0	2	99	0	0	126	0.785714	0
<b>Water</b>	18	0	0	0	0	0	7	0	25	0.28	0
<b>No Data</b>	4	0	5	0	0	0	1	0	10	0	0
<b>Total</b>	168	270	77	3	54	173	12	0	757	0	0
<b>Producers Accuracy</b>	0.565476	0.611111	0.675325	0.666667	0.518519	0.572254	0.583333	0	0	0.59181	0
<b>Kappa</b>	0	0	0	0	0	0	0	0	0	0	0.495643

**Appendix B: Table 54.** Maximum likelihood NUMosaic\_NAIP Equalized Random Accuracy Confusion Matrix

<b>Class</b>	<b>Bare Ground</b>	<b>Grasses</b>	<b>Veg of Interest</b>	<b>Park Road</b>	<b>Sagebrush</b>	<b>Trees</b>	<b>Water</b>	<b>No Data</b>	<b>Total</b>	<b>Users Accuracy</b>	<b>Kappa</b>
<b>Bare Ground</b>	88	8	0	1	1	1	1	0	100	0.88	0
<b>Grasses</b>	2	86	1	1	8	2	0	0	100	0.86	0
<b>Veg of Interest</b>	1	28	35	0	9	27	0	0	100	0.35	0
<b>Park Road</b>	91	3	0	3	0	1	2	0	100	0.03	0
<b>Sagebrush</b>	24	34	1	0	34	6	1	0	100	0.34	0
<b>Trees</b>	2	4	14	0	1	79	0	0	100	0.79	0
<b>Water</b>	70	3	0	0	1	0	26	0	100	0.26	0
<b>No Data</b>	31	3	28	0	2	5	31	0	100	0	0
<b>Total</b>	309	169	79	5	56	121	61	0	800	0	0
<b>Producers Accuracy</b>	0.28479	0.508876	0.443038	0.6	0.607143	0.652893	0.42623	0	0	0.43875	0
<b>Kappa</b>	0	0	0	0	0	0	0	0	0	0	0.358571

**Appendix B: Table 55.** Maximum likelihood SUMosaic\_NAIP Stratified Random Accuracy Confusion Matrix

<b>Class</b>	<b>Veg of Interest</b>	<b>Bare Ground</b>	<b>Water</b>	<b>Trees</b>	<b>Park Road</b>	<b>Grasses</b>	<b>Sagebrush</b>	<b>Total</b>	<b>Users Accuracy</b>	<b>Kappa</b>
<b>Veg of Interest</b>	40	1	0	11	0	19	3	74	0.540541	0
<b>Bare Ground</b>	1	100	0	7	0	14	6	128	0.78125	0
<b>Water</b>	2	2	6	0	0	0	0	10	0.6	0
<b>Trees</b>	35	11	0	97	0	10	4	157	0.617834	0
<b>Park Road</b>	0	15	0	0	1	9	1	26	0.038462	0
<b>Grasses</b>	21	14	1	8	0	180	8	232	0.775862	0
<b>Sagebrush</b>	13	12	0	8	0	44	25	102	0.245098	0
<b>Total</b>	112	155	7	131	1	276	47	729	0	0
<b>Producers Accuracy</b>	0.357143	0.645161	0.857143	0.740458	1	0.652174	0.531915	0	0.615912	0
<b>Kappa</b>	0	0	0	0	0	0	0	0	0	0.506747



**Appendix B: Table 56.** Maximum likelihood SUMosaic\_NAIP Equalized Random Accuracy Confusion Matrix

<b>Class</b>	<b>Veg of Interest</b>	<b>Bare Ground</b>	<b>Water</b>	<b>Trees</b>	<b>Park Road</b>	<b>Grasses</b>	<b>Sagebrush</b>	<b>Total</b>	<b>Users Accuracy</b>	<b>Kappa</b>
<b>Veg of Interest</b>	43	0	0	17	0	34	9	103	0.417476	0
<b>Bare Ground</b>	0	84	1	3	3	10	2	103	0.815534	0
<b>Water</b>	0	47	41	4	2	7	2	103	0.398058	0
<b>Trees</b>	14	7	0	64	0	13	5	103	0.621359	0
<b>Park Road</b>	0	76	0	1	6	14	6	103	0.058252	0
<b>Grasses</b>	3	11	0	6	0	78	5	103	0.757282	0
<b>Sagebrush</b>	3	15	0	5	0	53	27	103	0.262136	0
<b>Total</b>	63	240	42	100	11	209	56	721	0	0
<b>Producers Accuracy</b>	0.68254	0.35	0.97619	0.64	0.545455	0.373206	0.482143	0	0.475728	0
<b>Kappa</b>	0	0	0	0	0	0	0	0	0	0.38835

**Appendix B: Table 57.** Maximum likelihood NAIPTalkington75(2) compared with UASTalkington75(2) Equalized Random Accuracy Confusion Matrix

<b>Class</b>	<b>Bare Ground</b>	<b>Grasses</b>	<b>Veg of Interest</b>	<b>Park Road</b>	<b>Sagebrush</b>	<b>Shrubby Veg</b>	<b>Taller Veg</b>	<b>Trees</b>	<b>Water</b>	<b>Total</b>	<b>Users Accuracy</b>	<b>Kappa</b>
<b>Bare Ground</b>	48	30	0	0	12	0	5	1	4	100	0.48	0
<b>Grasses</b>	2	81	1	0	0	0	13	3	0	100	0.81	0
<b>Veg of Interest</b>	1	11	8	0	2	4	61	13	0	100	0.08	0
<b>Park Road</b>	35	51	0	0	5	0	4	2	3	100	0	0
<b>Sagebrush</b>	1	61	0	0	13	1	21	3	0	100	0.13	0
<b>Shrubby Veg</b>	0	0	0	0	0	0	0	0	0	0	0	0
<b>Taller Veg</b>	0	0	0	0	0	0	0	0	0	0	0	0
<b>Trees</b>	2	28	0	0	11	6	32	19	1	99	0.191919	0
<b>Water</b>	29	21	0	0	3	0	3	8	36	100	0.36	0
<b>Total</b>	118	283	9	0	46	11	139	49	44	699	0	0
<b>Producers Accuracy</b>	0.40678	0.286219	0.888889	0	0.282609	0	0	0.387755	0.818182	0	0.293276	0
<b>Kappa</b>	0	0	0	0	0	0	0	0	0	0	0	0.203905